www.sciencemag.org/content/358/6369/eaao2648/suppl/DC1

Supplementary Materials for

Single-stranded DNA and RNA origami

Dongran Han,* Xiaodong Qi,* Cameron Myhrvold, Bei Wang, Mingjie Dai, Shuoxing Jiang, Maxwell Bates, Yan Liu, Byoungkwon An,† Fei Zhang,† Hao Yan,† Peng Yin†

*These authors contributed equally to this work.
†Corresponding author. Email: py@hms.harvard.edu (P.Y.); hao.yan@asu.edu (H.Y.); fei.zhang@asu.edu (F.Z.); dran@csail.mit.edu (B.A.)

Published 15 December 2017, *Science* **358**, eaao2648 (2017)
DOI: 10.1126/science.aao2648

This PDF file includes:

Other Supplementary Materials for this manuscript include the following:
(available at www.sciencemag.org/content/358/6369/eaao2648/suppl/DC1)

Table of contents **Pages**

Supplementary section 1: Concept of single-stranded DNA origami (ssOrigami)

In nature, a biological macromolecule such as a protein (or a protein domain) typically folds from a single polymer into a well-defined structure (Fig. S1-1).

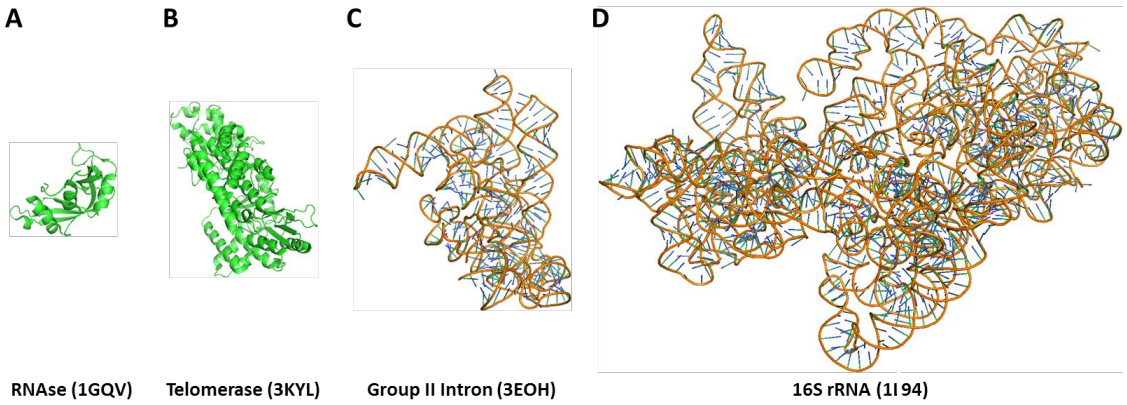

Figure S1-1. Examples of natural biomacromolecules folded from single strand components.

In contrast, in the field of DNA nanotechnology, 2D and 3D structures are typically constructed using self-assembly, in which many DNA strands bind to one another to form a structure (Fig. S1-2 A, B). The concept of ssOrigami is to fold a single long ssDNA into a target shape (Fig. S1-2C).

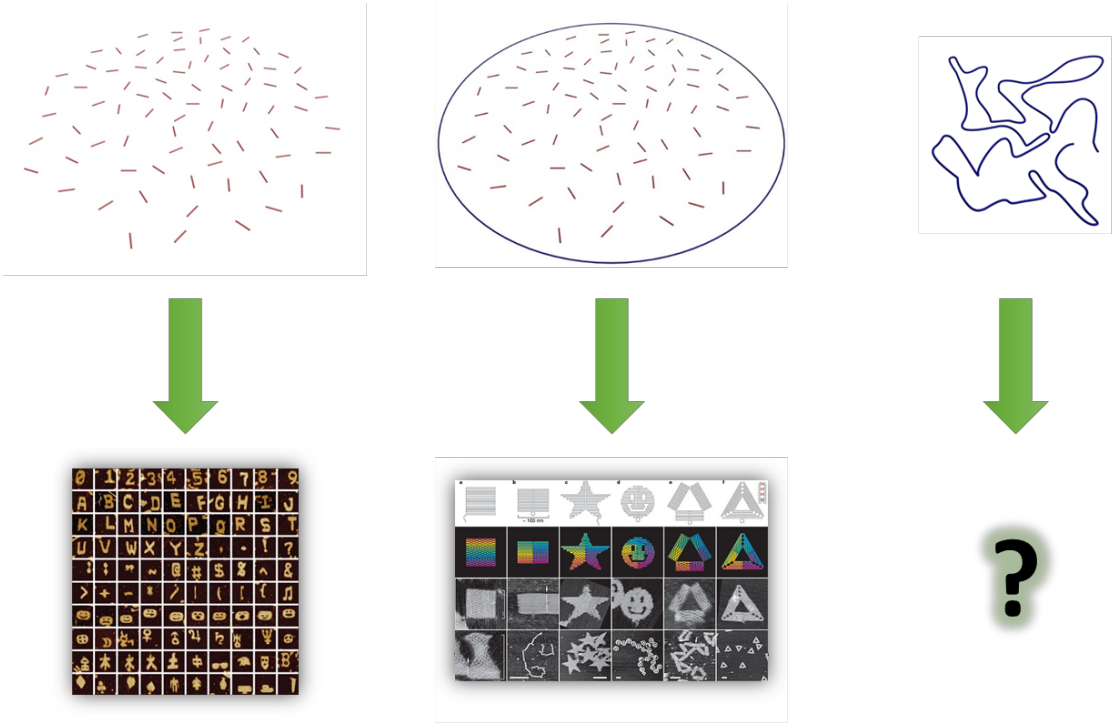

Figure S1-2. Current design strategies for complex discrete DNA nanostructures. **A.** Single-stranded DNA tiles (SST) have been used to self-assemble into finite size shapes. **B.** Long kilo-base scaffold strand and short staple strands have been used to construct scaffolded DNA origami structures. **C.** Long kilo-base single-stranded DNA origami has not been achieved prior to this study.

Supplementary section 2: One touch drawing of ssOrigami.

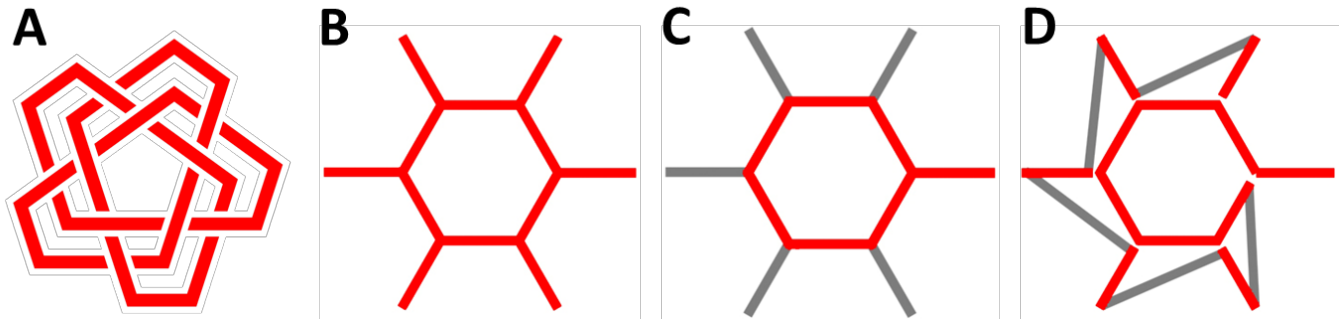

Figure S2-1. Concept of one touch drawing. **A.** A typical one touch drawing shape. **B, C, D.** A shape that cannot be drawn with one touch drawing unless extra bridging segments are introduced (**D**).

ssOrigami is designed to fold ssDNA into complex shapes similarly to those produced in one touch drawing artwork (Fig. S2-1A). For some patterns such as the one shown in Fig. S2-1B, one touch drawing cannot be achieved directly. Fig. S2-1C shows an attempt to draw the shape with one continuous line (the red segments) with several gray sections left undrawn. If additional bridging segments are added, such as the gray sections in Fig. S2-1D, the pattern can now be achieved using one touch drawing. In DNA nanostructure design, these extra bridging segments are replaced with ssDNA loops connecting distant 5' and 3' ends.

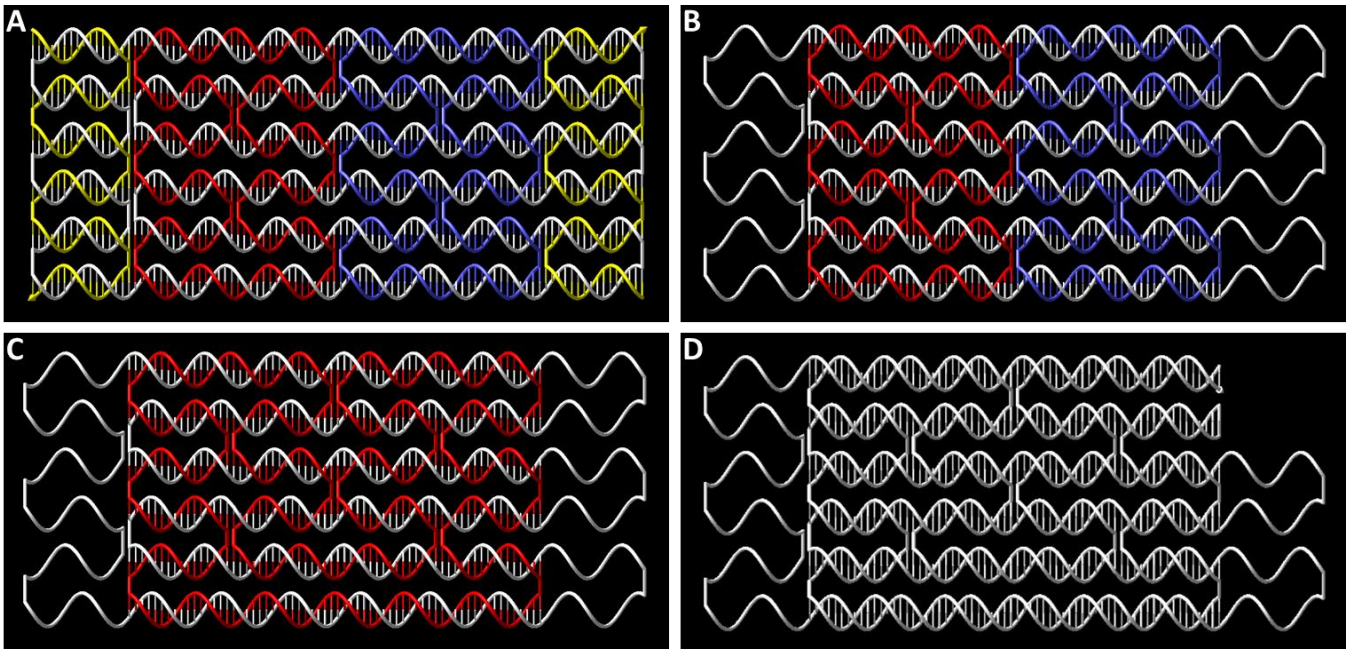

Figure S2-2. Breaking and reconnecting of a traditional scaffolded DNA origami into an ssOrigami.

One potential approach to create an ssOrigami is to break and reconnect strands in a traditional DNA scaffolded origami design so that all the staple and scaffold strands are merged into a single continuous DNA strand. This design idea could be realized via the processes shown in Fig. S2-2. In the first step, an antiparallel scaffolded origami structure in which staple strands are not cut into short pieces is used as a starting template (Fig. S2-2A). This design template contains one long scaffold strand (white) and four staple strands (from left to right: yellow, red, blue and yellow). Because the two yellow strands are not cyclized, and their 5' and 3' ends cannot be easily connected with the remaining part of the design, we can delete them to simplify the design into the structure shown in Fig. S2-2B. Here, there are three strands remaining. By breaking and reconnecting the crossover in the mid-bottom of the design, two staple strands (red and blue) can be

merged into one longer strand (Fig. S2-2C). This longer staple can be further merged with the scaffold strand at the top-right corner of the structure to become one continuous strand (Fig. S2-2D). Based on the principles shown in the above process, a typical traditional scaffolded DNA origami design can be converted into a single strand without creating long unpaired loop regions. However, such designs could fail due to the knotting issues discussed in Section 3.

Supplementary section 3: Knot theory and crossing number of ssOrigami structures.

While unimolecular folding is commonly observed in proteins, it is not straightforward to achieve similar bottom-up folding complexity using synthetic DNA. Although we can construct complex 2D and 3D shapes with scaffolded DNA origami or single-stranded DNA tile/brick strategies, converting them into single-stranded origami structures is difficult due to potential knotting problems, which will be discussed in this section.

Knot theory in topology can be used to distinguish different DNA knots to help guide the design process of ssOrigami. A 2D projection of a 3D ssOrigami model can be treated as a knot diagram, which also contains information about over-strand and under-strand at all intersection points. Fig. S3-1 shows a 2D projection of a typical ssOrigami design model, a simplified version of Fig. S 2-2D. The 5' and 3' ends of this ssDNA origami are shown on the upright corner of the design. The sticks illustrating the base pairing are not treated as part of the knot diagram.

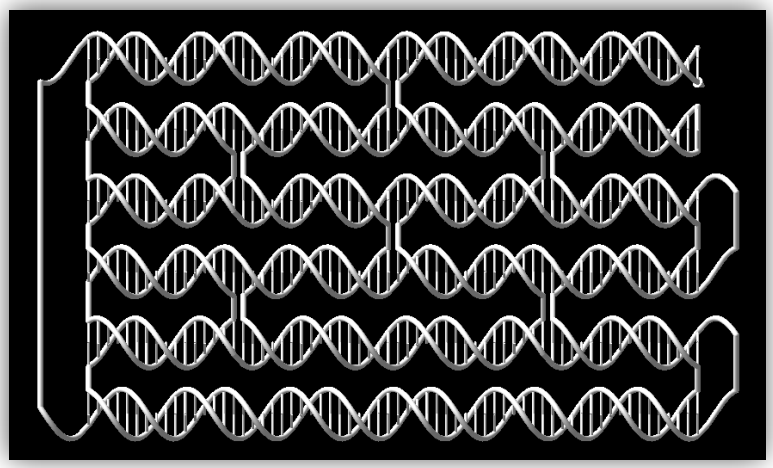

Figure S3-1. 2D projection of a typical anti-parallel ssOrigami design with ~800 nt.

When a 2D projection of an ssOrigami model is treated as a knot diagram, we assume the two ends of this ssOrigami model are connected in a way that keeps its knotting properties. For ssOrigami designs discussed in this paper, as their 5' and 3' ends are usually close to each other (e.g. the ssOrigami in Fig. S3-1, with its ends at the upright corner), direct connection of both ends will result in a closed loop (Fig. S3-2A and B). In general, for any 2D projection of a biological macromolecule with exposed ends, if there is a way to connect each of its two ends to a point at infinite distance using a straight line segment that does not intersect the remaining part of the projection, we can further connect these two points at infinite distance to convert the projection into a closed loop (Figure S3-2C and D). In this way, every ssOrigami design in this study can be converted into a closed loop while preserving its knotting complexity.

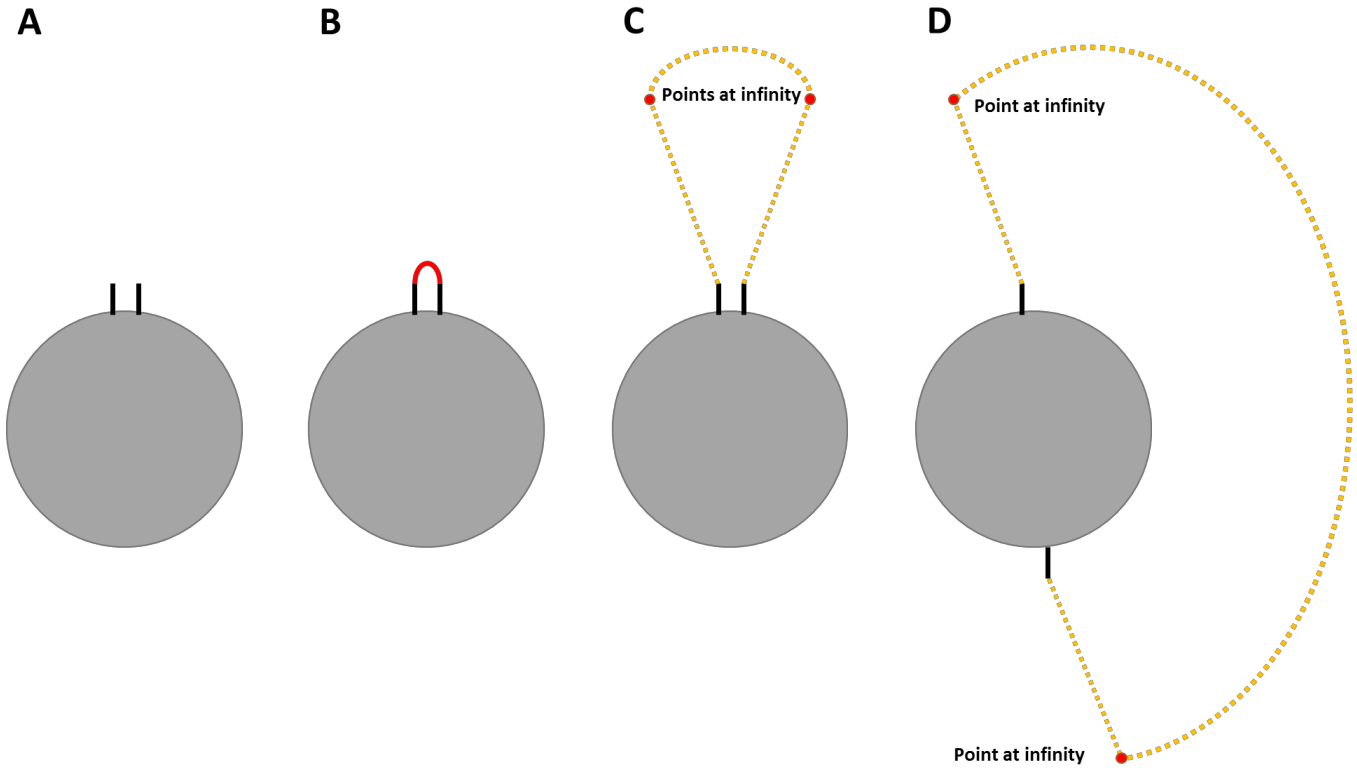

Figure S3-2. Converting the knot diagram of an open-ended biological macromolecule into a closed loop. **A.** A linear macromolecule with exposed ends that are close to each other. **B.** Direct connection of open ends in **a** without intersecting with the remaining part of the knot diagram results in a closed loop. **C** and **D**. If each of the two ends of an open-chain molecule can be connected to a point at infinite distance via a line segment that does not intersect the remaining part of the 2D diagram, we can then connect the two points at infinite distance and convert the open-chain molecule into a closed loop while preserving its knotting complexity.

In knot theory, two knots are topologically equivalent if they can be related by a sequence of three kinds of moves on their diagrams. These operations, called the Reidemeister moves, are shown in Fig. S3-3A-C. The Reidemeister moves ensure that no intersections are allowed in the operation of a mathematical knot. This restriction also applies to the operation of ssOrigami models. For example, by applying Type I Reidemeister moves (or by twisting), DNA hairpin structures can be converted into an unknotted open loop (Fig. S3-3D).

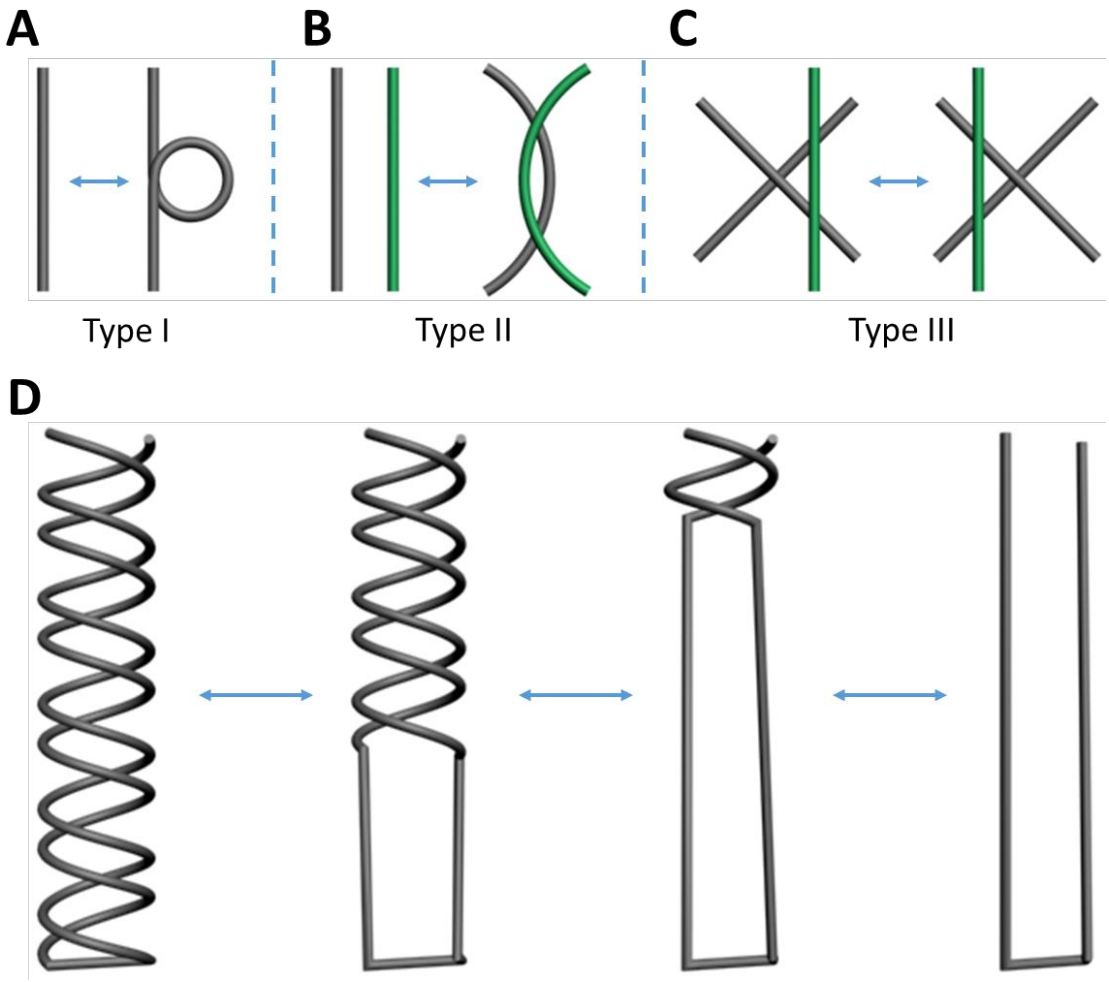

Figure S3-3. Reidemeister moves (**A-C**) and an example of Reidemeister moves operation over a DNA hairpin (**D**). **A**. Type I Reidemeister move: Twist and untwist in either direction. **B**. Type II Reidemeister move: Move one strand completely over another. **C**. Type III Reidemeister move: Move a strand completely over or under a crossing. **D.** DNA hairpin structures can be converted through continuous Type I Reidemeister moves to an unknotted open loop.

If we apply all Type I Reidemeister moves to the diagram shown in Fig. S3-1, the ssOrigami model can be further simplified into a reduced diagram (containing no reducible crossings) shown in Fig. S3-4.

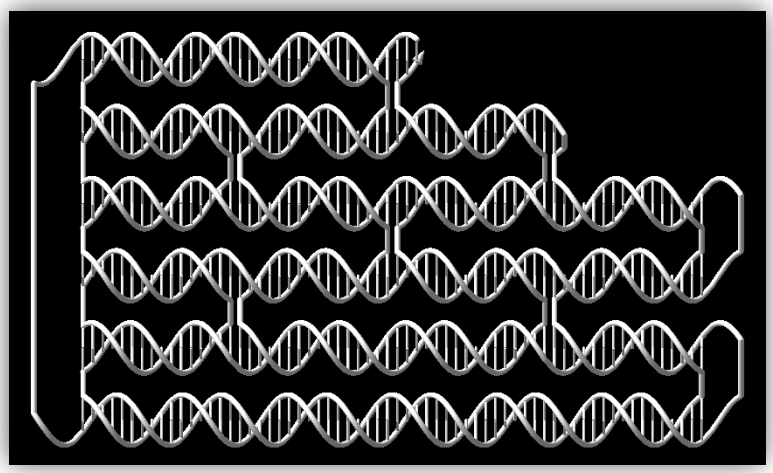

Figure S3-4. 2D projection of a typical anti-parallel ssOrigami design pattern.

The next question for ssOrigami design is to determine the knotting complexity of a DNA knot diagram so that we can roughly estimate the likelihood for it to fold correctly. One indicator to approximate the knotting complexity of an ssOrigami design is the crossing number, a knot invariant defined as the smallest number of crossings in any diagram of the knot. A knot invariant is a "quantity" that is mathematically the same for equivalent knots. In other words, if the invariant is computed from a knot diagram, it should give the same value for two knot diagrams representing equivalent knots. Note that the reduced diagram shown in Fig. S3-4 is also an alternating diagram[67], in which the crossings alternate under and over each time the strand intersects itself. If we follow the track of the ssDNA from the 5' end to the 3' end, it always passes alternately over and under crossings. According to Tait conjectures [67], any reduced diagram of an alternating knot has the fewest possible crossings. Here, we can count the crossing number of the design (Fig. S3-4) to be 63.

For anti-parallel crossovers, as shown in Fig. S3-5A, the local strand arrangement is alternating. At the same time, double helical DNA is alternating because its two strands are always intertwined along its helices. As a result, if an ssOrigami is designed from anti-parallel crossovers and double helices, such a design will be an alternating diagram because all its components are alternating after simplification on the edges (similar to Fig. S3-4). If we place a central plane containing all DNA helical axes (dashed lines in Fig. S3-5A and gray semitransparent central plane in Fig. S3-5B), we can see that we need to thread a needle through that central plane 126 times to weave the shape for the design with a crossing number of 63.

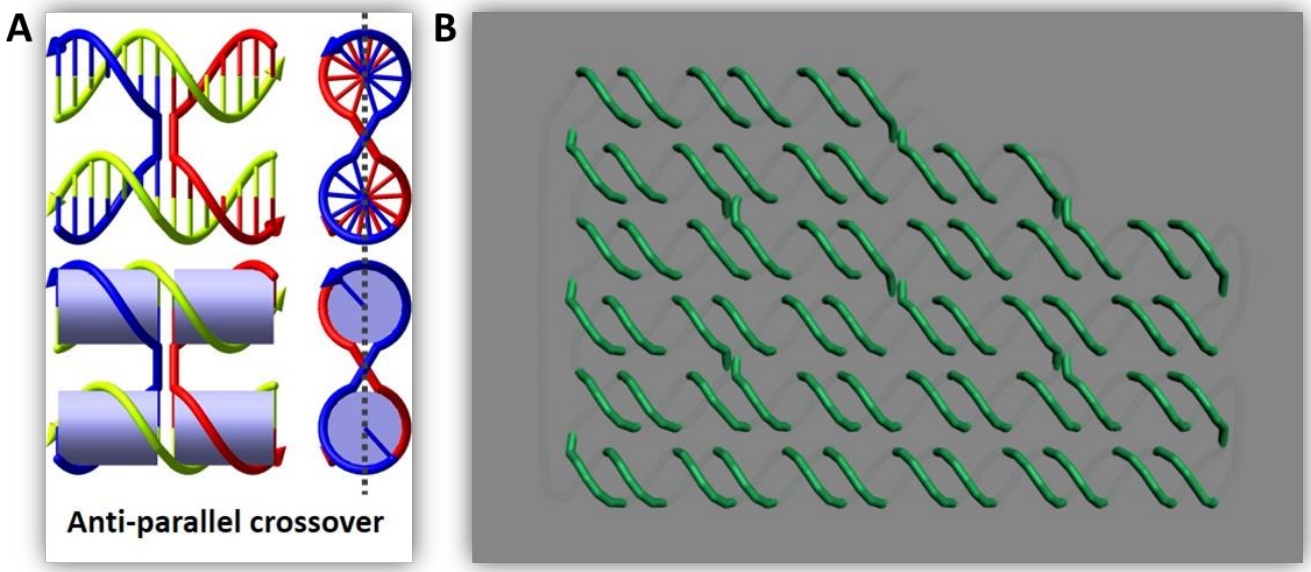

Figure S3-5. A. Anti-parallel crossover model and **B**. anti-parallel ssOrigami design with inserted gray semitransparent central plane, which contains all DNA helical axes. DNA strand travels through this plane 126 times in this design pattern, which would make the folding of such a structure difficult.

Supplementary section 4: Dynamic relaxation model for knot simplification.

To study the knotting complexity of a structure, we introduce a novel dynamic relaxation model to that simplify the knot structure without changing its knotting complexity. In this model, both the 3' and 5' ends of a 3D ssOrigami model are fixed while the remaining part of the strand falls under simulated gravity. The falling process will relax the unknotted crossings, and thus simplify the diagram. For example, if a structurally "complex" 3D knot model is actually an unknot (crossing number 0), the relaxation will simplify the model into an untied loop (unfolding), e.g. as in the DNA hairpin shown in Fig. S4-1A. On the other hand, if a 3D knot model is knotted, the crossings will be kept during the falling process, e.g. as in the double helical DNA structure shown in Fig. S4-1B.

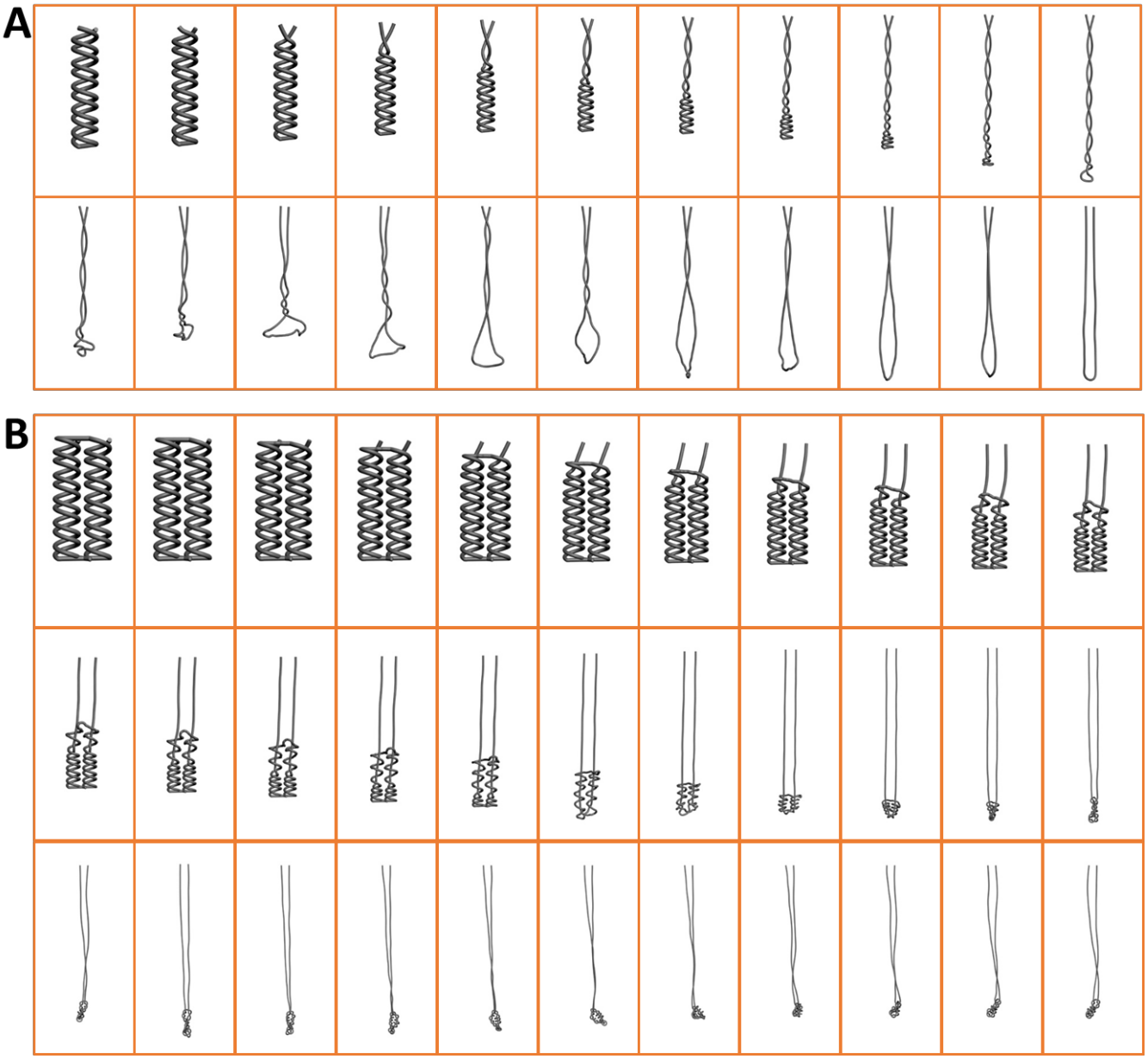

Figure S4-1. Dynamic animation to demonstrate the knot relaxation process of **A**. a simple DNA hairpin [Movie-1] and **B**. a paired double helical DNA with antiparallel crossovers analogue [Movie-2].

Our dynamic relaxation model is implemented using the Autodesk 3ds Max software. Linear models of target shapes are first created according to the target shape such as the first snapshot in Fig. S4-1 A and B. Such a **line/spline** object is then treated as a **reactor rope** and added to a **rope collection.** The relaxation is performed with **0.5 Friction** and **0.5 Air Resistance** with both ends of the rope fixed**.** The **Rope Type** of the object is set to be **Constraint** and **Avoid Self-**

Intersections. This dynamic relaxation model can also be applied to RNA or protein structures such as the ones shown in Fig. S4-2 to S4-5. In these cases, the PDB data of an RNA or protein structure is first converted to a **line/spline** object in the software, and then treated as a rope for relaxation.

Note that in the dynamic relaxation, the falling direction is chosen in a way that the falling process does not change the knotting complexity of the model. For simple cases such as the ones shown in Figure S4-1, both ends of the structure can be easily fixed at the top, and it is obvious the falling of the rest of the structure will not change the knotting complexity. More generally, for complex natural biomolecules such as the 16S rRNA shown in Fig. S4-2 where its two end points (highlighted with the red spheres) are not exposed, the falling direction is chosen according to the following procedure: 1, the molecule is positioned properly so that both of its ends (red spheres) are at the same height; 2, a horizontal plane is arranged at the height of the red spheres (Fig. S4-2C and E); 3, the portion of the molecule above the horizontal plane is projected onto this plane (Fig. S4-2D and F); 4, if neither red sphere is surrounded by a closed loop (Fig. S4-2D), the falling direction is legitimate; 5, if either one of the red spheres is surrounded by a closed loop (Fig. S4-2F), the falling direction needs to be changed because the end point may go through that closed loop during falling process, potentially changing the knotting complexity of the structure. The above procedure ensures that the knotting complexity will not be artificially changed during the relaxation process.

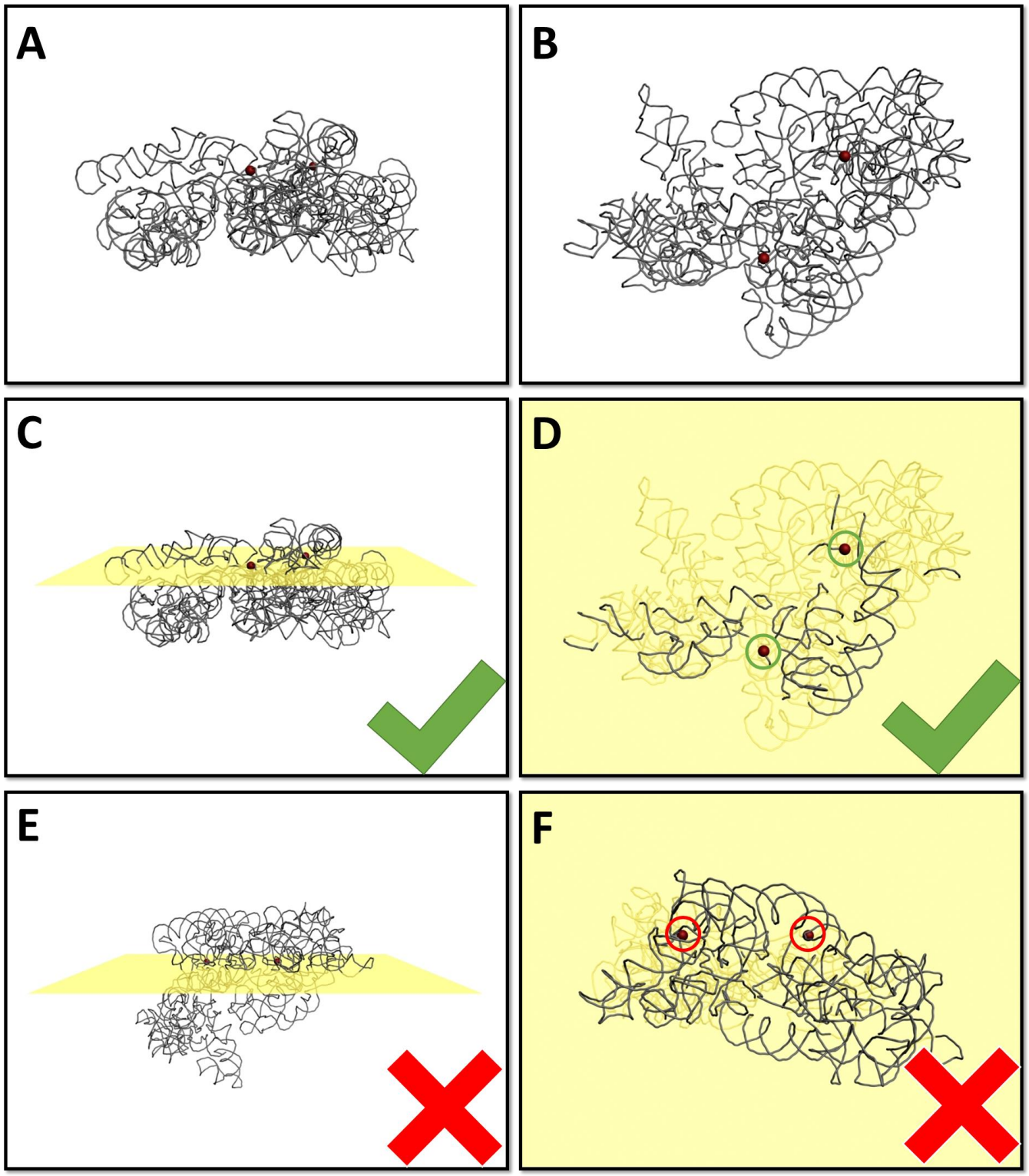

Figure S4-2. Choosing the falling direction of the molecule during the relaxation. **A**, **B**. Side view (**A**) and top view (**B**) of 16S rRNA (PDB: 1I94). Both ends of the molecule are highlighted with red spheres. **C, D.** Side view (**C**) and top view (**D**) of 16S rRNA with a horizontal plane placed at the height of the two red spheres. **D** can be viewed as a top-down projection of the molecule on to this horizontal plane. **E, F**. Side view (**G**) and top view (**F**) of 16S rRNA with a different falling direction. Considering the top-down projection of the molecule on the horizontal planes contains closed loops surrounding the red spheres (indicated by red circles), such falling direction is not permitted.

For more information about our dynamic relaxation model, please refer to the relaxation movies files in the supplementary information package.

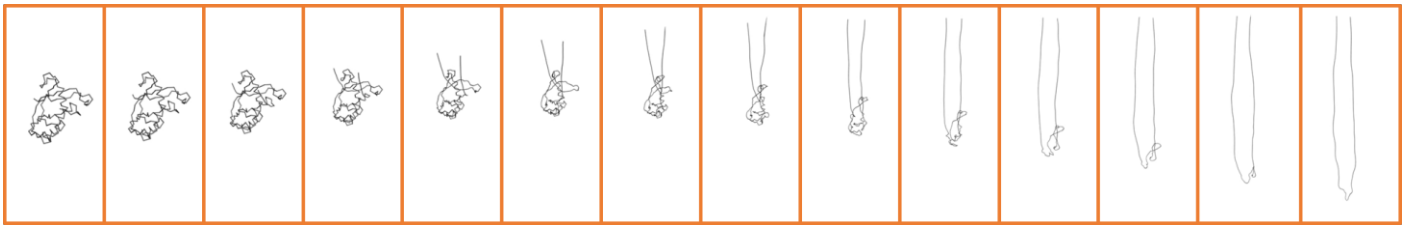

Figure S4-3. Selected screenshots of dynamic relaxation to demonstrate the knot relaxation process of RNAse (PDB: 1GQV). Relaxation movies are available in the supplementary information package [Movie-3].

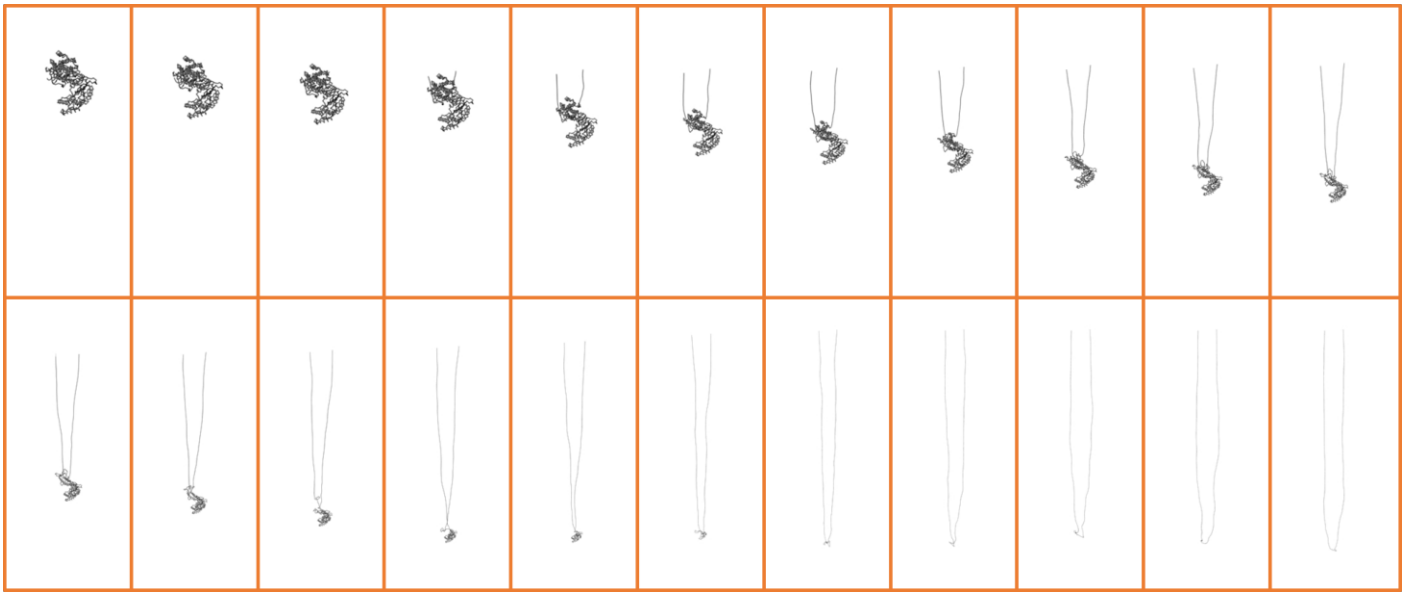

Figure S4-4. Selected screenshots of dynamic relaxation to demonstrate the knot relaxation process of Telomerase (PDB: 3KYL). Relaxation movies are available in the supplementary information package [Movie-4].

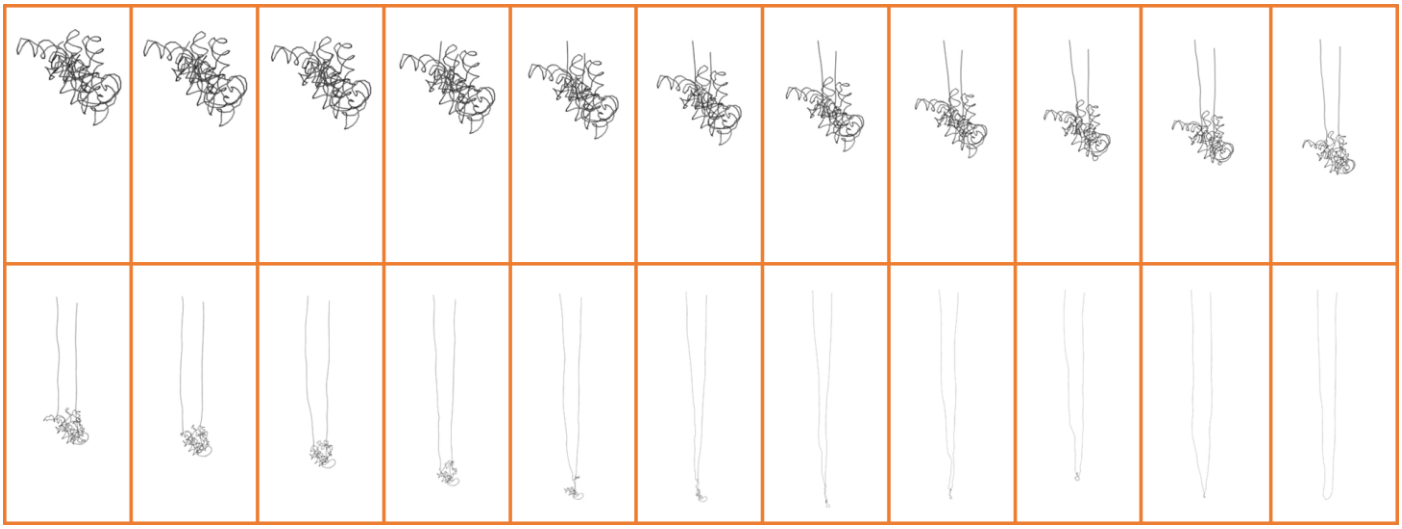

Figure S4-5. Selected screenshots of dynamic relaxation to demonstrate the knot relaxation process of Group II Intron (PDB: 3EOH). Relaxation movies are available in the supplementary information package [Movie-5].

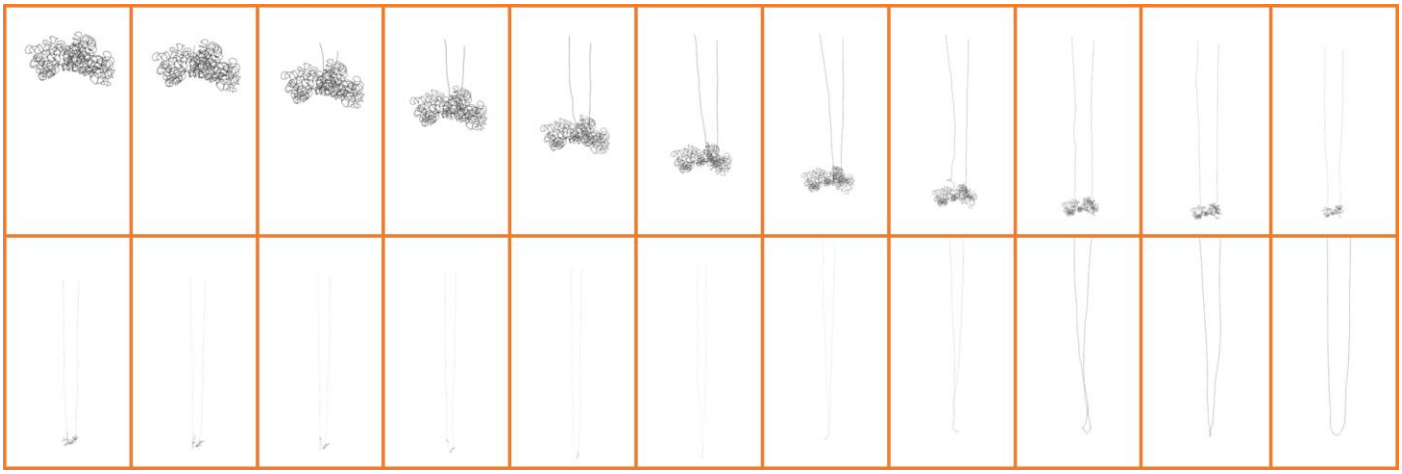

Figure S4-6. Selected screenshots of dynamic relaxation to demonstrate the knot relaxation process of 16S rRNA (PDB: 1I94). Relaxation movies are available in the supplementary information package [Movie-6].

As demonstrated in Fig. S4-3 to S4-6, RNAse (PDB: 1GQV, length: 135 amino acids), Telomerase (PDB: 3KYL, length: 596 amino acids), Group II Intron (PDB: 3EOH, length: 412 nucleotides) and 16S rRNA (PDB: 1I94, length: 1514 nucleotides) can all be relaxed into unknotted open loops via our dynamic relaxation system, which reveals that they all have a crossing number of 0.

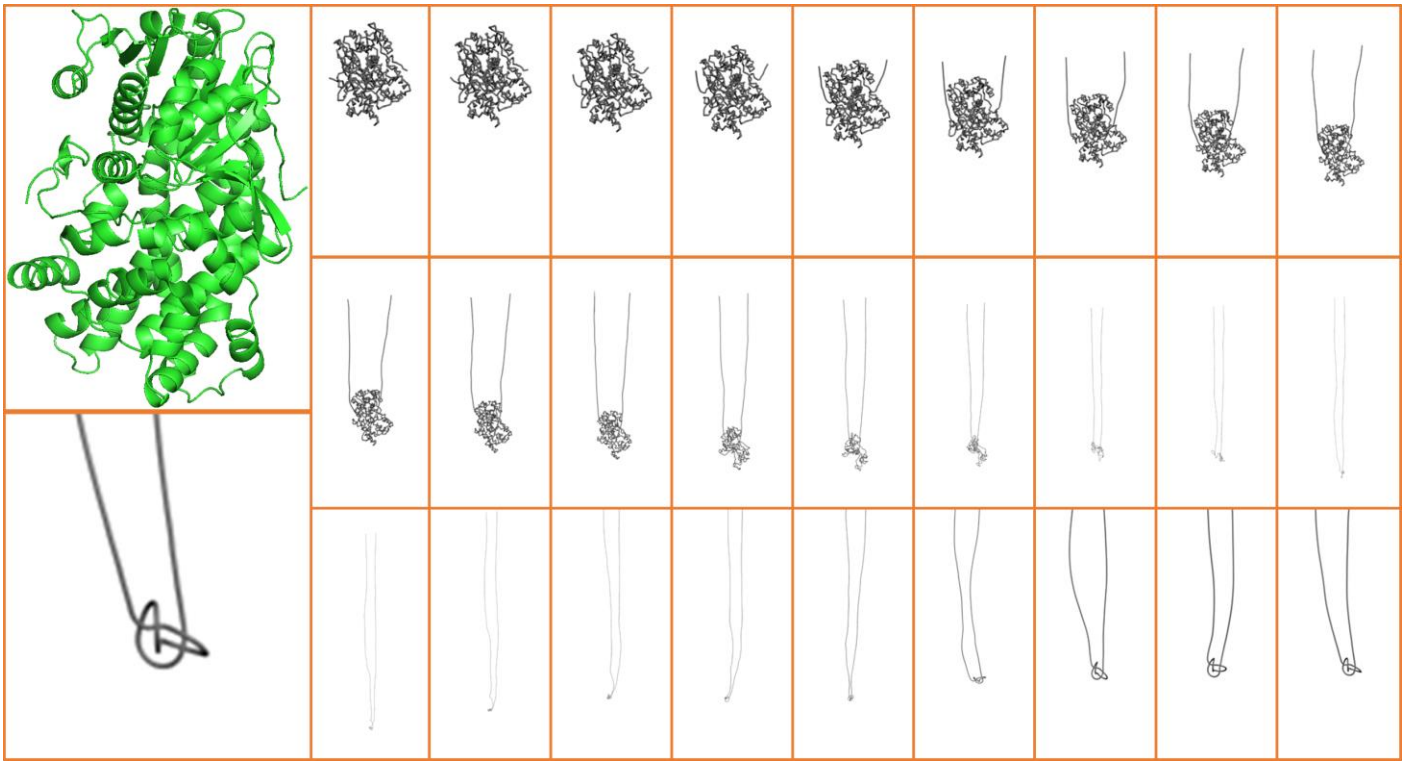

Figure S4-7. Selected screenshots of dynamic relaxation to demonstrate the knot relaxation process of acetohydroxy acid isomeroreductase (PDB: 1YVE-L). Top left: cartoon model of acetohydroxy acid isomeroreductase (1YVE-L). Bottom left: final state of dynamic relaxation. Relaxation movies are available in the supplementary information package [Movie-7].

If this dynamic relaxation is applied to a knotted protein (which is rarely observed) such as the carboxy-terminal domain of acetohydroxy acid isomeroreductase (PDB: 1YVE-L) [68] shown in Fig. S4-7, the rope will become as a simple knot. The crossing number of this knot is 3, which is the simplest knot [67].

We can also apply this dynamic relaxation to the previous anti-parallel ssOrigami design (Fig. S4-3) with a crossing number of 63. The snapshot of the relaxation process is shown in Fig. S4-8. Different from all previous examples, such a high crossing number design will not be relaxed into a simple final shape, but instead a knotted ball. Folding of such a high crossing number pattern could be challenging.

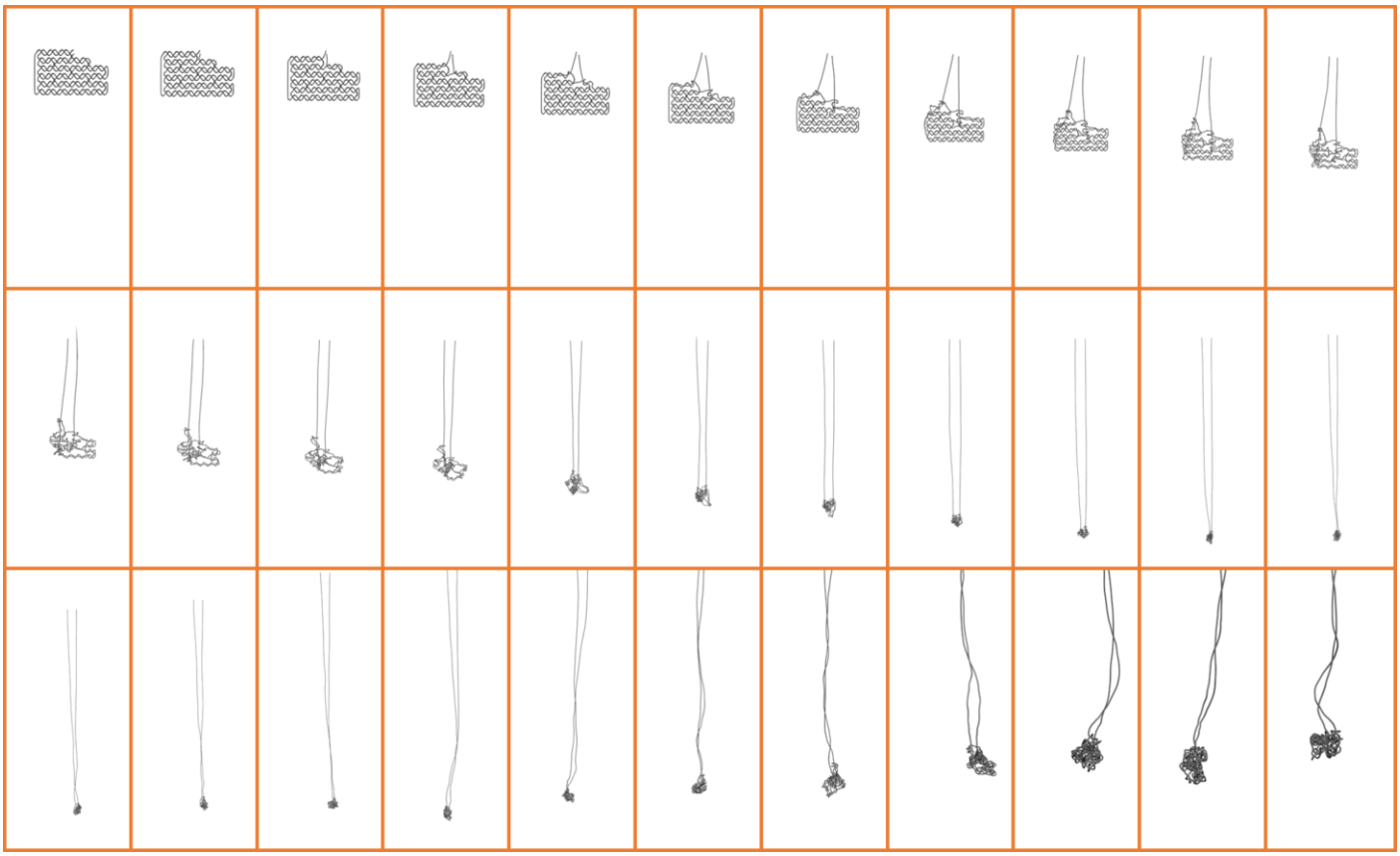

Figure S4-8. Selected screenshots of dynamic relaxation to demonstrate the knot relaxation process of an anti-parallel ssOrigami model. Relaxation movies are available in the supplementary information package [Movie-8].

Supplementary section 5: Design of ssOrigami with crossing number of 0.

As we have shown in Supplementary Sections 3 and 4, anti-parallel-crossover based ssOrigami designs have high crossing numbers. Here, we focus on *parallel-crossover* based ssOrigami designs. At parallel crossover positions, DNA strands do not need to go through the central plane containing all DNA helical axes, which could reduce the folding complexity of the structure.

Based on this assumption, if an ssOrigami design contains only locking domains but not helical domains, DNA strands in this structure does not need to thread through the central plane. To achieve this goal, we create a folding pattern as shown in Fig. S5-1a, which has the maximum crossover points so that DNA strands never intertwine more than 180° on to the double helices before jumping to adjacent double helices. However, such simple folding pattern could also reduce the stability of ssOrigami as it contains a large number of unperturbed 5, 4 or even 1 base pair (bp) sections. In Fig. S5-1a, the wider cylinders contain 5bp, the thinner cylinders contain 4bp and the sections without a cylinder contain only 1 unperturbed continuous base paring. In our preliminary experiments, we created one ssOrigami design with this pattern. As expected, this structure did not form and only linear unfolded DNA was observed under AFM imaging (data not shown).

To get rid of these 1 base pair sections, some of the crossover points need to be deleted. In Fig. S5-1b, we create a parallel ssOrigami design with 16-bp between adjacent crossovers, a similar crossover density to a typical traditional 2D scaffolded origami structure. This design strategy should be sufficiently stable since it contains only 16bp unperturbed sections; however, it also results in a large crossing number despite that it uses only parallel crossovers. In this design, the green strand goes horizontally to tangle with both blue and red strands. Such entanglement cannot be eliminated by the aforementioned Reidemeister moves. To further examine its folding complexity, we created an ssOrigami design based on this strategy (Fig. S5-2 top) and applied our dynamic relaxation animation to the structure. From the screenshots, we can see that the structure appears severely knotted.

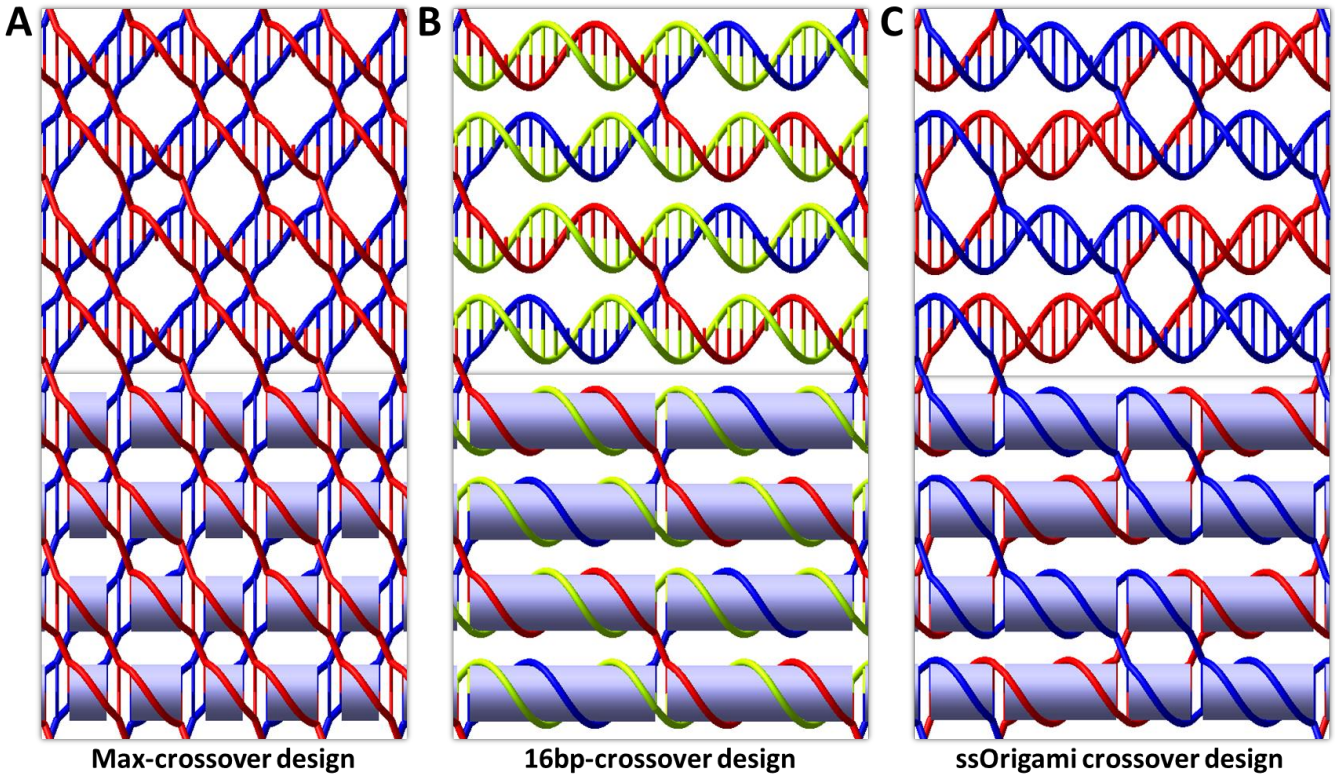

Figure S5-1. Design principles for parallel crossover ssOrigami. **A.** A maximum crossover design in which parallel crossovers are created in all possible positions. Blue strands are always on top of the red strands at crossover positions. This design contains sets of 5, 4 and 1 unperturbed base pairs. **B.** 16bp-crossover design which contains only 16 unperturbed base pairs between adjacent parallel crossovers. The green strands do not travel between adjacent helices. **C**. Our final ssOrigami crossover design in which local interlocks happen only between strands with the same color (at the helical domain positions). Top: 3D double helical model. Bottom: double helical model with wrapped cylinder showing the unperturbed base pairs.

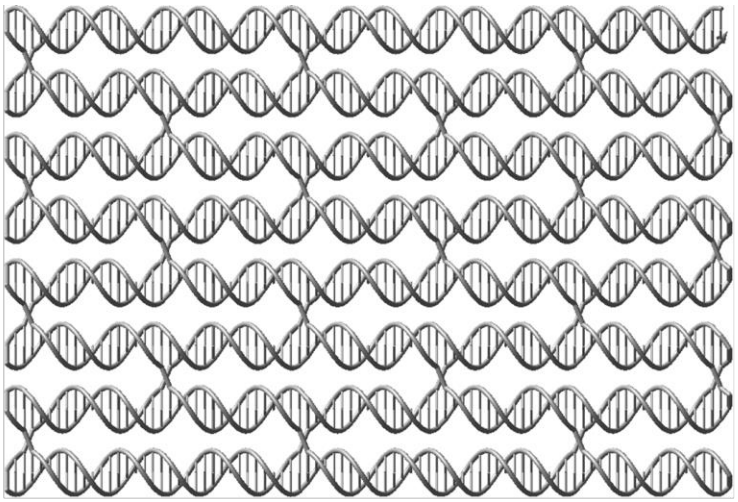

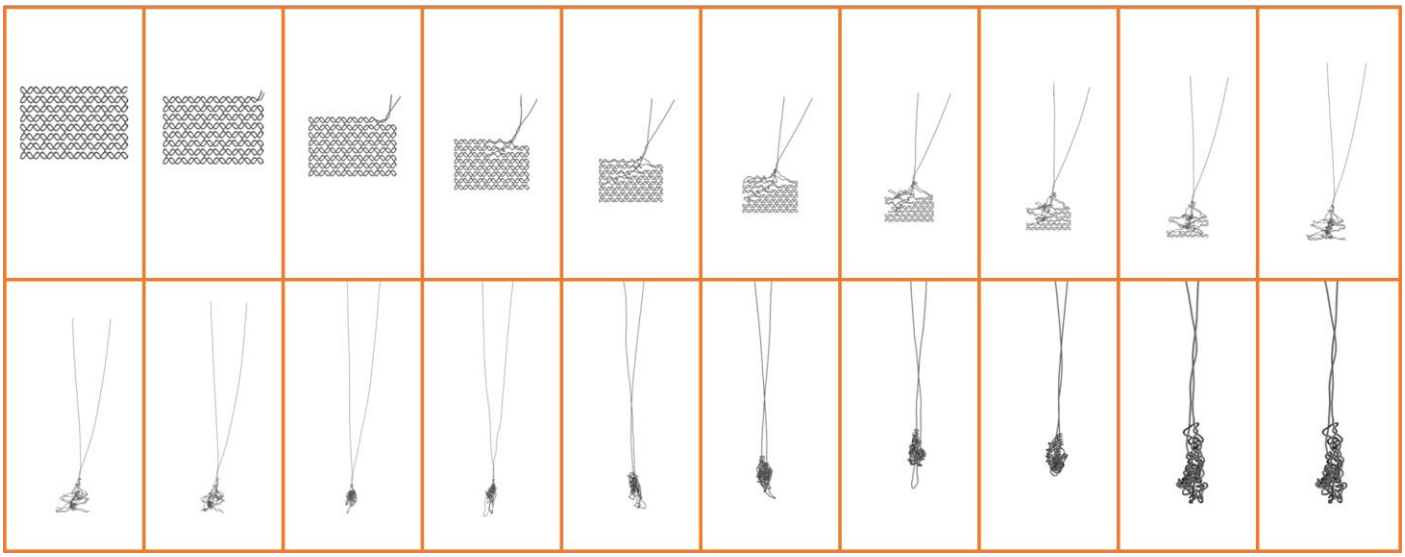

Figure S5-2. Selected screenshots of dynamic relaxation to demonstrate the knot relaxation process of a parallel ssOrigami model with 16bp crossover distance. Relaxation movies are available in the supplementary information package [Movie-9].

Our final design adopts the design pattern shown in Fig. S5-1C, in which a putative, partially paired double-stranded intermediate is first formed and then folds into the final structure (Fig. 1C and S5-3).

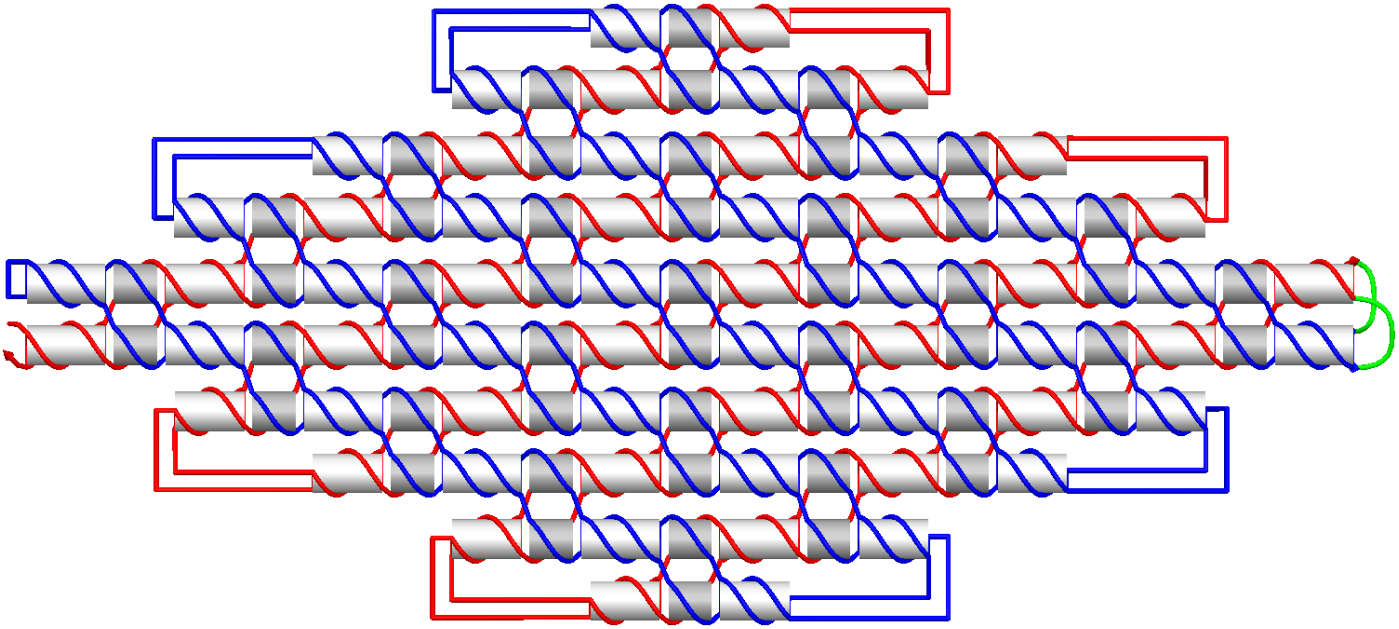

Figure S5-3. A 5 × 5 ssOrigami design model.

As shown in Fig. S4-1A, a helical double-stranded DNA has a crossing number of 0. Our putative, partially paired double-stranded intermediate is similar to such a double-stranded DNA and can be treated as an unknotted structural unit (similar to Fig. S4-1A) for further folding. As such, we can illustrate the 5 × 5 ssOrigami design model with the simplified pipeline style model shown in Fig. S5-4. It is also easy to tell that such an ssOrigami design is not knotted since the pipeline model never threads through any hole within the structure.

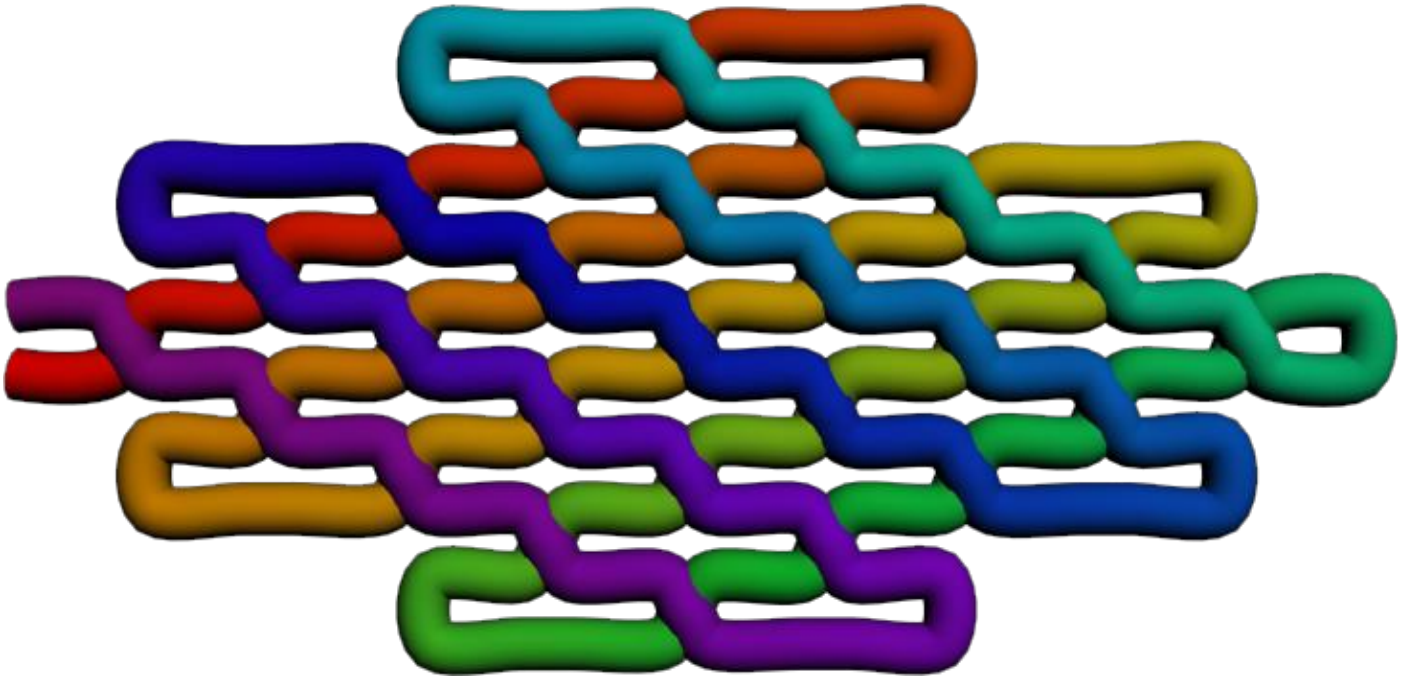

Figure S5-4. Pipeline style model of a 5 × 5 ssOrigami design. The model is colored with rainbow gradient starting from the 5' and 3' ends (red) to the middle of the strand (purple).

Complex ssOrigami structures are also achieved with similar helical and locking domain arrangements, such as those shown in Fig. S5-5, S5-6 and S5-7. These designs contain 26bps helical domains, indicated by the long green rectangles in the cartoon model (top). As that synthesis of a DNA strand with many 26bps complementary section is difficult, we cut the synthesis DNA template into two halves so that within each half of the strand there is no strong self-complementarity. As a result, such a DNA template becomes accessible via commercial synthesis.

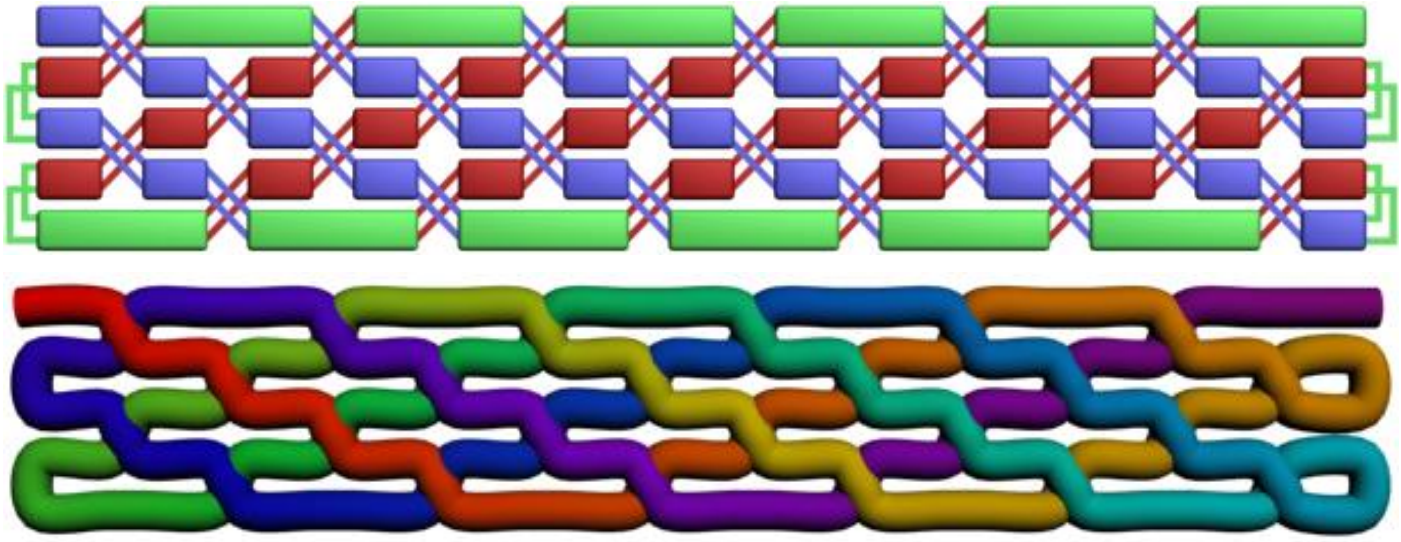

Figure S5-5. Cartoon (top) and pipeline style (bottom) model of the strip-shape ssOrigami design. The long green rectangles in the cartoon model stand for 26bps helical domains. The pipeline style model is colored with rainbow gradient starting from the 5' and 3' ends (red) to the middle of the strand (purple).

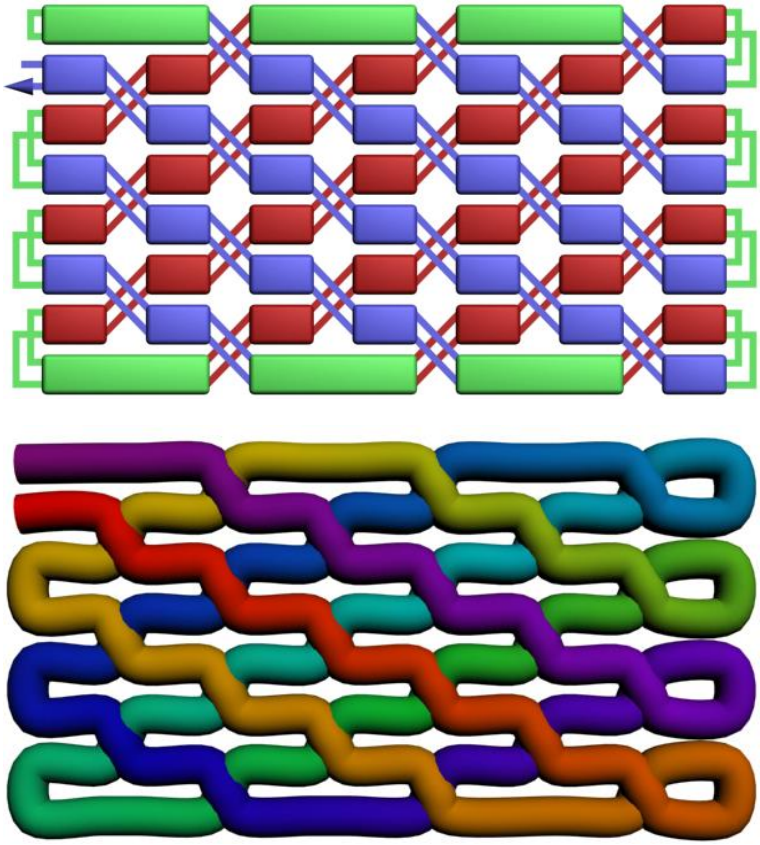

Figure S5-6. Cartoon (top) and pipeline style (bottom) model of a rectangle-shape ssOrigami design. The long green rectangles in the cartoon model represent 26bps helical domains. The pipeline style model is colored with rainbow gradient starting from the 5' and 3' ends (red) to the middle of the strand (purple).

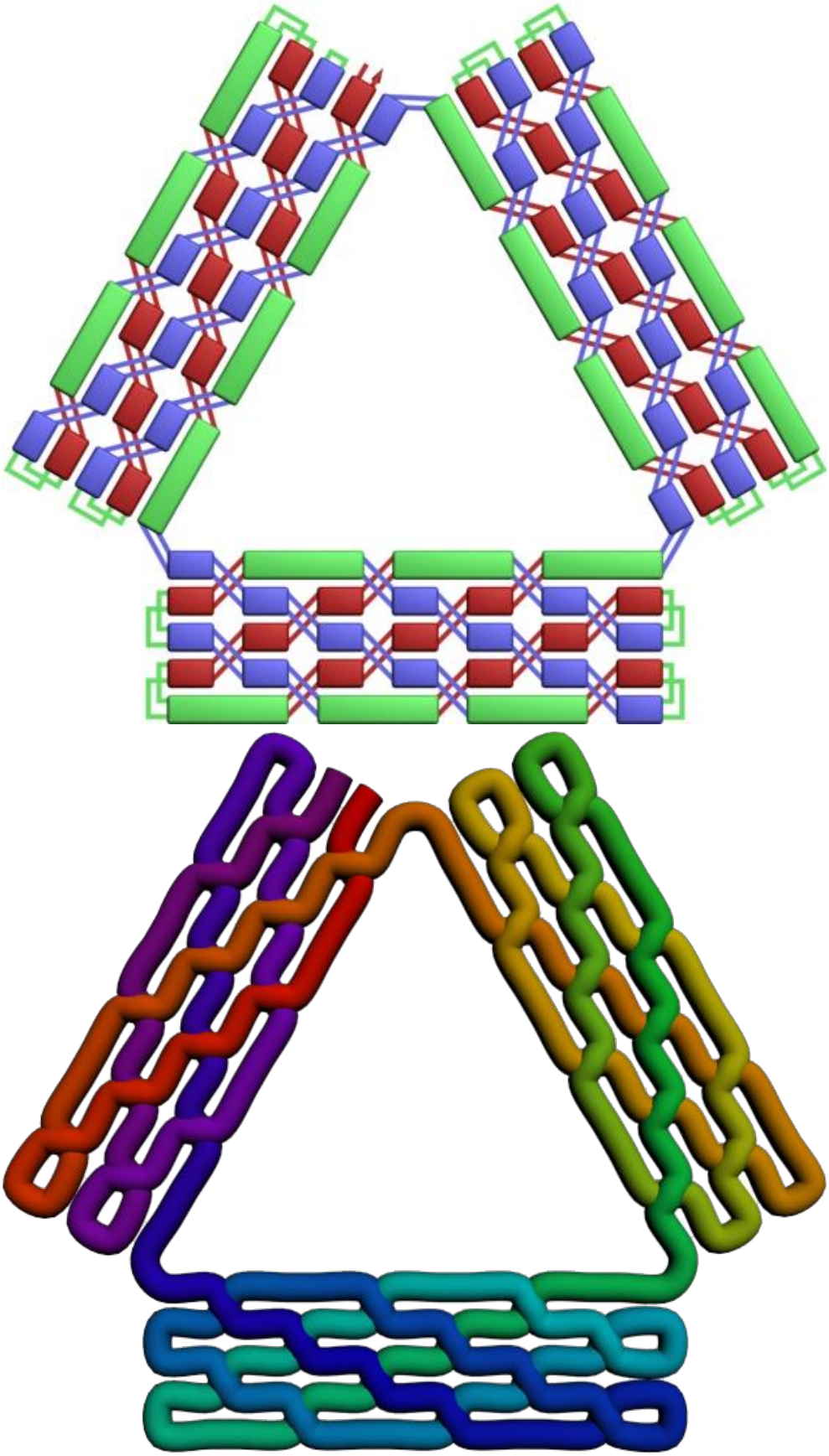

Figure S5-7. Cartoon (top) and pipeline style (bottom) model of a triangle-shape ssOrigami design. The long green rectangles in the cartoon model represent 26bps helical domains. The pipeline style model is colored with rainbow gradient starting from the 5' and 3' ends (red) to the middle of the strand (purple).

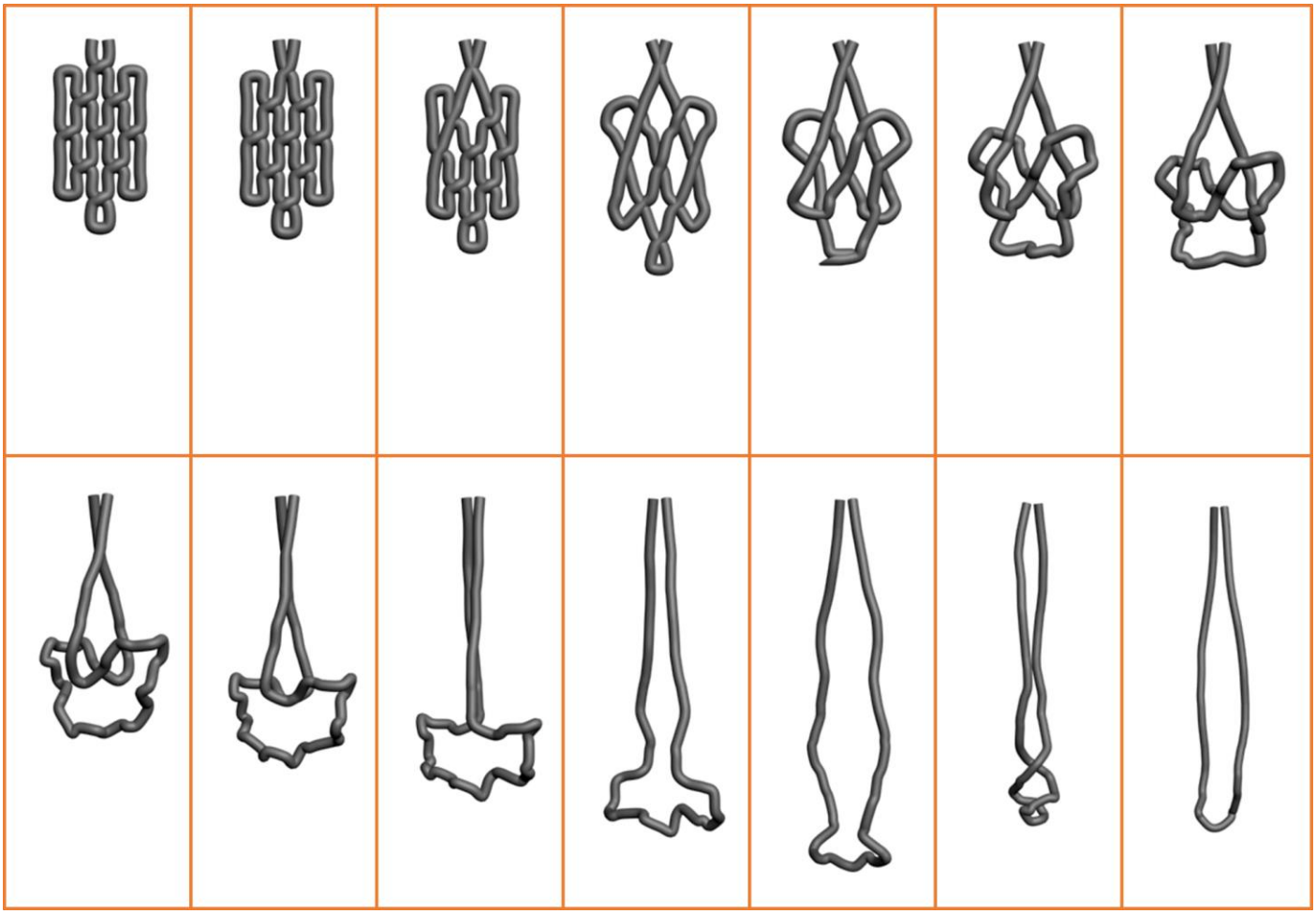

Figure S5-8. Selected screenshots of dynamic relaxation to demonstrate the knot relaxation process of our 3 × 3 ssOrigami model. Relaxation movies are available in the supplementary information package [Movie-10].

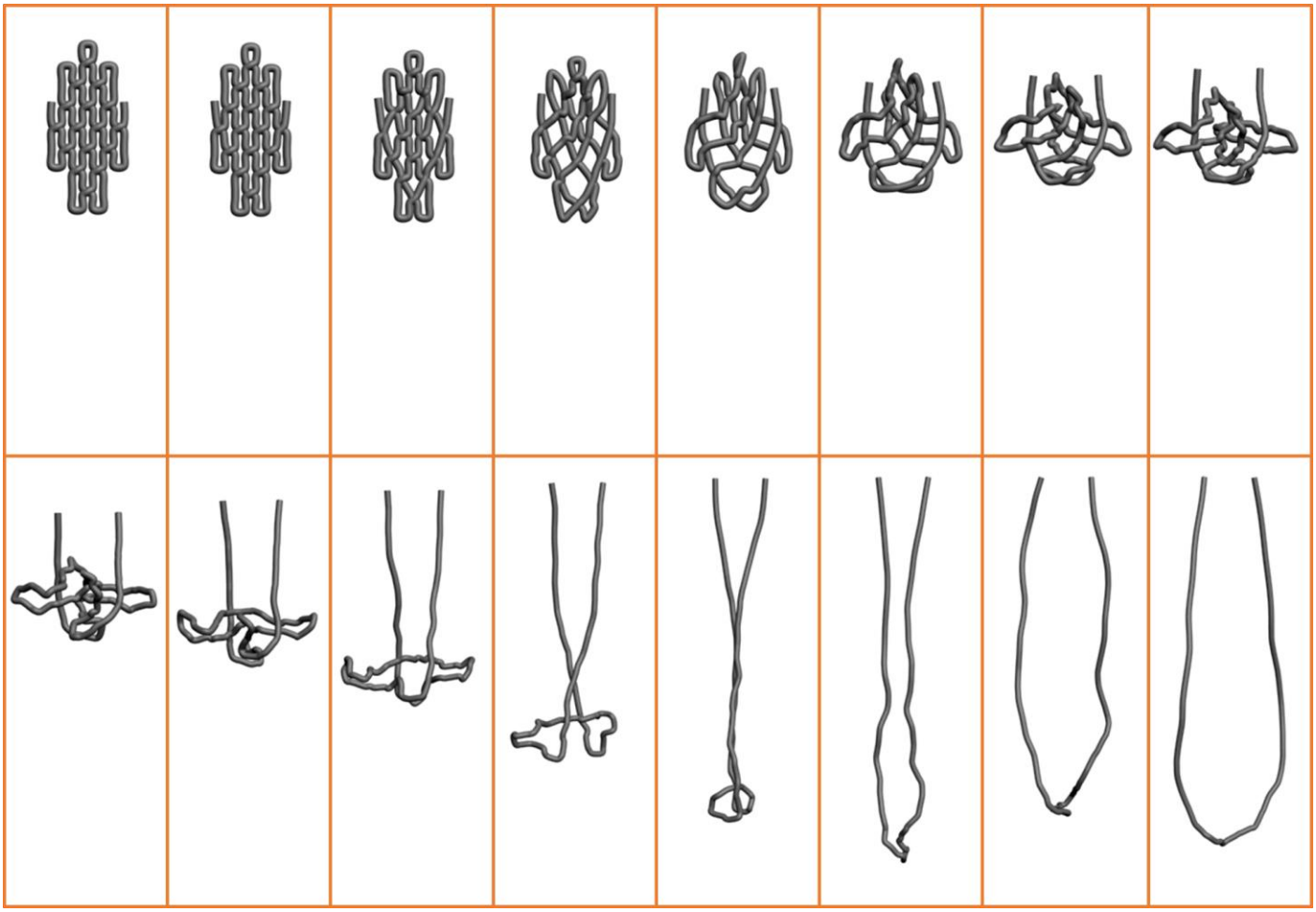

Figure S5-9. Selected screenshots of dynamic relaxation to demonstrate the knot relaxation process of our 4 × 4 ssOrigami model. Relaxation movies are available in the supplementary information package [Movie-11].

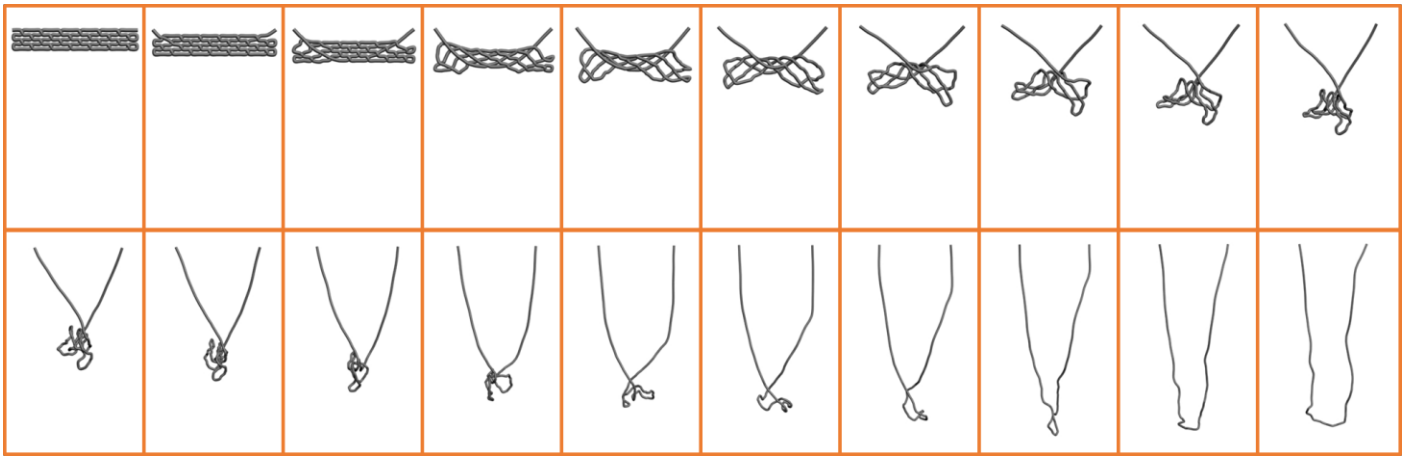

Figure S5-10. Selected screenshots of dynamic relaxation to demonstrate the knot relaxation process of our strip-shape ssOrigami model. Relaxation movies are available in the supplementary information package [Movie-13].

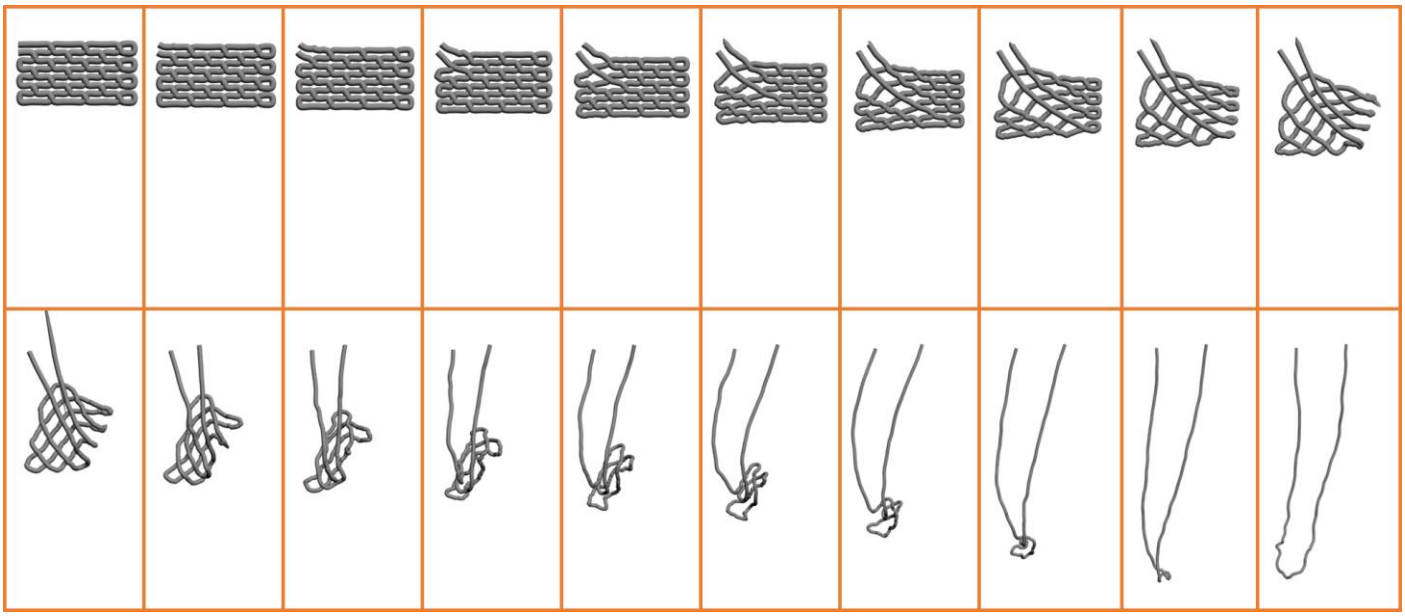

Figure S5-11. Selected screenshots of dynamic relaxation to demonstrate the knot relaxation process of our rectangle-shape ssOrigami model. Relaxation movies are available in the supplementary information package [Movie-14].

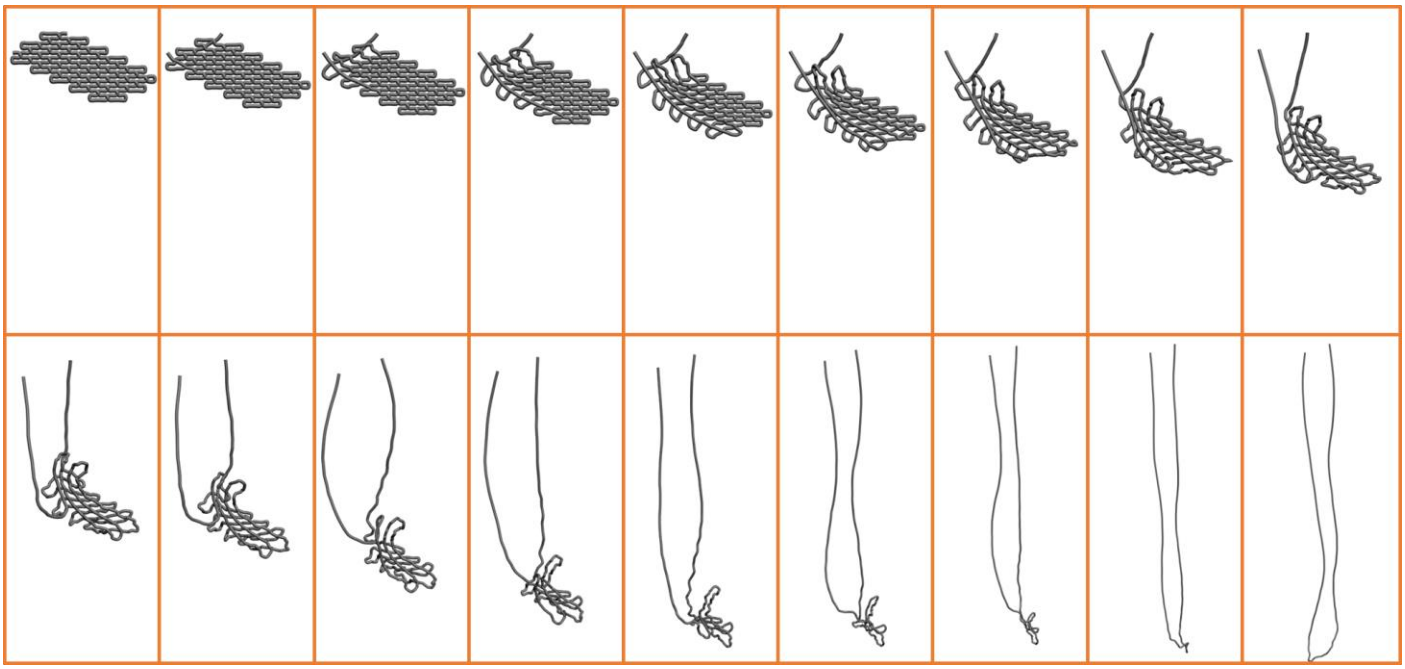

Figure S5-12. Selected screenshots of dynamic relaxation to demonstrate the knot relaxation process of our rhomboid-shape ssOrigami model. Relaxation movies are available in the supplementary information package [Movie-16].

Supplementary section 6: *In vitro* synthesis and replication of ssDNA for ssOrigami structures.

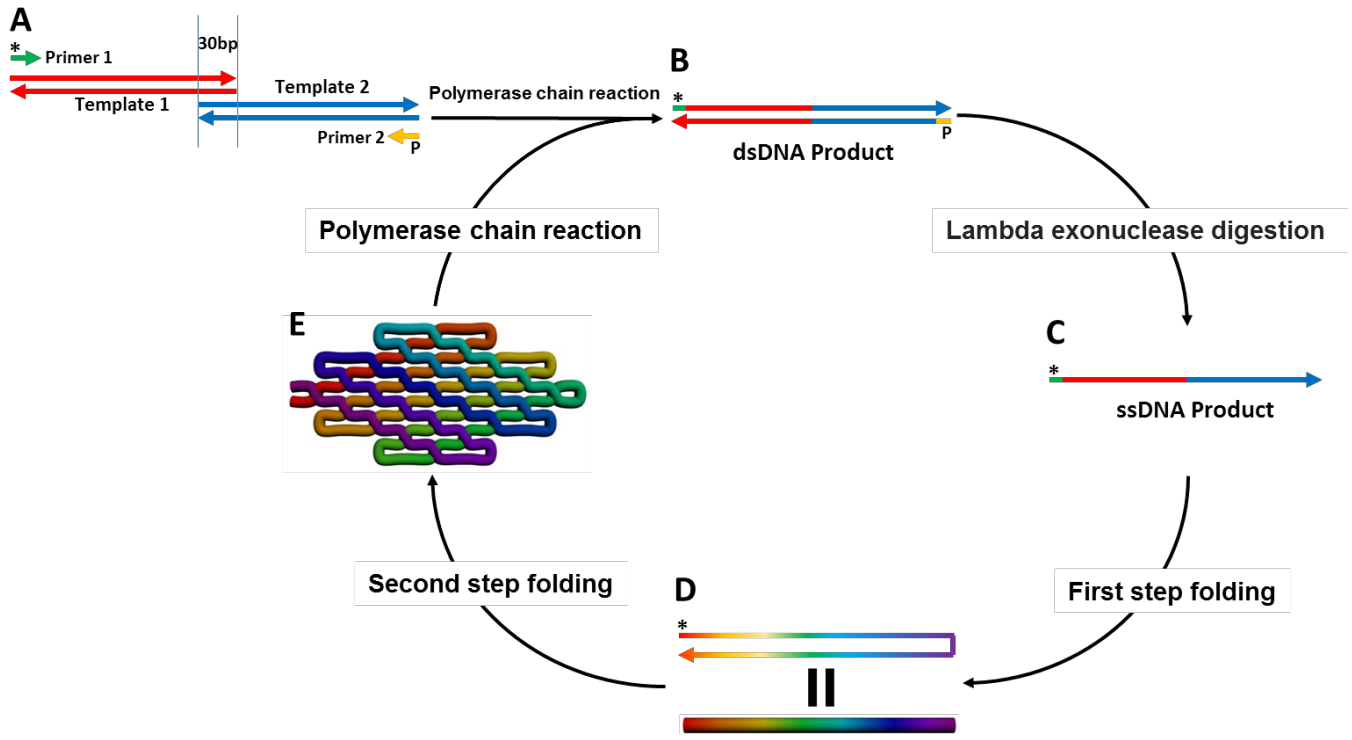

Figure S6-1. Synthesis and replication of ssDNA and folding of ssOrigami.

Double-stranded gBlocks (Fig. S6-1A) were purchased from Integrated DNA Technologies Inc.. Sequence of primer 1 was T*T*T*T*T*T*TACGGCACGTAAGCCTTGCATTGACTAGCC and sequence of primer 2 was /5Phos/GATTCGCGAAGATGAATCGCGATGCCGGAT. In primer 1, T* stands for phosphorothioate bond modification. In primer 2, /5Phos/ stands for 5' phosphorylation. Shown in Fig. S6-1B, dsDNA was synthesized by multi-template PCR. ssDNA was obtained after Lambda exonuclease treatment (Fig. S6-1C) and then purified by 2% agrose gel electrophoresis (if purified). Purified ssDNA was used for the fast 2-hour annealing to fold into the target shape (for larger structures such as the triangle and the rhomboid, slow annealing was applied). Note that the putative, partially paired double-stranded intermediate shown in Fig. S6-1D is for illustration purposes only. The ssOrigami product can be used as a template for its replication in the next cycle (Fig. S6-1E).

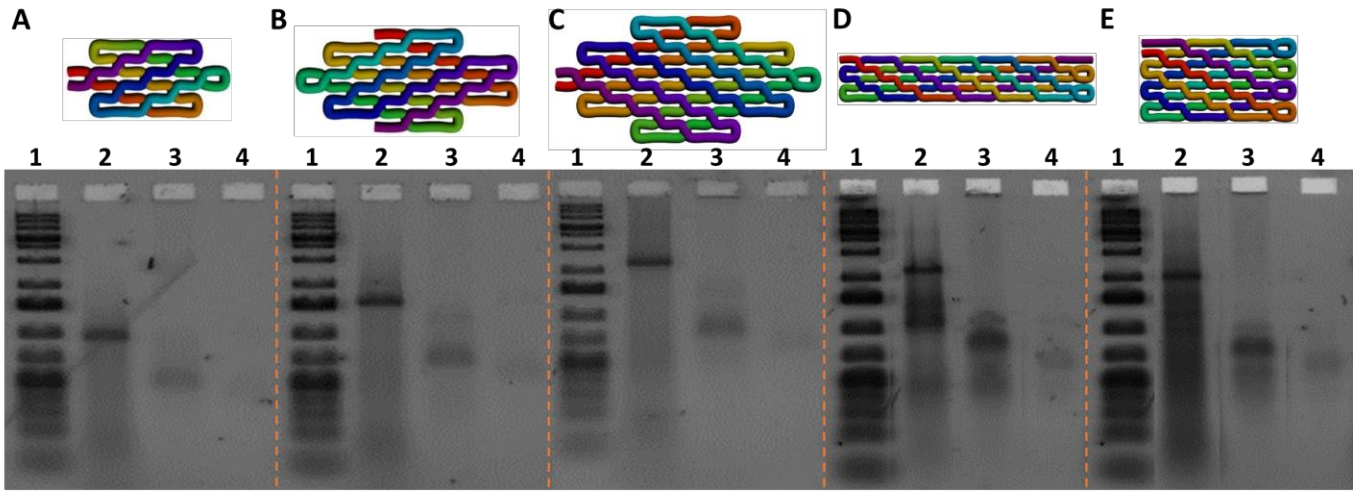

Figure S6-2. Agarose gel images of example ssOrigami products. Lane 1: 1 Kb ladder; lane 2: PCR product; lane 3: exonuclease treated product; lane 4: annealed products. In some cases, the concentration of folded DNA is too low to

be visualized on a gel.

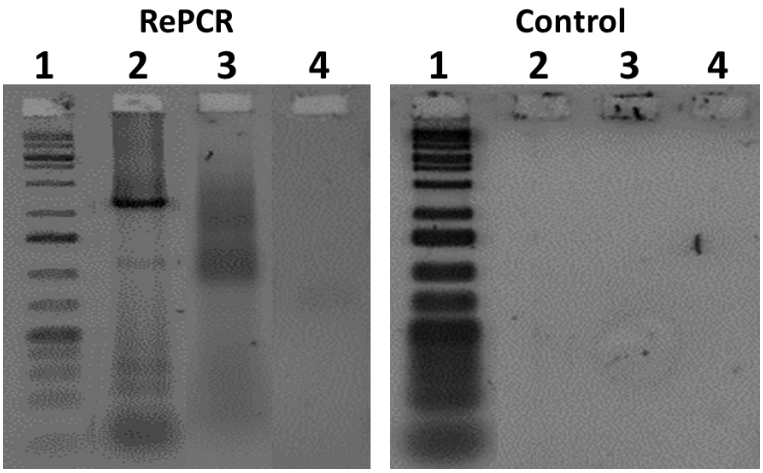

Figure S6-3. Agarose gel images of 2.3k 5×5 ssOrigami rePCR products and the control experiment. Left: Standard rePCR Products. Lane 1: 1 Kb ladder; lane 2: PCR product; lane 3: exonuclease treated product; lane 4: annealed products. Right: rePCR control experiment with no polymerase added. Lane 1: 1 Kb ladder; lane 2: PCR product; lane 3: exonuclease treated product; lane 4: annealed product.

Supplementary section 7: *In vivo* synthesis and replication of ssDNA for ssOrigami folding.

In our *in vivo* experiment, the ssDNA origami was divided into two DNA sequences with restriction sites designed on both sides and ordered from IDT as gBlocks fragments. For example, in the case of 2.3k 2.3k 5×5 structure, the first fragment had EcoRI and XhoI sites, whereas the second fragment had XhoI and HindIII sites (Fig. S7-1A). The Nb.BbvCI site was designed next to EcoRI site on the first fragment for the purpose of nick generation in the final step. The two gBolcks fragments (blunt-ended) were individually ligated with pMiniT vector (Blunt end vector from NEB PCR cloning kit) following the manufacturer's instruction (Fig. S7-1B). The ligation products were transformed into E. coli NEB-10 β competent cells (included in the PCR cloning kit). E. coli colonies were formed after overnight growth and single colonies were picked up for overnight growth in LB medium (Fig. S7-1C and D). Plasmid minipreps were performed from overnight E. coli cultures. The plasmids with inserts were sent for DNA sequencing to screen for error-free clones. The mutation-free plasmids were digested by restriction enzymes accordingly (EcoRI and XhoI for fragment 1 plasmid, and XhoI and HindIII for fragment 2 plasmid) (Fig. S7-1E).

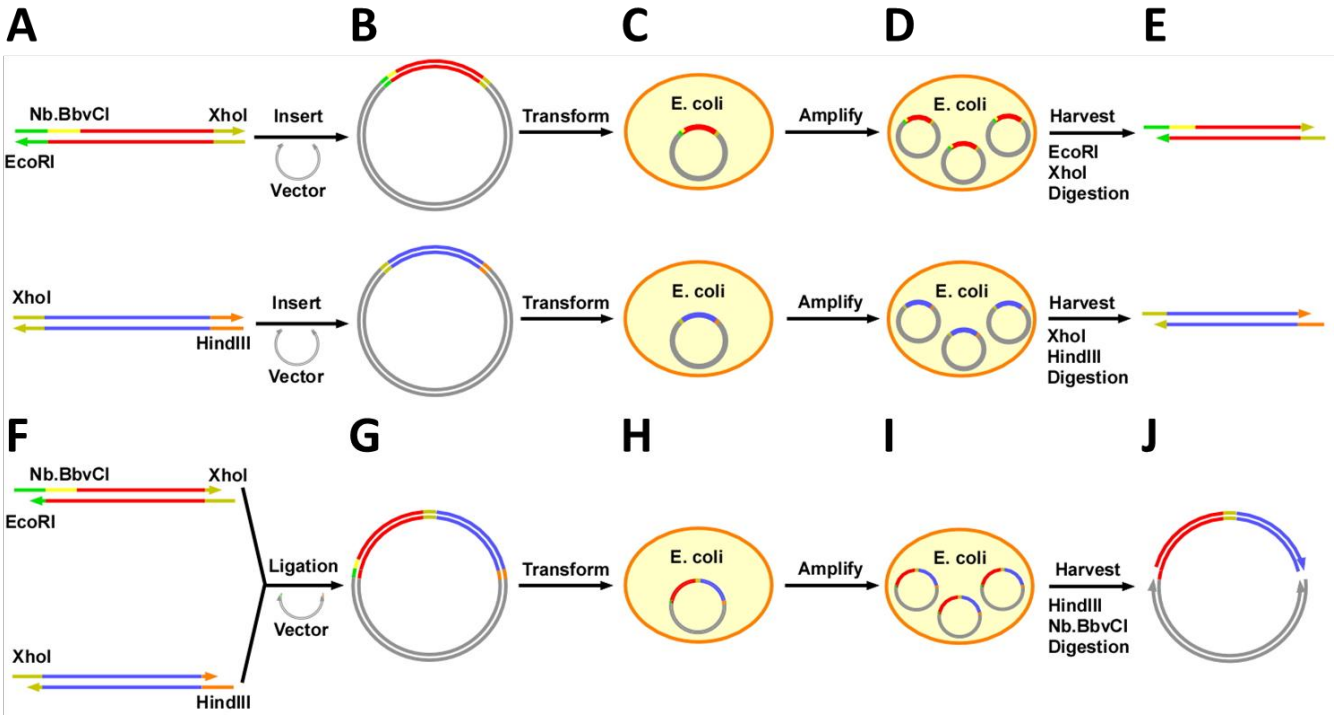

Figure S7-1. *In vivo* replication processes of ssDNA for ssOrigami folding.

In the next step shown in Fig. S7-1F and G, the digested two fragments were ligated with EcoRI and HindIII digested pGEM-7zf(-) vector, and transformed into E. coli cells (NEB stable competent cells). This was a three-fragment ligation to form a circular DNA. The Vector EcoRI sticky end was ligated with fragment 1 EcoRI sticky end; fragment 1 XhoI sticky end was ligated with fragment 2 XhoI sticky end; and the fragment 2 HindIII sticky end was ligated with the vector's HindIII sticky end. After the same cloning steps (Fig. S7-1H-J), single colonies were picked the next day and plasmids were purified.

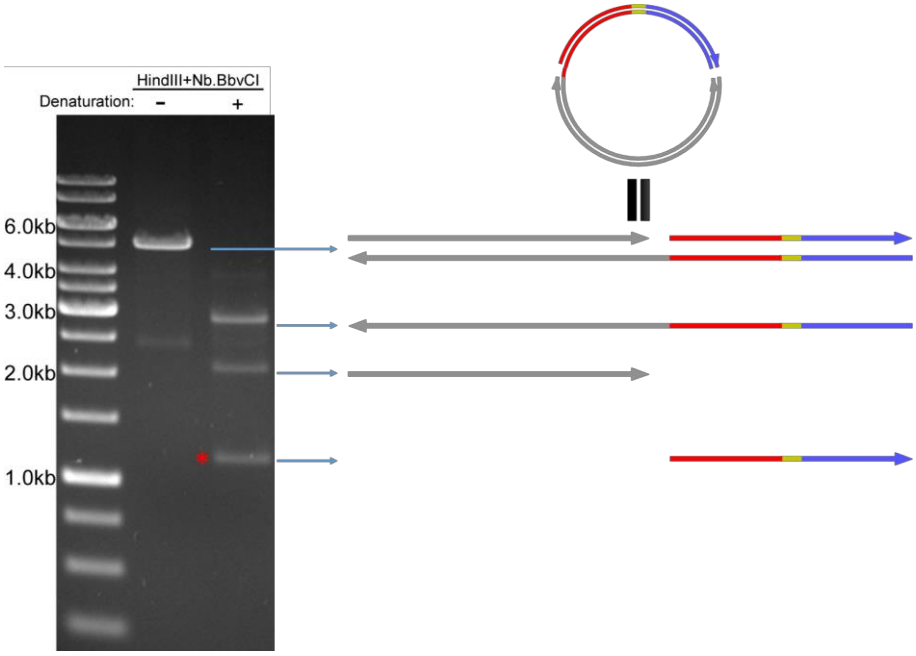

Figure S7-2. Denaturing agarose gel separation of target ssDNA from other byproducts. Left lane: DNA was mostly double-stranded when no heating denaturation was performed. Right lane: ssDNA was separated from heating-denaturized samples.

HindIII and Nb.BbvCI double digestion were then carried out. The digested products were heated at 90℃ for 10 minutes in denaturing buffer (10mM Tris-HCl, pH 8.0, 1mM EDTA and 8M urea) and loaded onto a 1% urea denaturing agarose gel (in 1× TAE with 1M urea) shown in Fig. S-7-2 with an unheated sample as a control. After extraction, the ssDNA was annealed using slow or fast annealing programs and imaged with AFM. The AFM images are shown in Supplementary Section 11.

We tested three different designs with *in vivo* cloning strategy. The ssDNA products were characterized with agarose gel (in 1× TAE) as shown in Fig. S7-3. These ssDNA products were annealed and subjected to AFM imaging without further purification.

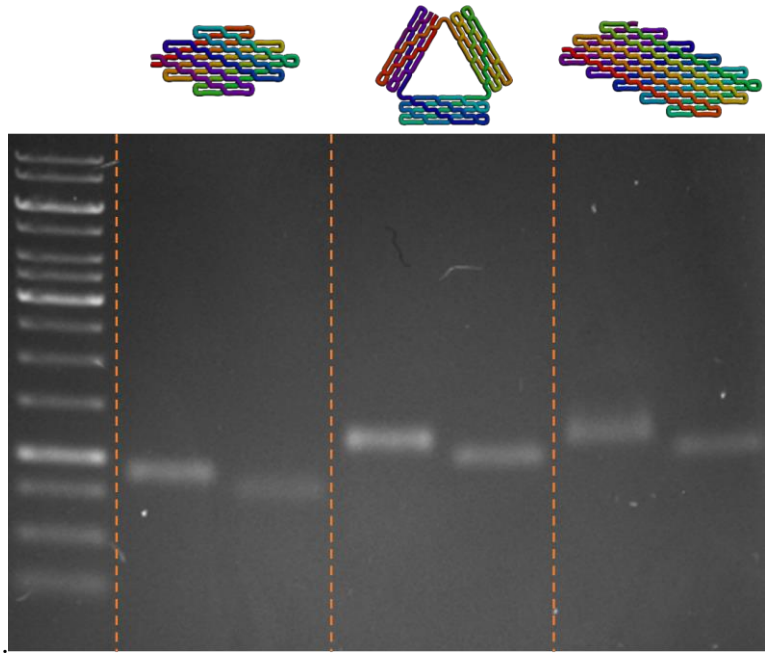

Figure S7-3. Native agarose gel characterization of cloned ssDNA product. For each sample, left lane contains ssDNA before annealing, and right lane contains ssOrigami after annealing.

The yield of ssOrigami structures was estimated using native agarose gel electrophoresis. The measurement of gel yield was based on the fluorescence intensity of the target band and the entire lane. Software ImageJ was used for the intensity measurement. The total intensity of a certain area was the integration of intensity per pixel over all pixels in that area and expressed with its average intensity. When the intensity of a target area was calculated, the background intensity was subtracted from the measured intensity for correction.

In Fig. S7-4A, intensity of the area inside the yellow rectangle refers to the intensity of the entire lane; in Fig. S7-4B, the rectangle contained the target band; in Fig. S7-4C, background intensity was measured in the rectangular area. The yield of each structure was calculated as the ratio between target band intensity and entire lane intensity:

$$\text{Yield} = \frac{\text{Intensity}_{\text{Target band}}}{\text{Intensity}_{\text{Entire lane}}}$$

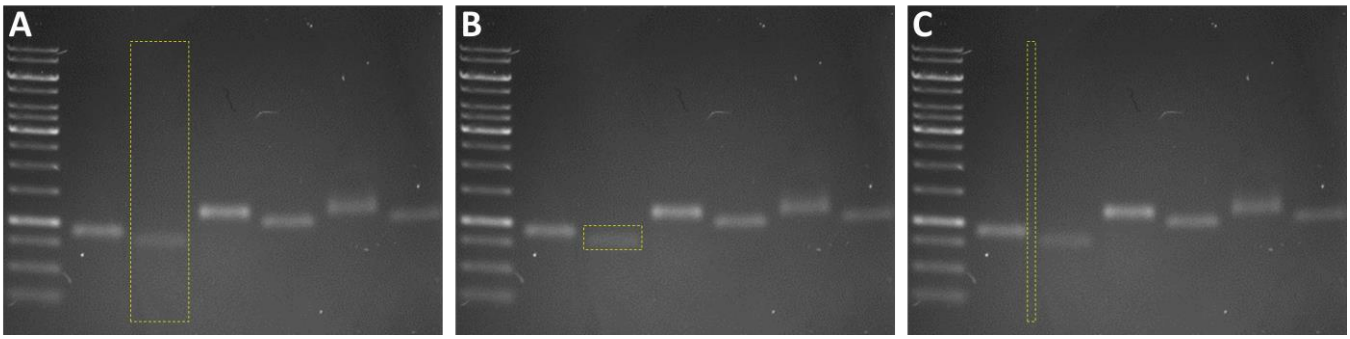

Figure S7-4. Example of yield quantification for ssOrigami structures. The yellow rectangle contains the area for entire lane (**A**), target band (**B**) and background (**C**).

Based on this yield calculation method, we measured the yield of the *in vivo* cloned ssOrigami structures. The 5×5 ssOrigami had an estimated yield of 95%, the triangle ssOrigami had an estimated yield of 93%, and the 5×10 ssOrigami had an estimated yield of 90%.

In comparison, the counting yield from AFM images (pixels in well-formed structures vs all pixels) of the abovementioned structures are 97% for 5×5 ssOrigami design, 74% for triangle ssOrigami design, and 86% for the 5×10 ssOrigami design (raw data not shown here). Note as native gel electrophoresis cannot separate DNA Origami structures (including ssOrigami structures) with minor defects, such yield estimation is expected to be higher than the real yield.

Supplementary section 8: Synthesis and replication of ssRNA for ssOrigami folding.

The DNA templates for transcribing ssRNAs were divided into two DNA sequences with both T7 and T3 promoter sequences added to the ends, and ordered as gene synthesis products from BioBasic Inc. The two fragments were then subcloned into pUC19 vector using the same restriction sites as ssDNA origami. The final plasmids were linearized by EcoRI and HindIII, and transcribed by T7 or T3 RNA polymerase following manufacturer's instruction (New England Biolabs). The transcription reaction mixture was purified by RNA Clean & Concentrator kit as described in the manufacturer's instruction (Zymo Research). After purification, the ssRNA was annealed using the same program as ssDNA origami, and characterized by AFM.

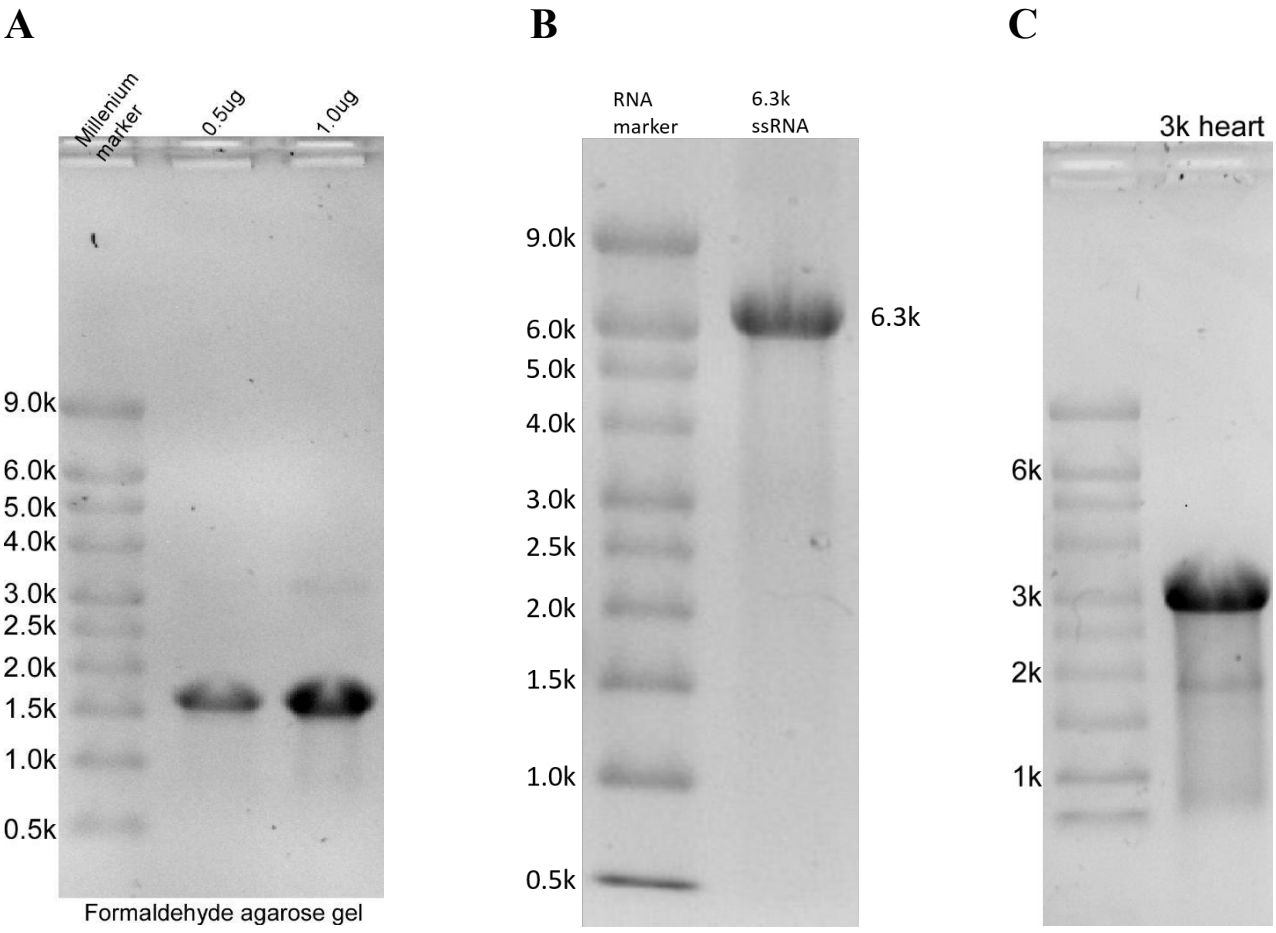

Figure S8 Rectangle ssRNA (A), 9x9 ssRNA (B) and 3k heart-shape ssRNA (C) denaturing agarose gel image. The in vitro transcribed RNA was purified and loaded onto the formaldehyde agarose gel.

Supplementary section 9: Melting study for DNA/RNA ssOrigami structures

DNA ssOrigami structures:

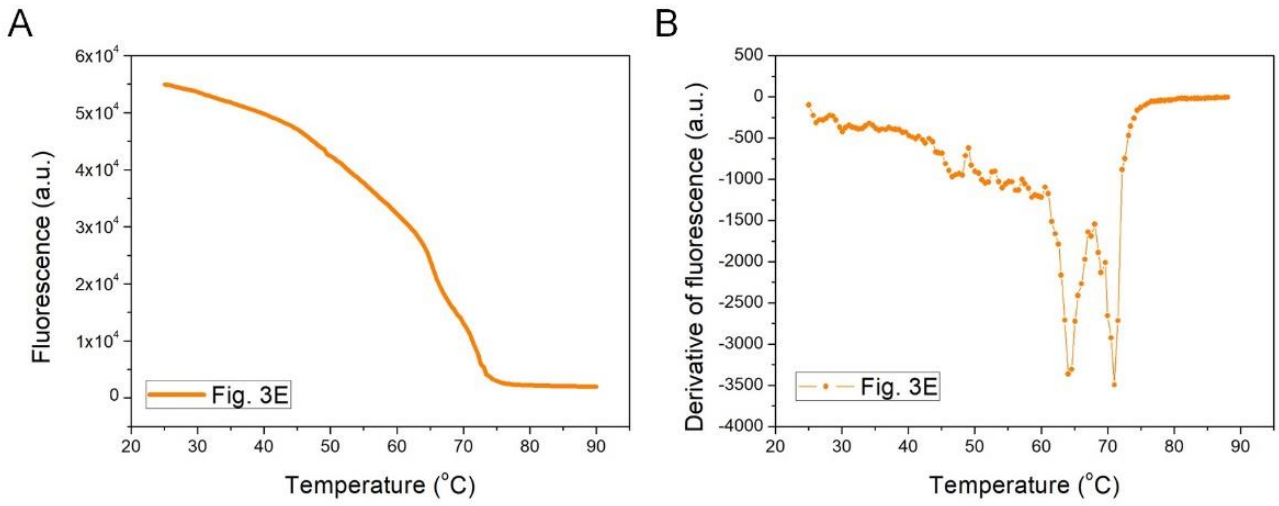

Figure S9-1 Melting analysis of the heart-shaped ssDNA origami in Fig. 3E. (A) The plot of raw data (SyBr Green intensity vs. temperature) of the melting curve. (B) The plot of the first derivative of SyBr Green intensity as a function of temperature.

We carried out the melting assay by staining the well-formed structures with 1× SyBr Green, and monitored the fluorescence intensity of SyBr Green as a function of temperature in 1× TAE/Mg^{2+} buffer. In Figure S9-1, we plotted the melting assay for three heart-shaped ssDNA origamis reported in Fig. 3E. The samples were heated from 25 °C to 90 °C at a rate of +0.05 °C/min.

RNA ssOrigami structures:

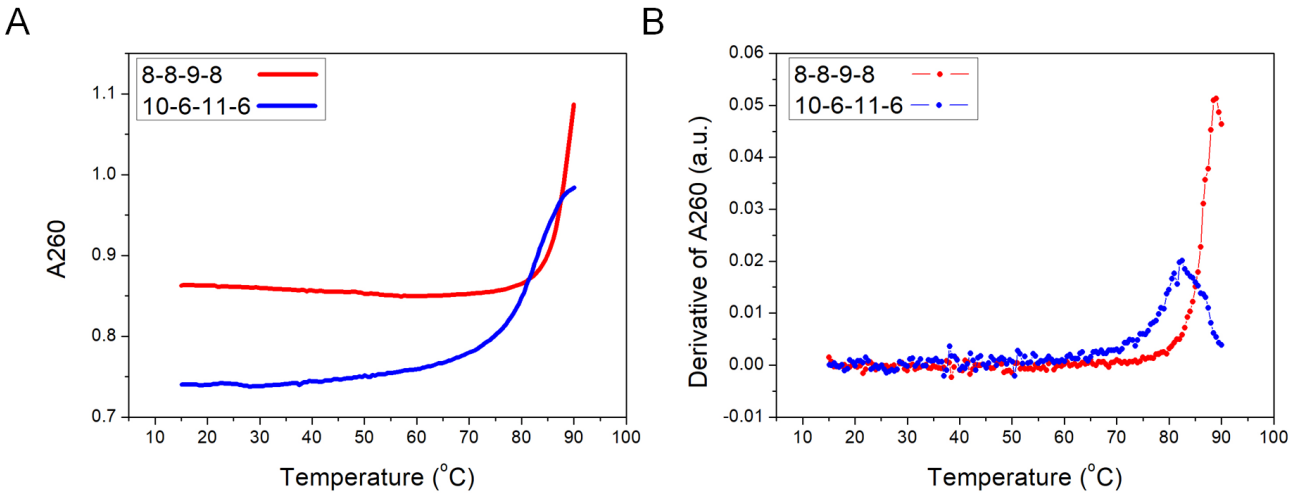

Figure S9-2 Melting analysis of the RNA ssOrigami structures from Fig. 5E (10-6-11-6) and 5G (8-8-9-8). (A) The plot of raw data (A260 *vs.* temperature) of heating and cooling curves in red and blue, respectively. (B) The plot of the first derivative of A260 as a function of temperature.

To compare the thermal stability of two different design strategies for the ssRNA origami, we carried out the melting assay by melting the well-formed origamis, and examined the absorbance changes at 260 nm as a function of temperature

in 1× TAE/Mg^{2+} buffer. The samples were heated from 15 °C to 90 °C at a rate of +0.05 °C/min. The results of the melting assay are plotted in Fig. S9-2.

Supplementary section 10: 5×5 ssOrigami designs assembled from multiple strands.

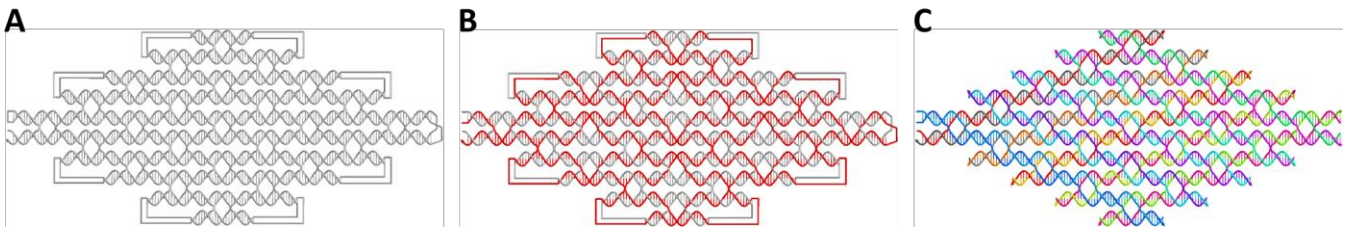

Figure S10-1. Models of 5 × 5 diamond-shape designs constructed from single-strand (**A**), two half strands (**B**) and twenty short strands (**C**).

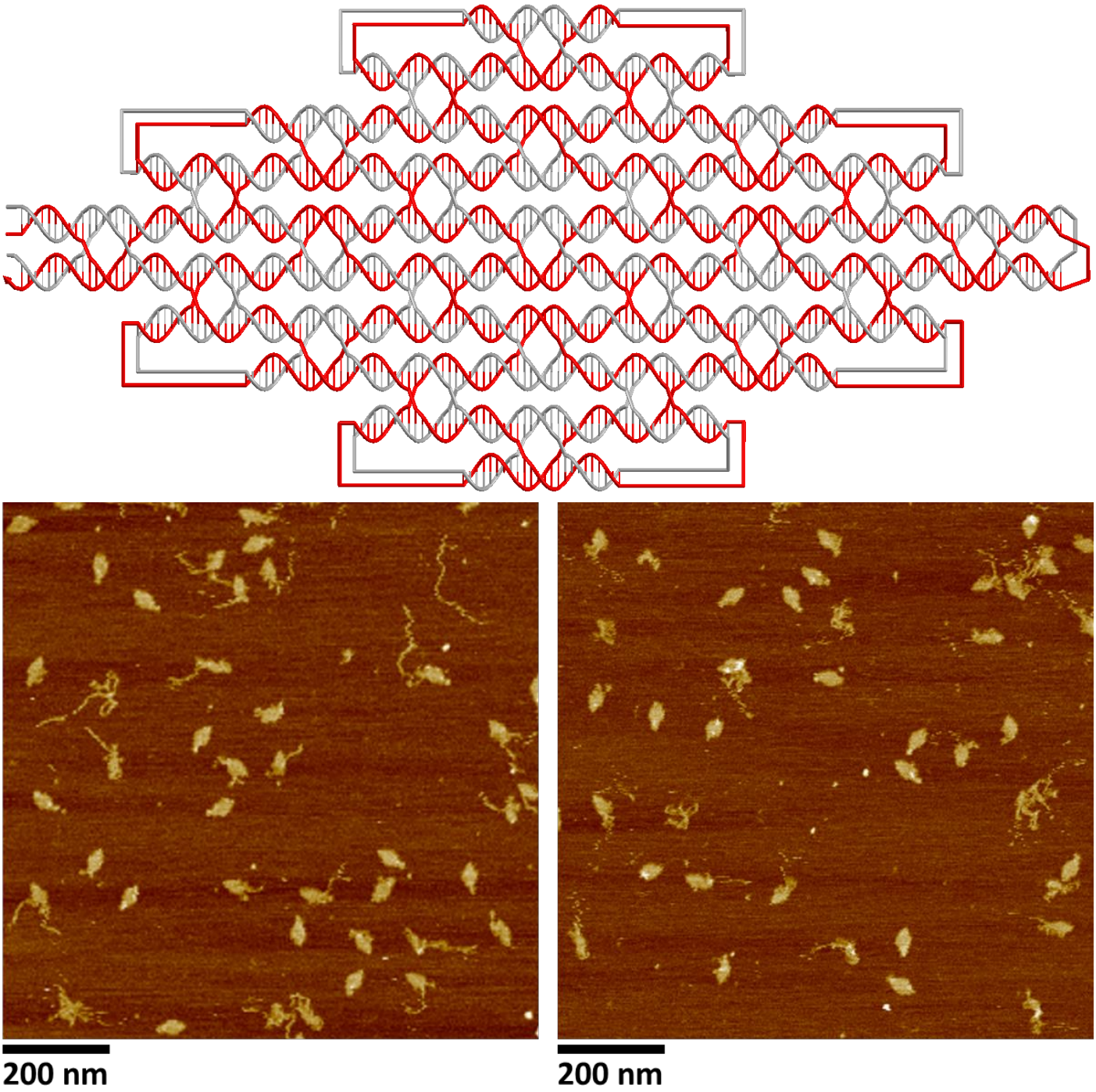

Figure S10-2. Model (top) and AFM images (bottom) for 5 × 5 diamond-shape ssOrigami structures self-assembled from two half strands (not connected).

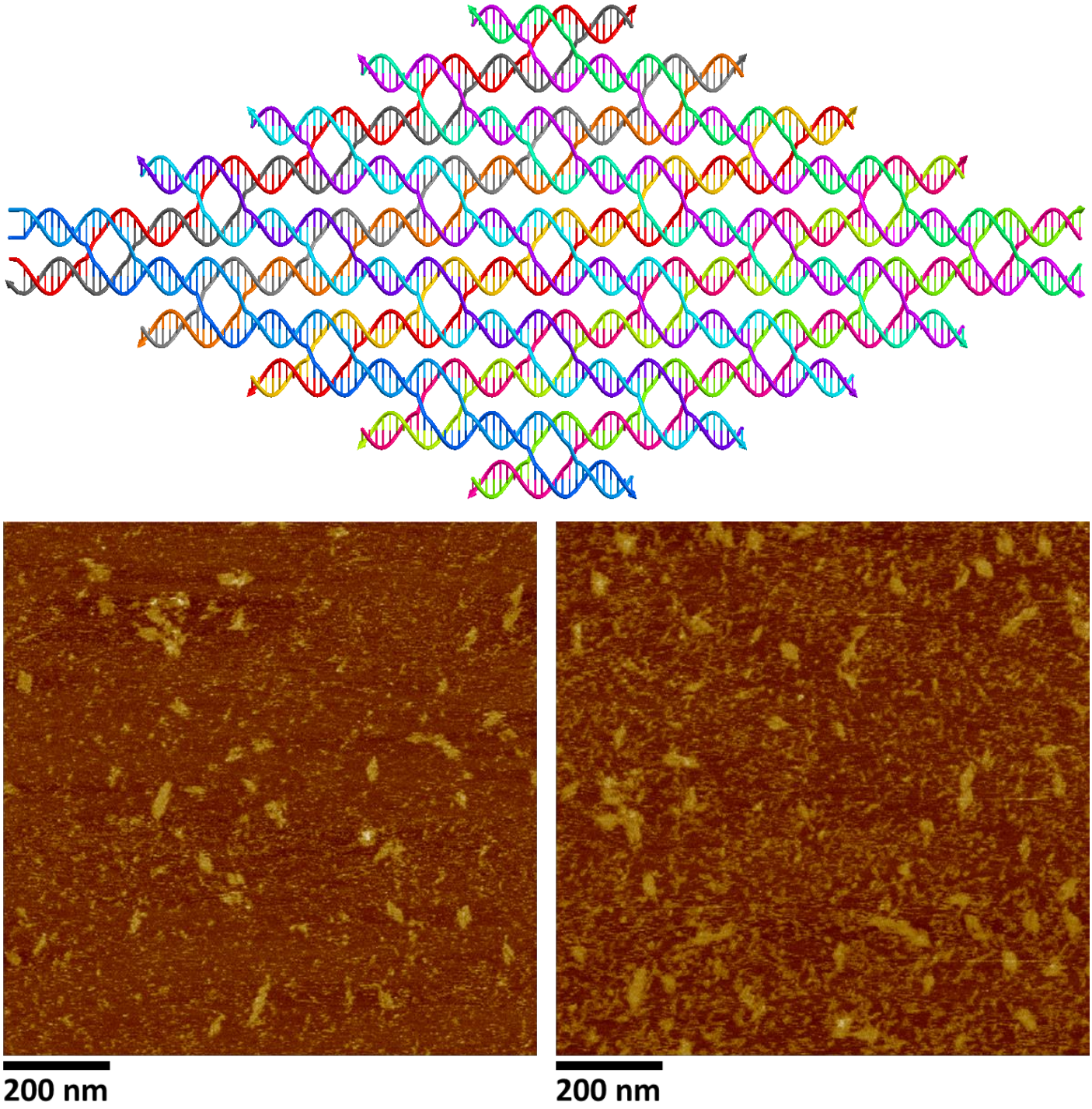

Figure S10-3. Model (top) and AFM images (bottom) for 5 × 5 diamond-shape DNA origami structures self-assembled from twenty DNA strands.

Supplementary section 11: Additional AFM images for ssOrigami structures.

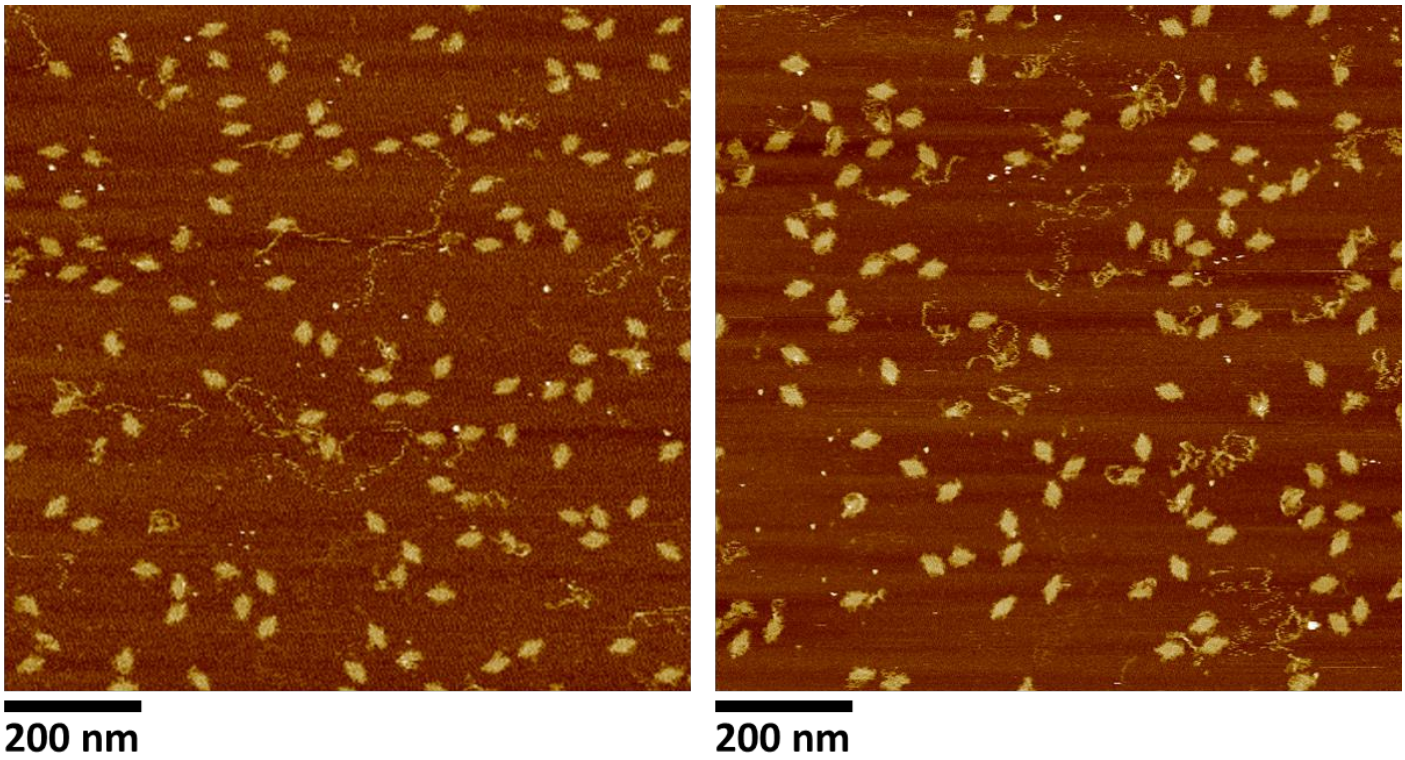

Figure S11-1. Additional AFM images for 4 × 4 diamond-shape ssOrigami structures.

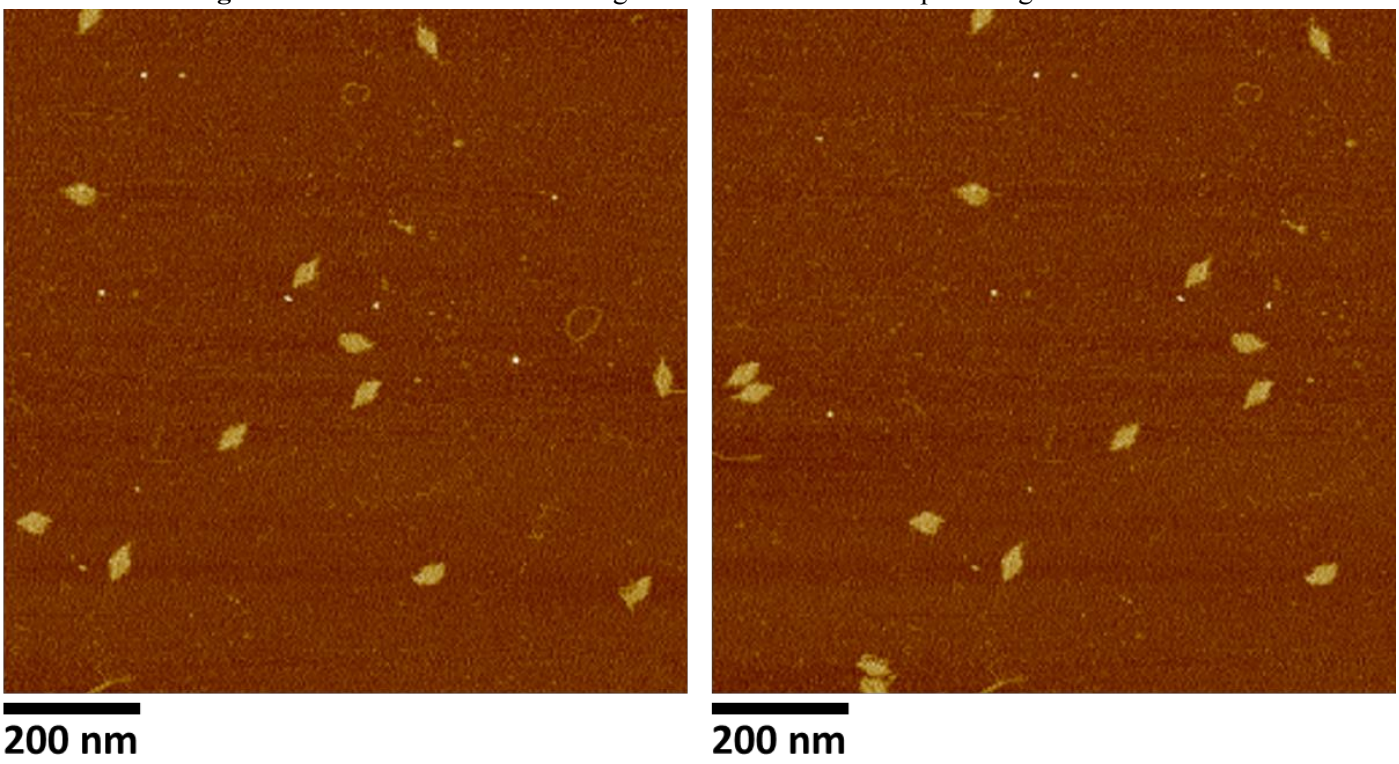

Figure S11-2. Additional AFM images for 5 × 5 diamond-shape ssOrigami structures.

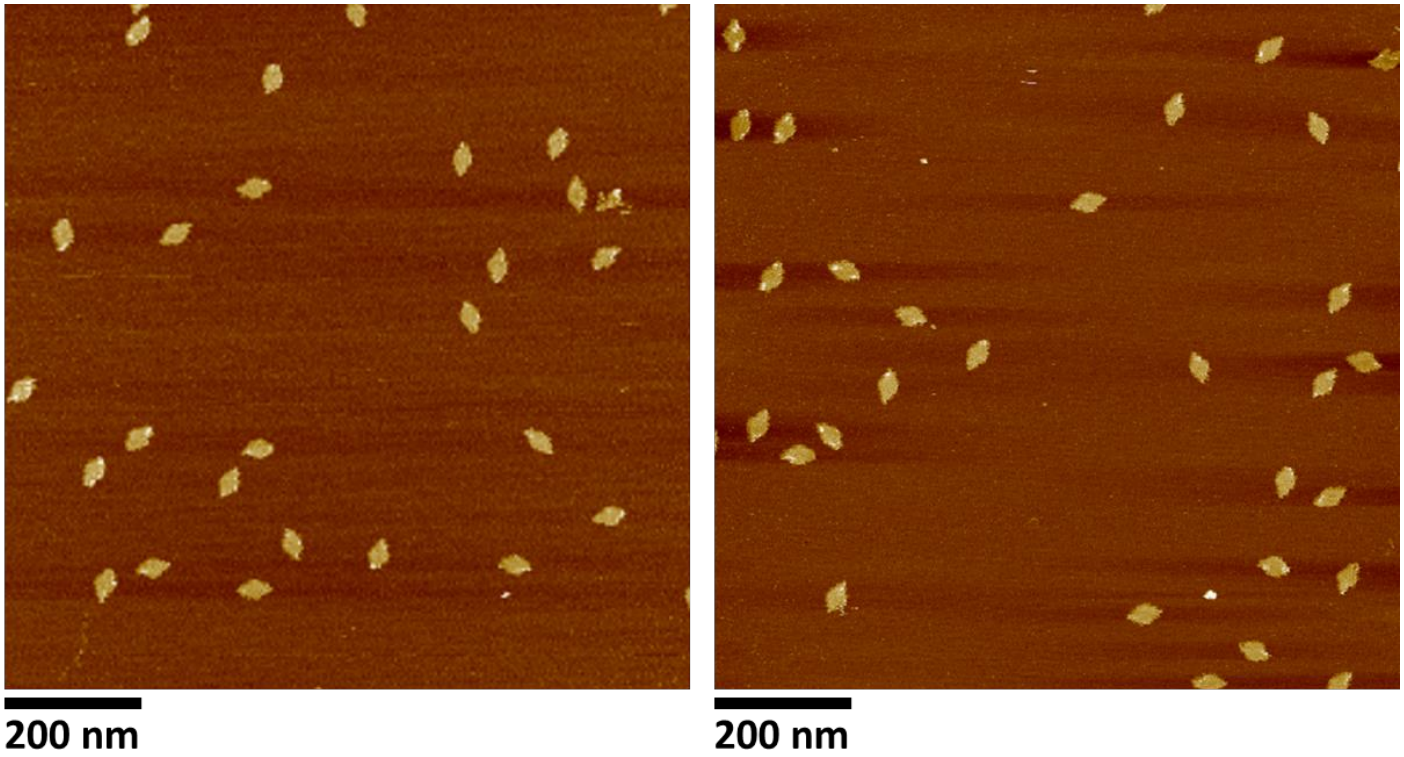

Figure S11-3. Additional AFM images for 5 × 5 diamond-shape ssOrigami structures (continue).

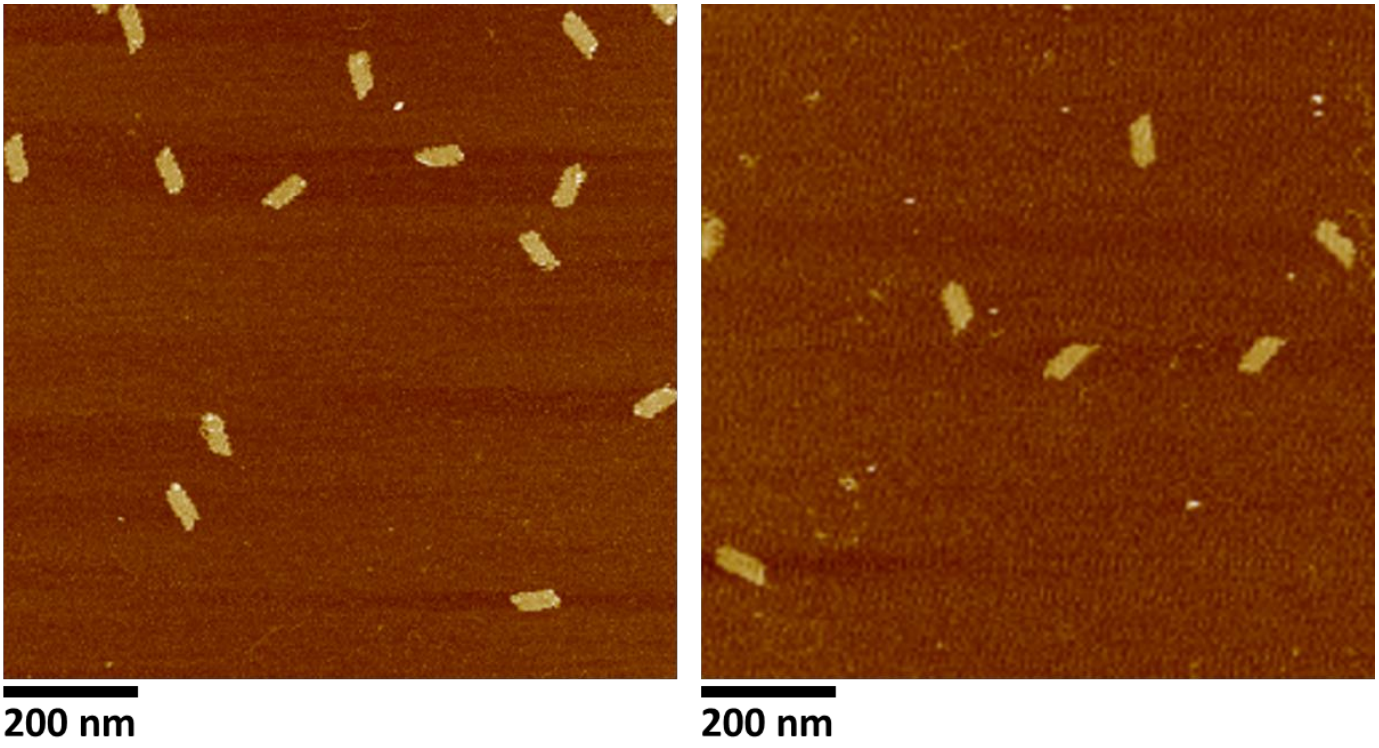

Figure S11-4. Additional AFM images for 5 × 10 rhomboid-shape ssOrigami structures

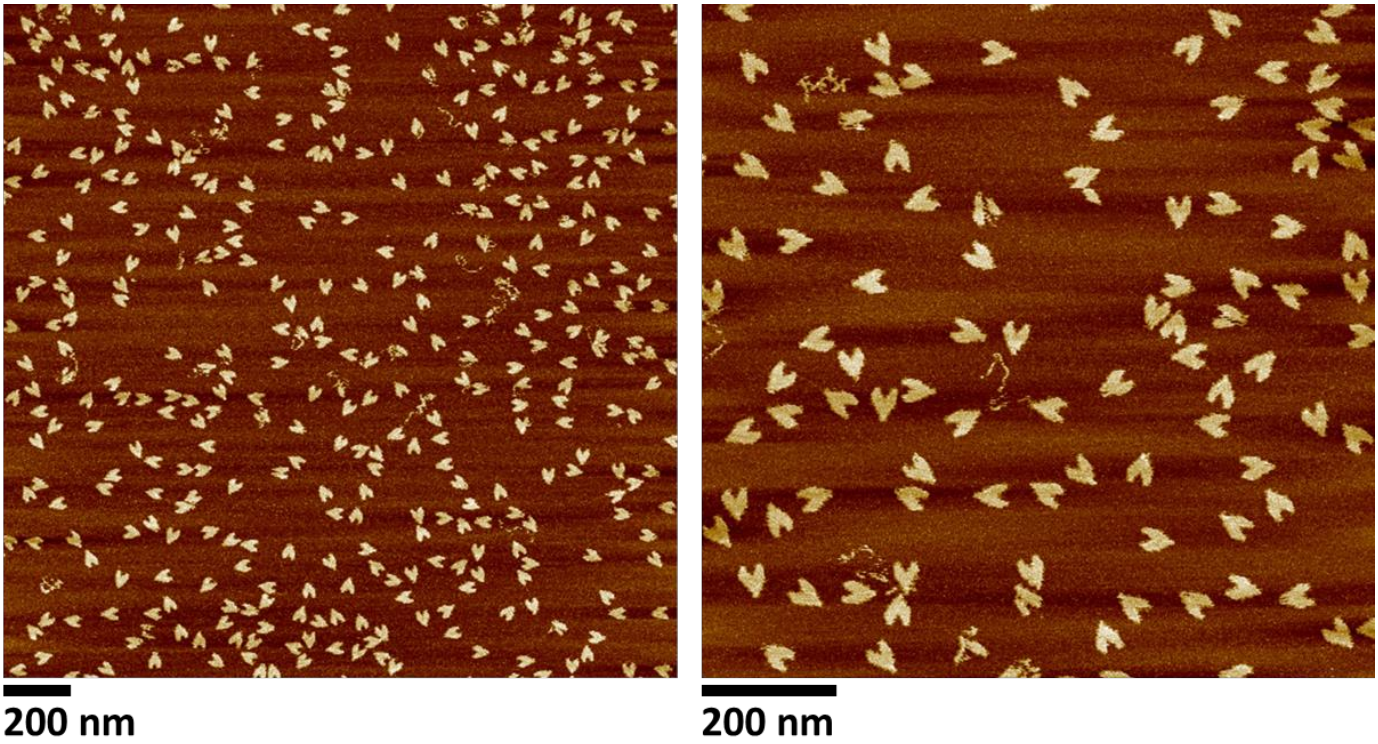

Figure S11-5. Additional AFM images for heart-shape ssOrigami structures

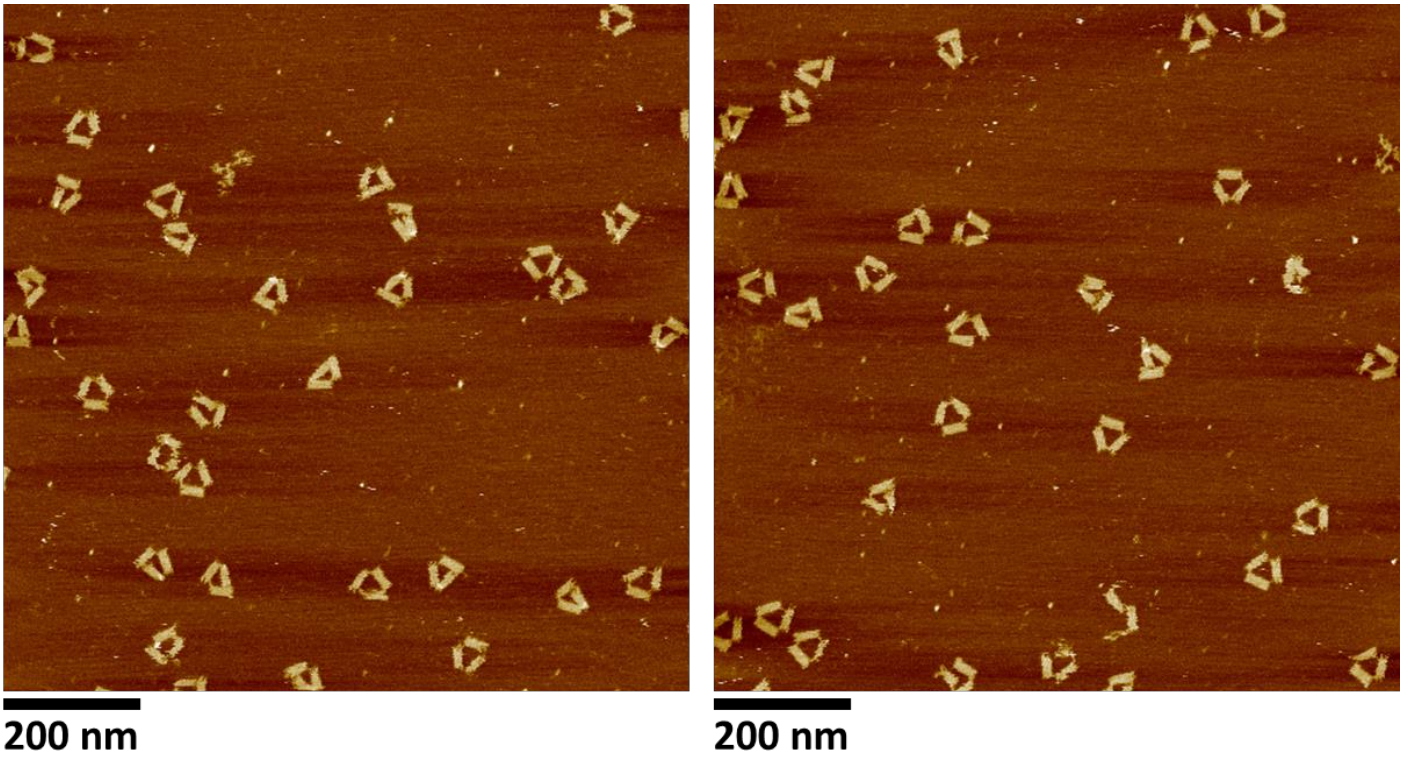

Figure S11-6. Additional AFM images for triangle-shape ssOrigami structures

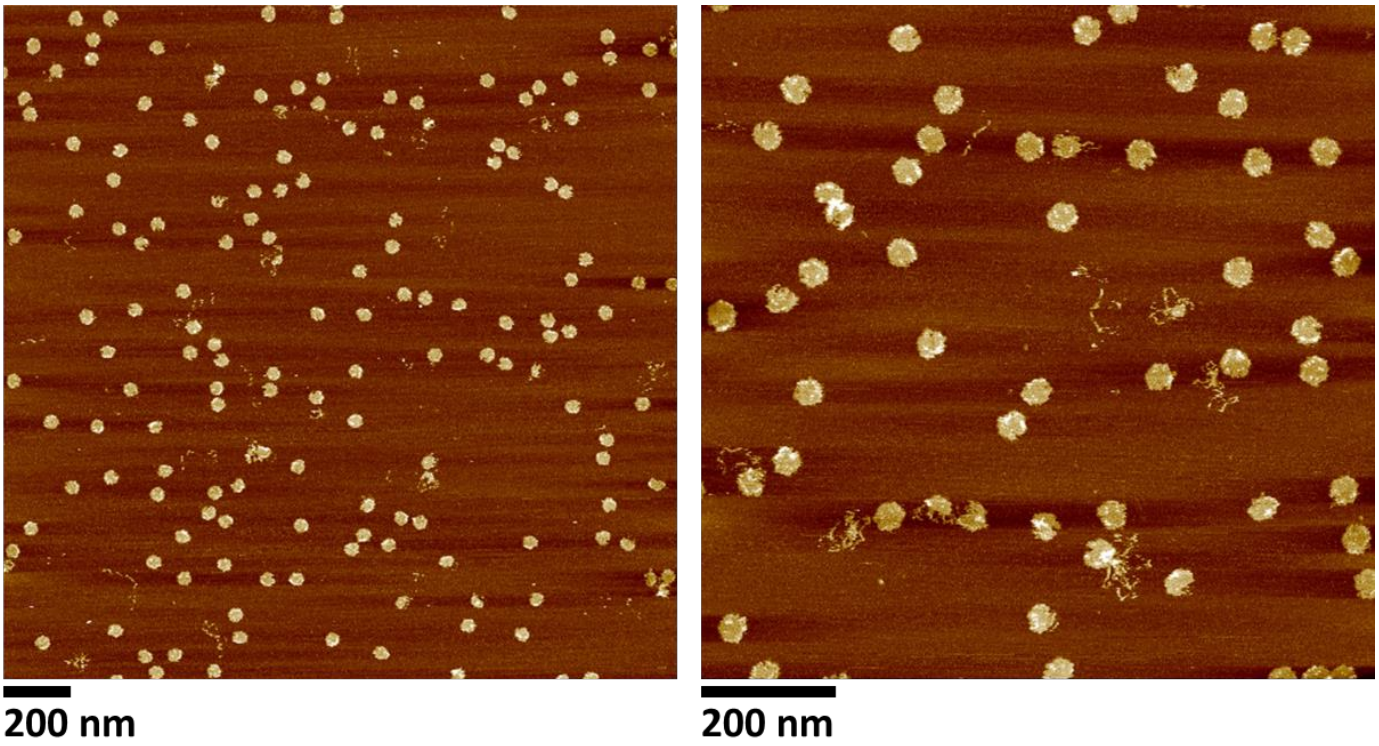

Figure S11-7. Additional AFM images for hexagon shape ssOrigami with patterned smile face

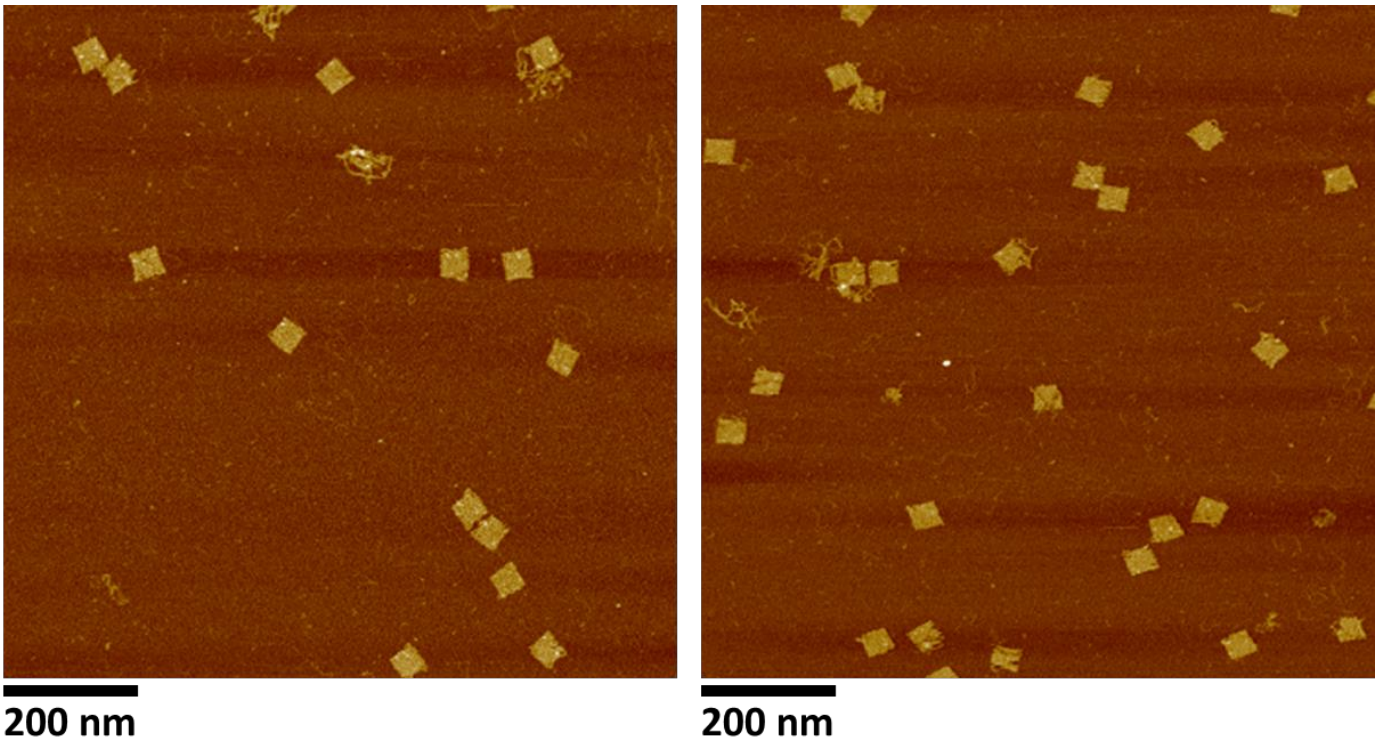

Figure S11-8. Additional AFM images for rectangle shape ssOrigami with single-stranded loops

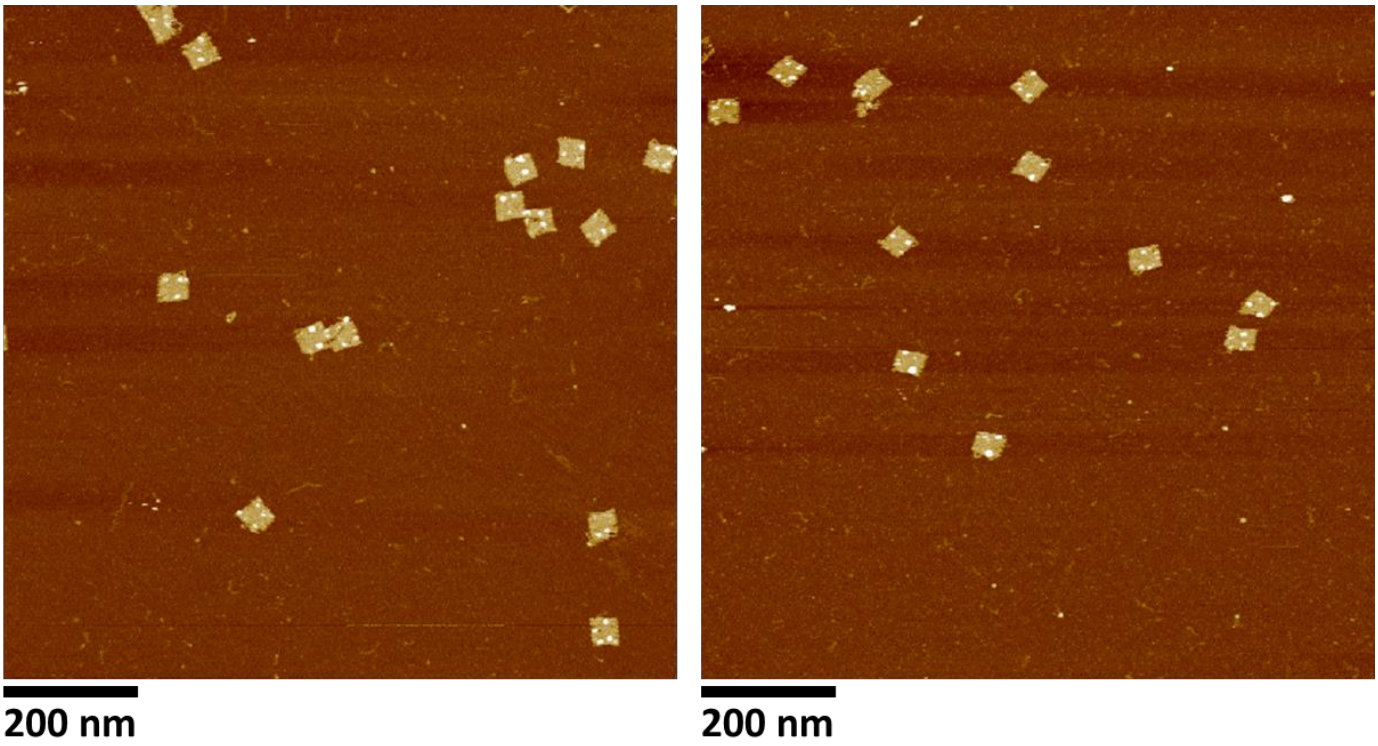

Figure S11-9. Additional AFM images for rectangle shape ssOrigami with single-stranded loops attached with biotin molecules

Supplementary section 12: Design details of ssOrigami structures.

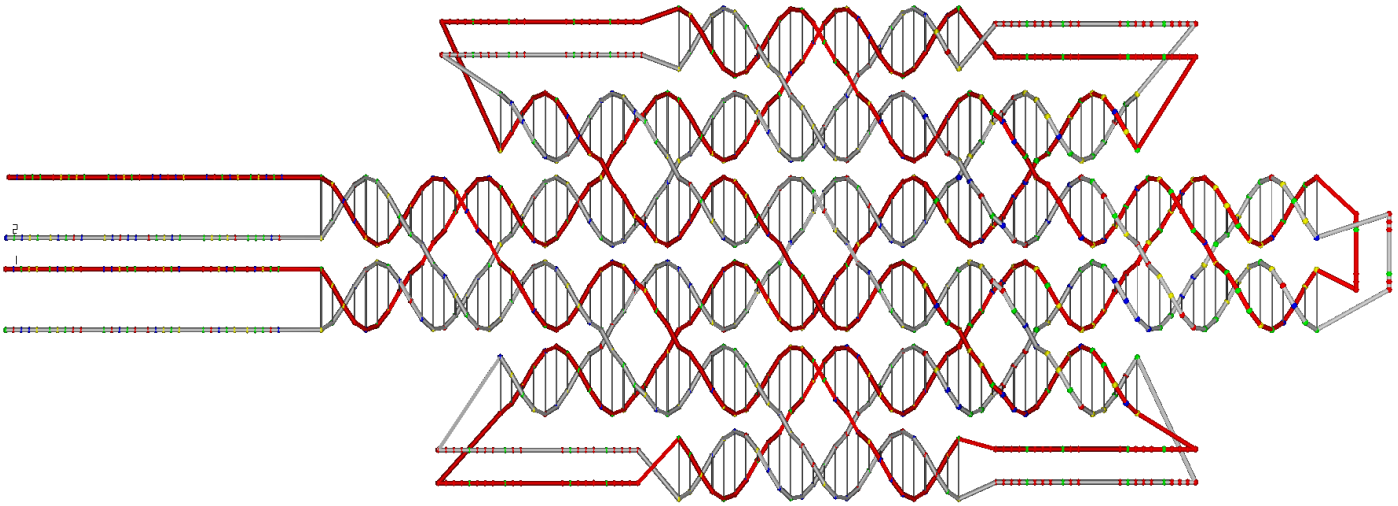

Figure S12-1. Design detail of 3 × 3 diamond-shape ssOrigami. Red strand is the forward strand and gray strand is the reverse strand.

Forward strand：

TACGGCACGTAAGCCTTGCATTGACTAGCCCGGTACGTATTTCTTACGCAGCCATGTCTGGCCTCGGACC
TCAGAGGGAATGCGTCACTTTTCTTTCTTTCTTTCTTTTCGAGGCGTCCAATGATTGCTGTTTAGCAAAGT
GGCGCACGTTGTCGGCACCCTACGCTTTTTCTTTCTTTCTTTCTTTTCCGTCTACTTCCGGTAAGGGAGAC
TTCCAAGTGCGTGGGTTTGCGAGTGGCGGACGCTTTCTTTGGTACGCCCGACTCGCACGAGATTTGCAAC
GCCAATTATAGCCCCTCTCCAGCTCTGCTTTTCTTTCTTTCTTTCTTTTGTTGTCAAGTTTGAGTAAGCTGG
CAAACTTTGATGGCGGACGGGCAAATCCGACCGAGTTTTCTTTCTTTCTTTCTTTTCGAATAAAGATACC
GGTCCGGGATTCTCGAGAGTCCTCATGCTAAGAATGGCGGAAGCACAGCGACTAGATAATCGACCGCGT
CCCAT

Reverse strand：

ACAGCGACTAGATAATCGACCGCGTCCCATGCTTCCGCCACAGCTGGCATGAGGACGCCGACGAATCCC
GGAGTTGAATCTTTATTCGTTTTCTTTCTTTCTTTCTTTTCTCGGTCGGAACTTGGCGTCCGCCATAGTCGT
TTGCCAGCTTGCCAGAACTTGACAACTTTTCTTTCTTTCTTTCTTTTGCAGAGCTGGTGGAGTGCTATAAT
TGATCATTCAAATCTCGTTGGTTCCGGGCGTACCTTCTTTAGCGTCCGCCGAACCAAAACCCACGCTTTG
CCAAGTCTCCCTTTCAACAAGTAGACGGTTTTCTTTCTTTCTTTCTTTTAGCGTAGGGTTCTCGAAACGTG
CGCCACGACTCTAAACAGCAGCGTTGGGACGCCTCGTTTTCTTTCTTTCTTTCTTTTGTGACGCATTACTC
CAGAGGTCCGAGACTCAACATGGCTGCGCAGCTGATACGTACCGATCCGGCATCGCGATTCATCTTCGC
GAATC

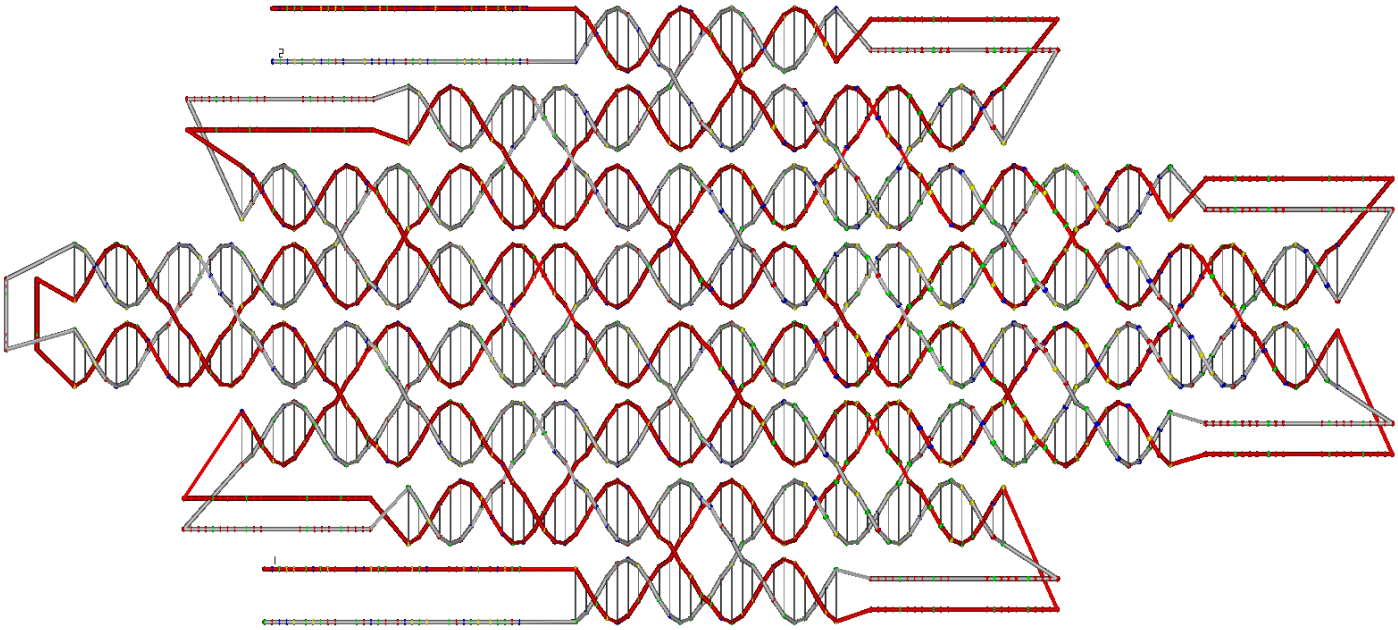

Figure S12-2. Design detail of 4 × 4 diamond-shape ssOrigami. Red strand is the forward strand and gray strand is the reverse strand.

Forward strand：

TACGGCACGTAAGCCTTGCATTGACTAGCCGTCGATCAGTGGTTATGGGTGGCTGCCCGCGGGAAGGGA
TGGTAAACACGAGCATAACACAGCGGGTCGCTGTATTTTCTTTCTTTCTTTCTTTTGTTTCTACAGGCTGA
GAGCGTCCGCCGAACCAAAACCCACGCTTTGCCAAGTCTCCCTTTCAACAAGTAGACGGTTTTCTTTCTT
TCTTTCTTTTAGCGTAGGGTTCTCGAAACGTGCGCCACGACTCTAAACAGCAGCGTTGGGACGCCTCGAT
ATCTCCCTGCATACTTTTCTTTCTTTCTTTCTTTTTGGTGGGTAGTTCATCGTGACGCATTACTCCAGAGGT
CCGAGACTCAACATGGCTGCGCAGCTGATACGTACCGTTCTTTGCTTCCGCCACAGCTGGCATGAGGAC
GCCGACGAATCCCGGAGTTGAATCTTTATTCGGGCCACGGAAGGGTGGTTTTCTTTCTTTCTTTCTTTTGA
ACCGCCTCCCGCGGCTCGGTCGGAACTTGGCGTCCGCCATAGTCGTTTGCCAGCTTGCCAGAACTTGACA
ACTTTTCTTTCTTTCTTTCTTTTGCAGAGCTGGTGGAGTGCTATAATTGATCATTCAAATCTCGTTGGTTCC
GGGCGTACCCGGCCTGGTGTATGTGTTTTCTTTCTTTCTTTCTTTTTGAGCACATTCGCTGTAATCTCATC
GCCGCAATGGCTATGGGAGATATGCATAAGTTGCCCTAAATATAGCATTACAGCGACTAGATAATCGAC
CGCGTCCCAT

Reverse strand：

ACAGCGACTAGATAATCGACCGCGTCCCATAATGCTATATGATGAACAACTTATGCGTGGGTCCCATAG
CCACTCAGCCGATGAGATTTAGGATAATGTGCTCATTTTCTTTCTTTCTTTCTTTTCACATACACCTGTTT
AGGTACGCCCGACTCGCACGAGATTTGCAACGCCAATTATAGCCCCTCTCCAGCTCTGCTTTTCTTTCTTT
CTTTCTTTTGTTGTCAAGTTTGAGTAAGCTGGCAAACTTTGATGGCGGACGGGCAAATCCGACCGAGGGC
TCGGAGGCGGTTCTTTTCTTTCTTTCTTTCTTTTCCACCCTTCCATAACCCGAATAAAGATACCGGTCCGG
GATTCTCGAGAGTCCTCATGCTAAGAATGGCGGAAGCTTCTTTCGGTACGTATTTCTTACGCAGCCATGT
CTGGCCTCGGACCTCAGAGGGAATGCGTCACTTAGGGCTACCCACCATTTTCTTTCTTTCTTTCTTTTGTA
TGCAGGGACCCACCGAGGCGTCCAATGATTGCTGTTTAGCAAAGTGGCGCACGTTGTCGGCACCCTACG
CTTTTTCTTTCTTTCTTTCTTTTCCGTCTACTTCCGGTAAGGGAGACTTCCAAGTGCGTGGGTTTGCGAGT
GGCGGACGCTTTGCGGCTGTAGAAACTTTTCTTTCTTTCTTTCTTTTTACAGCGACCATCCTAGTTATGCT
CGAGGCCGCCATCCCTTCCGAGCCGCAGCCACCCGTGGCCACTGATCGACATCCGGCATCGCGATTCAT
CTTCGCGAATC

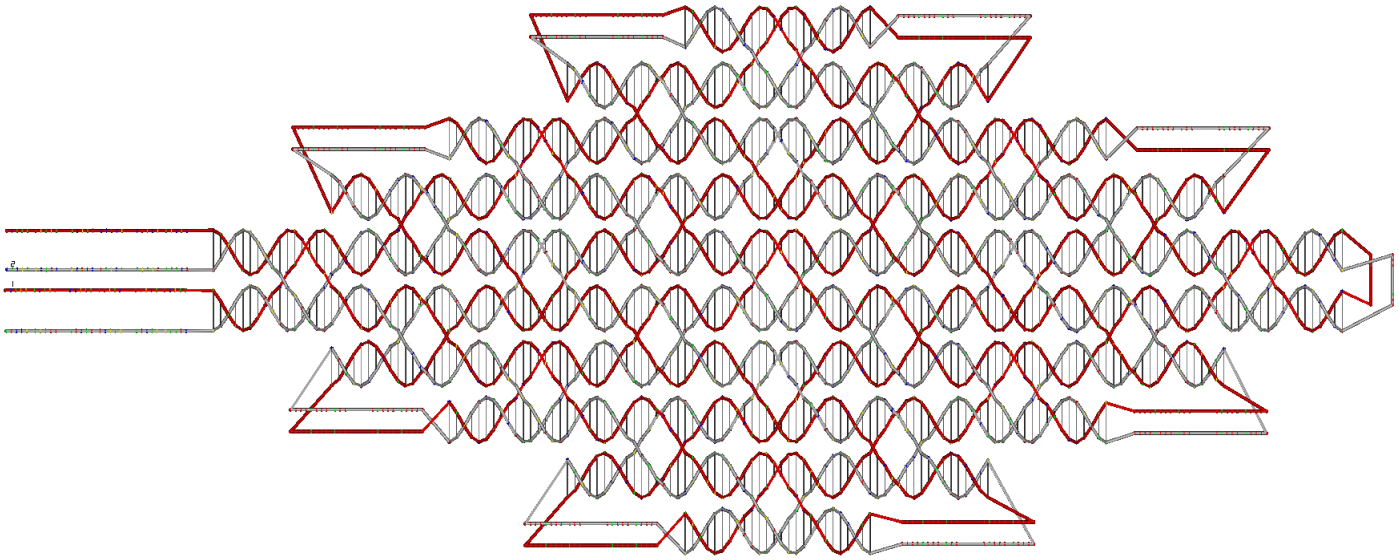

Figure S12-3. Design detail of 5 × 5 diamond-shape ssOrigami. Red strand is the forward strand and gray strand is the reverse strand.

Forward strand：

TACGGCACGTAAGCCTTGCATTGACTAGCCCTCCCCCACAACTGACTGATTGCTGAATCTTGCGGTGTGT
GGAGTTCATCTGCATCCTGCCCAACTCCGGCGGCGGTTGCACGATCAACATTTTCTTTCTTTCTTTCTTTT
ATGAAAGGCAGTTGGGCCAGTAGGCGGTCCACCTATGAGCACCAAAGGATCCTGGTCGTCGGGCCAGCC
ACCACGTATTGCTATTACGATTTTTCTTTCTTTCTTTCTTTTACGTATGCTAACTCATTGCTCCTAAGACCA
GTATAAGTTCCATGGCTGGACTCCGGCAATGAGCGGGAACCGCTGATTCAACGACCAGCATTTTCTTTCT
TTCTTTCTTTTACCATTCCGCGTCGAGGGACGAATTGGATCTATCTCTGTGTCATTCTGGACCGTAAGCGC
GCGTCAGAATTTGAAGAGGACAATCGACGTTTTTCTTTCTTTCTTTCTTTTCGCTCTTCAAACGAGTCGGT
TGCAATGTTGCGCCTCGGCGTGATCCTGCTTACTCGACTGCTCTAATGGACAAGGCTTAACCGCGCTTTC
TTCTTTATCTCTCTTGTTAAGCAGTCTGCGAAATCGGGGTAGAACCAATGAATCCTCAAGCACTGCCCGG
GTAGAGATGAGCAACCTTCTTGTCCTTTTTCTTTCTTTCTTTCTTTTTCTGAAGCAGACTATCTGACGCAG
GGGTGGACGAAACCGAGGTGCCGAAGACAAGGGCTAGATCGGATTTCTCCGGTCCGGATCACGCGTTTT
TCTTTCTTTCTTTCTTTTGGACAATCAGCAGGATTAAGTTCAACCTTGAATCGACTCCGGCAGCCACAGA
TCTCTACAGGACGAACGACACCTGAACTACGCTACCTCTTTTCTTTCTTTCTTTCTTTTGAAAGTGCTTAT
CTAGACGAAACATAGCCCGAGCCGAAGCGTATGTCGCGTGCCCCGAACGCGCCGTACAACCACAGGTTT
TGGAAAATCTTTTCTTTCTTTCTTTCTTTTCCTTTCCTCAACTCGTGTACGGGTCTAAACCATCAGGACAG
TATGAGTACAGGAAGGGCTCGAAGGCATGTTCAGTCAGTAGCCCCCGCAACAGCGACTAGATAATCGAC
CGCGTCCCAT

Reverse strand：

ACAGCGACTAGATAATCGACCGCGTCCCATTGCGGGGGCTAGTCTTTGAACATGCCCAATACCCCTTCCT
GTGGGTGTACTGTCCTGATCCTCTAGACCCGTACCGTGGGTGAGGAAAGGTTTTCTTTCTTTCTTTCTTTT
GATTTTCCAACGCAACTGGTTGTACGAAGTGCTCGGGGCACGACTGGTACGCTTCGGCGGTCTTTATGTT
TCGTCAAGATAAGCACTTTCTTTTCTTTCTTTCTTTCTTTTGAGGTAGCGTTTTCCTGGTGTCGTTCCCTTT
GTAGAGATCTGGCCAGACCGGAGTCGACAGAATGTTGAACTTACGCATTCTGATTGTCCTTTTCTTTCTT
TCTTTCTTTTACGCGTGATCAGAGCAGGAGAAATCCAATTCTGCCCTTGTCTGCTCATCCTCGGTTTCAGA
ATCCCCTGCGTCATTGGGCCTGCTTCAGATTTTCTTTCTTTCTTTCTTTTAGGACAAGAAACGGCTTCATC
TCTACCCCAACAGTGCTTGAGCGGTAGTTGGTTCTACCTCGACTTCGCAGACTCACGCTCAAGAGAGATT
TCTTTGAAAGCGCGGAGCGTGCTTGTCCATTCGGACCGTCGAGTAAGAATGCGCACGCCGAGGAACCTG
ATTGCAACCGCCCACGTTGAAGAGCGTTTTCTTTCTTTCTTTCTTTTACGTCGATTGTGGTTTTCAAATTCT

GGCACTTGCTTACGGTCTTCAAGGACACAGAGAAGAATTCAATTCGTCCCCCGATGCGGAATGGTTTTTC
TTTCTTTCTTTCTTTTTGCTGGTCGTCTACCGAGCGGTTCCCTCGGCATGCCGGAGTCTCTGGCTGGAACT
TATCGACATCTTAGGAGCAACACCCTAGCATACGTTTTTCTTTCTTTCTTTCTTTTATCGTAATAGTTCGA
GGTGGTGGCTGAAGACCCGACCAGGATGTCCTGGTGCTCATAGGATTCTCGCCTACTGGCCGGGCTGCC
TTTCATTTTTCTTTCTTTCTTTCTTTTTGTTGATCGTAGCCGTGCCGCCGGAGGATAGTAGGATGCAGAAG
GAAACCACACACCGCTAGATTCAGCAATCAAAGACTTGTGGGGGAGATCCGGCATCGCGATTCATCTTC
GCGAATC

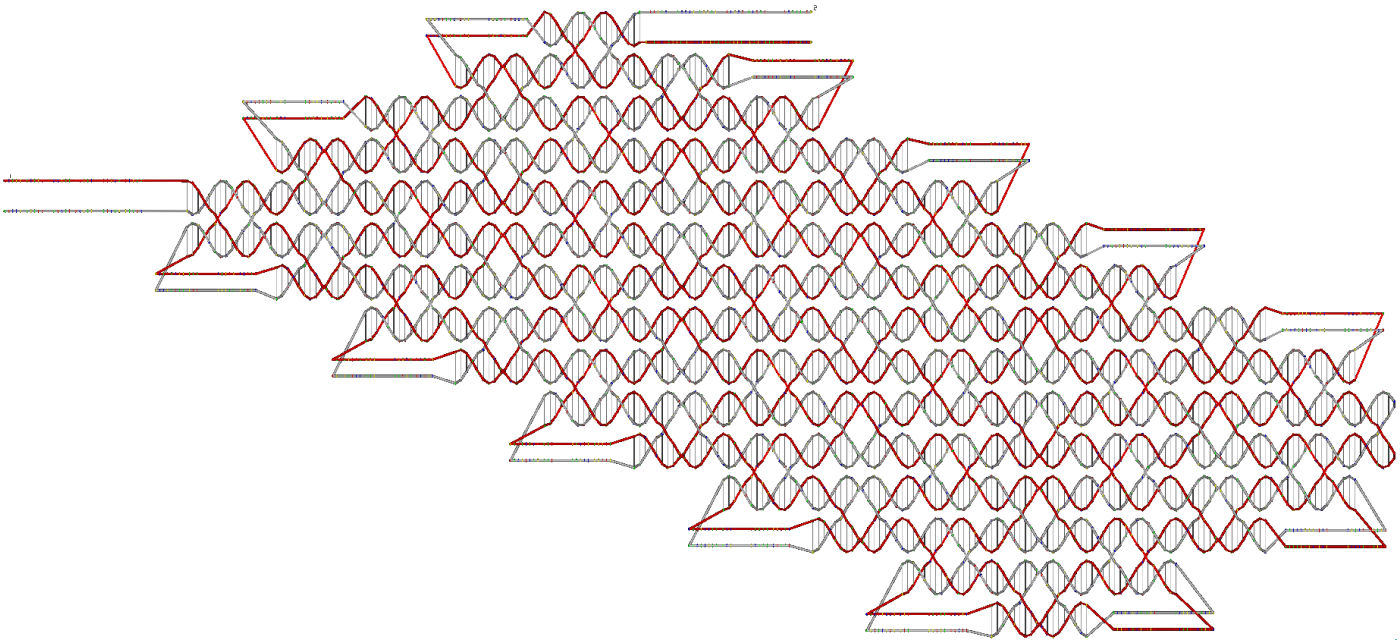

Figure S12-4. Design detail of 5 × 10 rhomboid-shape ssOrigami. Red strand is the forward strand and gray strand is the reverse strand.

Forward strand：
TACGGCACGTAAGCCTTGCATTGACTAGCCCTTTCGATCGTGTTAGCTTTTATATCCCCACCACTAGCAA
ACGCGCGCCGTGCGGACTACAGAAGCTGAGTACGAGACCTTGTATCCTGCTGGTCTTGCAGGAGGACTC
GTGTCATAGCCGCTTTTTTTTGGCCGTGACTCATAACTTGTAAGAAGAGACTGTGGTACAGTGTTACCTA
CGTATGCTGAGTGGCTAGTTCACGCCACCTCGGGTACATGCGCCCCGCCGAGATGTAGACATCTGCGTC
ACCGTCGGCGTTAGCACATTCTACCATTTCACTCACAGGCGCCTCTCCCGGGTCCTGTTTCGTCAAGGAT
TCAGGGCCCCTTCCTCGTACGAGAGCGCACCCGCCCAACCGTGGCGCGCACGGCGAAGAAGCGGCGGC
CCCTAGTCGTCATTGCAAACTCTAGCTCGGGTTCTATTATTTCGTCATCAGTAGTCTAGTGACGAGTGGT
TTGCGGCGGTTCTCGACTTGAAAGTTAAGATTCCAACAGCTATTGACGGTGTACACTCTGGGCTGCTCGG
CTCCCCGCGAGAGGAAACTCGTTTTGTCCAACGGGCTGATCGCTCGGATGCAAGACCGGGTACCACTTC
TGAGTGTGTTTTAGAGGTCCACGGCCGGCGCGCCGGACATAACGGCAGTACAGGCACTAGCGCAGATGA
GGCCCTGCTCTACCTTGGCACGCTTTCGTGGGGCCGTGTTAAACGGGAAAATGGCCTGCGCAGGTCCCT
GTCCACTATAGCACTCCTACTTACACTTAATTTTACGAGATGGCAAGAACAGATGCCAAGGCTTAGAGT
GGCCCGCCCAAGGGCTCTCGTACTAGGGAGCGGGGAGCAGACCCACTCGCCGCTGTGCGTCTGCAACTC
AGTGCGTAGGATCTAGACCATTGTCCTTTGGGGTCTACCAGGGGCAGCCAGAGCGGCGAATAGACCGTT
GATACGCTTCTTTGGGACAGTATCCTCTTGAGAAGTACAGGCGCAATAGGTCGAGTGGAACCGAGGTCT
ACAAATCTAATGGAGAACTTCTGCGCATCCGGAGAGTGCTAATTGTAGACACCTGATGTAATAGGAGGG
TTCGTACATCAGCGGCTCTCGACTTCATACAGCCCAACACTGGGAATCAGTTTTCGGAAGGTGGTGAAA
TAACCAAGCGGCCACCCACTGGCCCCTAACCCAAGTCACGGGAGATGCTATTGCAAGTGTAGATGTTCT
ACCCAGACCAGGAGCGAGATGGACTAAAAGGCGGTGTTGTACTTGACAATTTGAGCAAAGCACAAGTT

GCTGCTAGAGTACGAGCGACGCTTGCGCGCTGGACACGACGAAAACCAAGCACGCACTACGACTTCGCC
AACCGCAGCAGTAGAGGCTGGCGTACGTCCTACACTCGCCTGAGAGCCAATCATGTACTCATGGTAGTC
ACATCACACTATTCTGAGCAGTGGCCGTTTGTGACAGGTGATCGGCACCCCTGGTACAATGCCAGTCAC
CGCCTGGACTTGGCATCGACACCGGGTTTCACGGTTGCCGTATAATACTAACGCTCGTTCAGGAGAATC
AAGAGTAGTCTCCTCGGTCATCAGGAGGGCTTGCTCTCCATGCAGGTAGCAACGCTGGCAACAGGTCCC
GAAGTAATAGCCTTTGGTCTCAAGCAGGCCAGGAAAGATATCTTGCAGCAGCTAGCACGCTTGGTCCTC
GGGAAGTGAGTGTATGAGTAAGTACCCGCACAAAGCTCGCGACTAGTGTAATCTCTTCCCGATCAGGGA
CCCGGGATAGGAACGTCTAAGTGCACCCGGACTCAGTGCGTGAGGACGCGTGGGCATCCGTACGTTTCT
CGCTAGGGCTTCCCGCTCAATTAACACCCTGCCGTTTCGGGGATAATTGGTCTATCGGCGTAAGTGCCTC
CGGCAGCGACCCTGTATGCAAGGGTACATTGAGCACAGCGACTAGATAATCGACCGCGTCCCAT

Reverse strand：
ACAGCGACTAGATAATCGACCGCGTCCCATTCTACTAGATGCGGCGAAACACGTTCAATTACTATAGAA
ACGGCAGGTCCAGCATTGAGCGGGTTCTTCTAGCGAGAAATAACACGATGCCCACGCACGATCACGCAG
AAGCTCCGTTGGGCCGCTGACGTTCCCCACTTGGGTCCCTGACCTGAAAGAGATTACAGTAACGGCGAG
CTTTGAAGCGTTACTTACTCAAAGGGCCACTTCGTGATTAGCATGACATTGATCTGCTGCCCATCTTCTTT
CCTGGCAACAGTGAGACCAAATAGAGTTACTTCGGGATTCACCGCCAGCGTTGGCGTTTGCATGGTGCG
CTAACCGCCTGCTATGACGAGGACCCGACTCTTGATTCTGGCGCCCGAGCGTTAGTGTGAGACGGCAAC
CGCGCTAGCCGGTGTCGATAGCTTGTCCAGCACAAAATCCTTCTTGGCGCAGGGGTGCGGGCCACCTGT
CACAGGAACTCACTGCTCAGGACTACGTGATGTGACAATAGTGAGTACATGACTCGTACTCAGGTCAGT
ACGCCTCCGAAGGTTGCCTCTACGAGAACGGTTGGCGAACGCCGAGTGCGTGCTAGCAGCTCGTCGTGT
CCGCCGGGCAAGCGTCGCCCGCGCTCTAGAACTGTGGGACCCAAGGAACAAATTGTGCTCCCCAACACC
GCCCGCGGTTCCATCTCGCAGTCGATCTGGGTAGACTGGGGACACTTGCAAAGTCCTCTCCCGCCACAG
CCCAGGACCCATCCTGGGTGGGTCTGGGGTTATTTCAGCGGGGTCCGAAAACTGCTGGCCAGTGTTGGG
AGTGGTGAAGTCGAGAGCCCCTGATGTACGAACTACAGGCCATCCGTATGTGTCTTGAGTTAGCACTCT
CCGCAGGAGCAGAAGTTCACCGTCAGATTTGTAGCATTGTGTTCCACTCGAGTCACTGCGCCCGTCAGTG
GTCGGTGCTTATTGTCCCAGCGACCCGTATCAACGAGCCACTCGCCGCTCTGGCCTACCCTGGTAGACCC
GTTAGGACAATGGAGAACTTCCTACGCACACAATTGCAGACGCACAGGGGCGAGTGGGTCTCAAGTAC
GCTCCCTAGCGCGGGAGCCCTTGGGCCGATCACTCTAAGCCAAGCTATCTGTTCTTGAAGATACGTAAA
ATTAGCCCTTAGTAGGAGTGTCCCCGTGGACACGAATCTCGAGGTACCTAGGGCCCGTTGCTGGAGGCC
CCACGATGCGGGGCCAAGGTAGCTGTTGGCCTCATCTGTGAAACTGCCTGTACTAGTTCCATGTCCGGCG
CAGCGCCCGTGGACCTACCGCGCACACTCAGACTGTATACCCGGTCTTTCCTGCGAGCGATCAGCCCCA
AGGACAATGCGTTACGATATGGGAAACAAGCCGATAGGCCCAGAGTGTACTCCATTAATAGCTGTTGCC
AGCTTAACTTTCATCCTGGGAACCGCCGCGCTGCTCTCGTCACTAAATAGTTGATGACGAACTCACAGAA
CCCGAGCGGCTATTTGCAATGACCGTTACGGGCCGCCGCAAGCCCGCCGTGACTCTAGGTCCGCTGCTT
ATGCGCTCTGTGTTAAGGAAGGGGCTCGGGATCCTTGACGAGGTGAAACCCGGGAGACCTGAATGTGAG
TGAAACTATTGAATGTGCTAAGTCGTACGGTGACGCCCCCAGCTACATCTCGCCACCTCGCATGTACCAC
AATGGGCGTGAACTGTCTATTCAGCAGGACGAGGACTGCCAGAGAACCAGTCTGGTCGCACAAGTTATG
ACCTATGGCCAAAAAACCAGACCTATGACACGTAGCATCCTGCAAGACTTCTCGGATACAAGGTTTGGC
TCTCAGCTTCTGTCGGGCGCACGGCGCCTACCTGCTAGTGGTGAAGTGGTAAAAGCTAACGTCCTCGAA
AGATCCGGCATCGCGATTCATCTTCGCGAATC

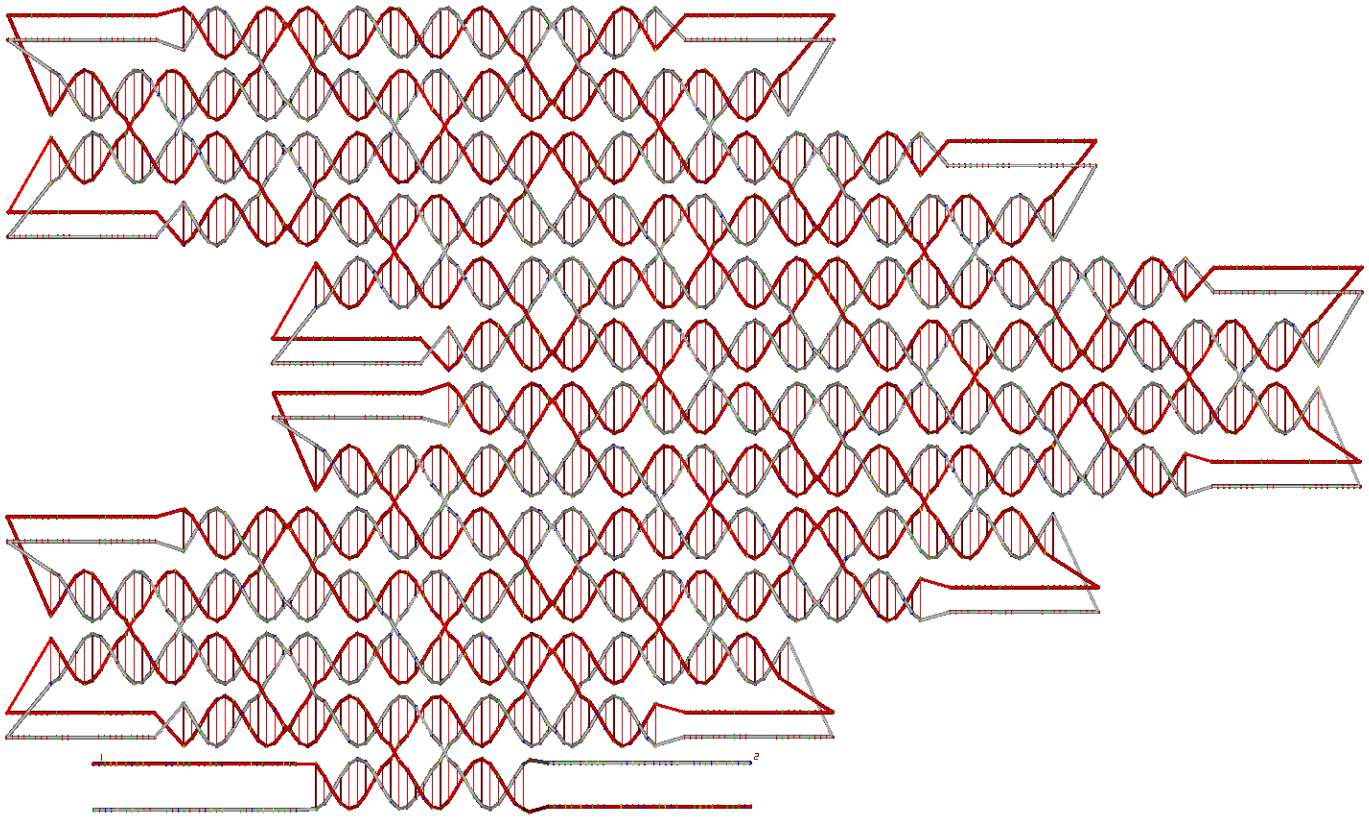

Figure S12-5. Design detail of heart shape ssOrigami. Red strand is the forward strand and gray strand is the reverse strand.

Forward strand:

TACGGCACGTAAGCCTTGCATTGACTAGCCGTTCGTTCATCCTCTTGAACAAGGATTCCGCGAGTACTTC
ACAGTAGAGGAGCCCCATACAGTTTATCGCACGGGATTGTGTATGGTTTGCTGTTGCTGTGCAGACATCG
CATTGTGTTAGCTTTTCTTTCTTTCTTTCTTTTCAAGGTCATGTGGCTTGTATCCCGCGCTTATCTTCAATT
GCACAAAGTAAGGAAAACACTGTAGGTGTATACGAGGCACAGCGCAGGGATGGCTGTTTCTTCAAGTTT
GCTGAGAGAAAGCGTTTTCTTTCTTTCTTTCTTTTTGTTGCTCACGGAGAGACAGTTTTCCTTGCATCAGT
GTTGATCGCATCGGCTCGCGCTATGAGAATGATAACGCTGTAAAACACTAAGGTTAGACGCTCGTGTGG
CACTATCTGGGATCTACTTTTCTTTCTTTCTTTCTTTTCAAGTTTGGTTCGTTGAAAGCCGGTCTCAAGTGT
TATCTAGCAGTTCAGTCGAGGTCATTTTCTTTCTTTCTTTCTTTTTCGCCTCTTTAAACCCAATTTAAACCT
ATGAGAGGCAGTCGCTAACTGGCATTGAACGTTTTCTTTCTTTCTTTCTTTTGTGTCTTACTCACGGTTGG
TTTGCATGATCAATAACTACACTACTCGACATACACACATTTTCTTTCTTTCTTTCTTTTCCGCTTAGCCCT
TTGGTCTGCATCATCTCCACGGCCAAACGGCGTAACAGATAATCGTACCGTGTAGACTGTAGCCGGAAT
GATAATGTGCAACGATTTCTGGCGGCAATGGATTATTCCCAAAGCCAAATGTATAACCAAACCGACCCT
TGCCTTTTCTTTCTTTCTTTCTTTTGAGCATCAGCCAACAGGTGAGCATTGTCCTTGGAAACGAGGGCGTC
TATGAGGTTCTAACTCACATCCGGTCTGCTCATACTTCATATAAAGTAGGGCCGTGTAATGTGGAGTGAG
TCTTGATTTTCTTTCTTTCTTTCTTTTCTACACCTCAGCAAGTGTTCACCATTTCGAGTTCGCTAATCTGAC
TTTATTACATACGTGAACTCCGATGATATGGGGTTCAGGGAGGTGACTTTGGATCCCTTGACGACCTCAC
CAGTTGTTTTTCTTTCTTTCTTTCTTTTCTTAGAAGGTAACTGTTATTGGAGAAAACCTTTTCCTTACTGTC
TCATAGTTGAAGTCTTTTCTTTCTTTCTTTCTTTTGTTTAGTGTGGATTTGTTCAGCACTTTGTGCCTGCAA
CCACGTCGGACGCAACAATTGTTTTCTTTCTTTCTTTCTTTTCTAAGGAACGCGCGGATGGTTCCGTTCAC
TGCGTCCACTTTAATGCAAGCGACCCATGTTTTCTTTCTTTCTTTCTTTTCATAGGTTTCCTATCAGTAACT
TCTCCAGCAAAAGCTGCTTGGTCAGCTACGTTCTAGTACAGCGACTAGATAATCGACCGCGTCCCAT

Reverse strand:

ACAGCGACTAGATAATCGACCGCGTCCCATTCTAGAACGTAAAGAGGCAAGCAGCTTGTTGACGAGAA
GTTACCTCTCCGAAACCTATGTTTTCTTTCTTTCTTTCTTTTCATGGGTCGCGGATCCTAAAGTGGACACA
GCCAACGGAACCATAGAACCGTTCCTTAGTTTTCTTTCTTTCTTTCTTTTCAATTGTTGCTCTACTCGTGGT
TGCACAACATAAGTGCTGAAGATGCGCACACTAAACTTTTCTTTCTTTCTTTCTTTTGACTTCAACTCCAA
TGCAGTAAGGAACTACAGTTCTCCAATACATACGACCTTCTAAGTTTTCTTTCTTTCTTTCTTTTACAACT
GGTGACAATCTCAAGGGATCGGTCCGCACCTCCCTGTTTACAATATCATCGGCACTAGCGTATGTAATGG
GTTTAGATTAGCGACAGACTAATGGTGAACCCAAAGTGAGGTGTAGTTTTCTTTCTTTCTTTCTTTTTCAA
GACTCAATGGGGATTACACGGCTTGATCTTATATGAAGCCGTAACAGACCGGATACTTGATAGAACCTC
AGCAGAACCCTCGTTTCGATAAGCAATGCTCACGTGCTTGCTGATGCTCTTTTCTTTCTTTCTTTCTTTTG
GCAAGGGTCTGCGATGTTATACATTGTCTTCTGGGAATAATGATAGTCCGCCAGAAATCTTCCCACATTA
TCACAGTTACTACAGTCTAAGACTCACGATTATCTGTTACGCCGTTTGGCCCCCCATATGATGCAGAACT
TGCGGCTAAGCGGTTTTCTTTCTTTCTTTCTTTTTGTGTGTATGAGTCTGAGTGTAGTTACCTACTATGCA
AACCAGAGTCTAGTAAGACACTTTTCTTTCTTTCTTTCTTTTCGTTCAATGCTTCCGGGCGACTGCCTTTA
CGGGGTTTAAATTAAAGTCAAAGAGGCGATTTTCTTTCTTTCTTTCTTTTTGACCTCGACCTAGTGGCTAG
ATAACGTGAGTGACCGGCTTTGGAAGAACCAAACTTGTTTTCTTTCTTTCTTTCTTTTGTAGATCCCACCA
TTGGCCACACGAGTTCTGCACCTTAGTGTAACCCCGCGTTATCATCATTGGAGCGCGAGCCCAAATCATC
AACACTGGGATCCGGAAAACTGTTGATAGGTGAGCAACATTTTCTTTCTTTCTTTCTTTTCGCTTTCTCTG
TCAACACTTGAAGAAGCAGTGATCCCTGCGCATGTTGTCGTATACACAAGGTTTGTTTTCCTTCGGACCT
GCAATTGAACAAGGACGCGGGATACGAAGACCATGACCTTGTTTTCTTTCTTTCTTTCTTTTGCTAACAC
AAGGTTTGGTCTGCACAGAAGCACCAAACCATACAGGTCGCCGTGCGATACGTATGATGGGGCTCCGTC
CGAGTGAAGTACTGTTCTAATCCTTGTTCGCTGACATGAACGAACATCCGGCATCGCGATTCATCTTCGC
GAATC

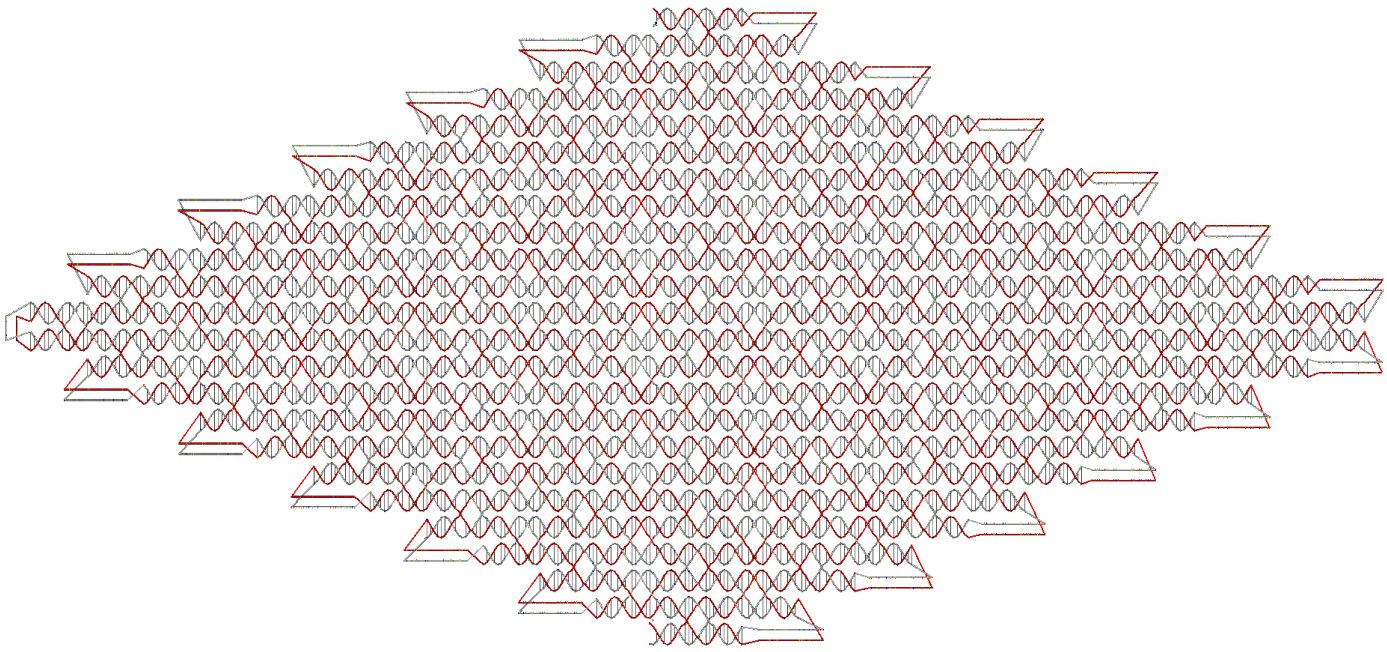

Figure S12-6. Design detail of 12 × 12 ssOrigami ssOrigami. Red strand is the forward strand and gray strand is the reverse strand.

Forward strand：

ATCGAAGCGATTACCCGAAACTGCAGGGCCACCTCGCCCAGTTCAAGGAAGTAGAGACAAACGTAATC
AGCGAGGGCATCGAGGCAAGGCGACATAAGTTGGGTCGGGAGTAGCTTAAGGGTTCTACCCGACATAA

CCATTGAGCCAGGAGTTTCCGGTACAGAGACGGCGACGAGTGATACAACGGTGATCCTCACGGGATACG
AACTCCTCACGCTGAAAACAGTCCGGTACAAGCGCATGACTTCCGTCAATTGTGCAGCCGCTAGTCGCTT
GGCCACCCCTTCTTATGGGAGTGGGCAGCCGCCGGTAACCAATTTCTGCTGATGGCGAAGTCGATCTCC
AGCATAAGGTCGACTGTTCTCAGAGCCCCTAAACGTCGTGCGGTTTATGCGGACTTTCTTACTCTGCATT
CCGGGCTCGACAGAGTTGACCTGCCGAGGTATCGTAAGTCTGTGCCGGTCGTAGCATCAATGCATTAAT
CCGTGCGGTGCATACCCACATATGAGACGAGCGAGGGTGCAACCGGACTGATCACCCGAACATAGGTC
GCGCCTACATTCGAAATGTACAAGGGATGACATCACGCACGAGGAAGGACTGAACCTGTGACTCGAATC
AGTACGGCTACCTCCCAAAACATCTCGCTGCCGGGTAGCTTCCATCTCCTATTCGGTGCCCAGCCTGTGG
CACGCAAGCGTATGATCGAGAAGCACTGGATGGGGACTGGTTCGTAGAGTTGCACTGTATGCCTACTCT
GGGGTTATCCGTTGCTCTCCTACGTCTAACGCTTAACGTAGAATACCACGGGTTTGCACGGTCGGATGGC
CACCTCTGGTCCGGCGTAGGGAGGTCGAGGGGATAGTTTGGCCTCGGATTCGTGTCGTGCGAGGAGTCG
TCAAGAACCCACATCCCGTCTCTACATCCCCAGAATTGACATACCCGACCGTGAGCCCTCTAGCAGCCG
GGGTATGCATCGGATCGGTCAACCTGGTGGTGCGGGCCGTACAGGGTGTTAACGTACACTAACGATAGG
GGCAGGAAACAAAGAAGCACTGGAGCGCTAGCACTAACCATGAACGTCATCTTGTTCGTAATAAGCGTC
AGGCTTGATGCTCTCACCAGTAACAGTCGTTATGGTGGTCGTACCCAATGGCCCCTGCTGTAAGTGTAAA
ATAGGCCTAAAGGACCCAAGATCCGGCCAACGGTCCTCCTTTACCACCGAAGCGACACAGCCTCTTATC
TCTAAGAGACTCCCACATGATTCTACGTTCTGCCCCGACGTACGACGTAAGCCCCATGCACGACTGGGTT
GGACGTCGTTCAGATTCTTTAGTTATGGGACCCGCGCCATACACACGGGGCGAACGAGACCATGCCAAA
GCCAGACCTCTTAGGATGTCGCCGGCACCGCCCCGGAAGGAGACCCCGGCGAAGCCTTACGGCCATGGC
GACGTCCTGTGTCGCAGTCCTATGGAACAGGTCGGACCGGTACTTCGGCAGCTTCGCCCTATCTCAACTT
ACGGTAGCCGCATCGCCGGAGTGCGGGTGTTTACCCGATGGGTAACGAAATCGGCCTACTGGTGGTAGG
CTTACTCCTCCAAGTCTGGCGCGCATACAAGGTGGCCAAGCCGGTCTAAGTCCCATAAAGGGCCTGTCA
GACAGGACCTGGCATCGGCGAGCGTCGCTGGCTTCCGGTCGAGTTATCAAAGAAGTTAACAGGGCAAGC
TCCAGCACTCCAAATTCGGGACGTGACCCCTCCGGGAGTGGACCGGGGCTTAGTACTGTGTAGTCGGTC
TCACTGAGGCGGTGGGATTATAGTCCGCCCGATCAAATCGAAGGCCGGTTTCCGTGGAGCCCACTTGAG
TAACTCGATACCCATGACACTAGCAGTTTAACGATTGACTTGCACTTCTTGCCTGTAGTCGCGAGCGGAA
TGCTCTGTGCGAGTTTCGAGTGCCGCCCGATTGGGGCTGTCCCCGTCACTATGTTCAGGCGTTCACAGGT
ACACCGCAGACTTAAATAGGCGCTATAACTTTGACGGTAGATACATGTAAAAGAAGAATGTTCTGAGAA
GCTCAGCGTCGGCTACCCAATCACGGATCAAACGGAACGAACCACCCAACAGTAAGTGATCTAGCCGCG
TAGCATCCGTTCCTCGCACTGAAGCATACCACTTGAAGGGGTGTGTAGACACTAATGGCCTGCGCGAGA
CTACACCCAGTTAGGGTCACAACAAGGTCGGTGCTTCACACCGGCATCCTCTGCTCTTCTTCTGCGCTAG
TATTGGTATCGGCGGATGTACACGCGCAGCCCGTTGGAGCTAGATAAGAGCATCCTCCCATCCTTCATTC
CTATACGGGCCGTTGTGGCAGGGCCCTGAGTGAGCGCTACCAGCATAGATTTCGGACCACTAACACTGA
TGTACGGGTTCCCTTCAGGAACTACGACCGGGTATTCCACAACGGTGTGCCCTCGTAAGCTCCTGCAAA
GGCATTATGTCAGCGGACGCGTGGTGTAAACCGGGACGATGTTATGGCCGGTCTGGCGCCCCAGACCAG
ATCCCCACCCCGAGTCCTTGCCAAGGAGTGTTAGTTGTCCCTTAGGATCGGGCTAGGACGGCCGCTGGC
GATAGGATCCACCACGACTTACAAACAAGCGTGGTAAATTGCCGTGGTCGACGCCGAATATCCATGACA
ACGTGTTAGTGTTCTTTCCCGCGGAGTCTTCTGGCATCACGTCATACGAGTTAACGTCCGTGTAGCGCTG
TCGTGAATTTTCAGCTTTGCTATAGTGCATATCCCCTGCGTCGGCCCACATGTATGTGTAACCGGAATGC
TTGTAGCTAGAACGCCTGACGCGGTAAATGATGGATGGCGCTCTCCTCGGATAACAGGTGGCGTCGGTA
CCCCGGAAGCCGTGACAATATGCATAGTTTCCCGCGAACTGCCACTCGCATATGTAGTAGCAAAATCTG
GGCGGTCAAGCTGATCGTTCGACGATCTCTCGGTCCTTCGAGGAACAATCCCGATTCCTCAGCAGCGTTG
TGCCGTGTGGATGCGAGGCCCCGAGCCGGAGCGACCAATGTCGTGTTCATATCGCGACACCTATGTGTA
AGGCCCGACGCAGAATGTAGACCTAACAGAATTGTTCAGTGCGTCAGCCGGAACAGAATGCACACGCT
GTTACGAAAATGTTAGCATTTTGCTGGGGTCAGAACTCGGCGATCCGTCCACGACTCCGCTGGGCCATA
AGTCCTCATCCGGCAGTGTTCTGCTCACGACGAACCATTGCGTTTATCCCGCATACACACCCTGAGTCTG

AACCTACTTATGTCCCCGTACGTTCCGCCTCGATTGCCGTTTATTAACTAGTCTCATCCTGGGAGAGCGA
AGCATAAGGCCTAGGGCTGGCCCCGGGCGACTCAACGCGCCAGGGACATCTCGAACAGTAAGCGTTCG
CTCGCCCTAAACCGCCGCATTCGTGTGGGATCGGTACTGCCGATACGTGGTCCCGGGGAGCCTCTACAG
GCTGGACACTCGCCTCAAAGTCCTGTTCGTTGACGCAAGGGGTACTACCGCGTAGATATTCCGTGGATC
ACTGGTGAGGTCAAGGTTCCAATCCCGCACAGCGACAAGTAATGGACCCGATCCGTTACTTGATAAGAT
CCGAGGGCGACCGAGCGAGTATGAACGTTAGGCTCGCCCAGACCCTGCTCGACGGTCTTATGCTGTCGG
TGCAGTAGCGCAGCTGAGCGCTCCGATCAGGGGCACGCAAGGCACAGCCCTTATGTTGGTGAGCAAGCC
TCCGTAAGAAGGATTCGGGGCACCGCAATTAACGGCCGGGGCAATTTGACCACGGTGCACATTCATTTC
ACGGCGCCTCGCCGATAGTCCCAACGGAGTATATCGCAGGTGGGTATCAGGTCCTCGCAGGCGCCACCC
GAACTAGCTTTGAAGGGGTAGGGGTCGACTAGGGATGGCCCGTCGCTGGCCAGGAGTGGTCTGGTGCGC
CAGCAGGAAGGTCTGTTCGTAGGTGGGTCATCCGTAGCGACTGGCCCAGCCCTTGTCACCCACAGGCCA
ACTCAAATTCGTCTGACCTTAAATAGGACCGTGACTTGGATTTGCCCGAAAGGGGCTAACCCACTGAGG
CATGGAAAGATGAAACTACAAATTGGTGCGGAATGCCGGCCACTCTTATCGACTTGTCGAAGAGAATGA
AACGTAGTCCCTGGGGTAGGGAGAGCAAACTAAGCTGGGGATGTCCTTGTAGCACGGACGACCTCGCGT
GTCCAATGCGTTAAGGCGAGTCACTACCGCGTTTGGGACGGCGACAAGGGTGGGTTACTGATTCTTCAA
TGGAGTGCATTTCCATGCTAGCACAACCTTTGAAATATAGGGGCTTCGCGCTGAAACTCCACCGCCTGTA
ACGTCCGCGATCGAGTTCCTATCTAACGCACCACCCACGCGGCGTAATGTTCTCATGGCCCAGAACGGTT
CCCAGCGGGTGAAAACCCATACCCACCTCATGGGCTGACAGCATTAGAAGGTGTCCTATTAATGGGCCC
CACGATCTGATCGAGCGCGAACCTATAAAGCTAAGCGGGTACGGGGCATAGAAGGTTACCGACTATGG
ACGGAGCAACTGAGTCCGACCTACGCTCCACGGCGTGGTTTCTCGTACCGCTAAAGTCTGCGACATCGT
GAGACTAGGTTCATGATGGCATTGATCCATTTTGGATGTCTTCTTAACCGTGGCCACGTTATGCGCGGTG
GCGAAGTGGGGAAGTATTCTCAAATATGTTTTGACAGAGGTAGCCCCGCCCTCTCTCACCGGTACGCGC
TCGTGTGAGCAAGCTACGGACGCCCCGATATTGCGCCTGTAACTGTCACGCTCGCGATAGGAGCTCTCG
AGGGGCCGGACTATCGCTGTGGCAAAGTGCTATCCGGCAGAGCGACCAAATGCTAAGCCTGAGCTGGA
CGTAGGTTGCTATCGATCTACGACCCTTAGACGACTCGTTGCTTCGTTATTACGCTTACCGGTGCGTCGA
TCCTGAGTATGGAATTGATCTCTCGAGACACGGCGGTAACACCAGAATTGTTATCATCCAGCGAGGCGG
TTACTAGGATCAGGGCCTACCGTCAATTATGTCGTCCCTTTGGGGCGAGATCGGTATCCCTAGACGATAG
TGACGTTGTCTTTGTCCGGACCGTCCGAAACCGGCTACATTGCCTGTTGTTAGACTGCGTTACTACAGCC
GACCCCTACCATAGCCAAATCCGCCATCAGTGAAAGTTTGGCGACGCTGAGCTTCTAG

Reverse strand：
CTAGAAGCTCCACCGTGCCAAACTTTTCGACATGGCGGATTTATTTAAGGTAGGGGTCAAAGCAAGTAA
CGCAGGGCCGAAACAGGCAATTGTATTGGTTTCGGACACTGTTGACAAAGACAAGTATTCTATCGTCTA
AGGCTGCCGATCTCGCAATTCCGGGACGACATGCGCTTCGGTAGGCCCTCACGGTAGTAACCGCTGCAA
CGCGCCTGAAGATGGATGGTGTTACCACTCGTTCTCGAGAGACACCTCCCATACTCAGACTGATCGCAC
CGGTAGATGCAATAACGAAGCTGCTAGTCGTCTAAGGGGTAACGATCGATAGCGATAGGCGTCCAGCTC
TACAAAAGCATTTGGTGGCACTGCCGGATAGCTTGTGGCCACAGCGATGAAATCGCCCCTCGAGGCGTG
CTATCGCGAGCACACACCGGCAATCATAAGCATCGGGGCGTCACATAATTGCTCACACATCTAAGTACC
GGTGATACATGGCGGGGCTACGGCGGCCAAAACATATCCAGACATACTTCCCCTGAAAACCACCGCGCA
AGCAGGGGCCACGGTTGGGGTAACATCCAAAACAGTGCAATGCCATCAATGCGTTAGTCTCACGCGACT
ACAGACTTTAGATACGAGAGAAACCACCGTCCCGCATCTCGCGGTCCCTCAGTTGCTCGCTCAATAGTC
GGTAAGACCCAATGCCCCGTAGTGCGTTAGCTTTATATAATCTCGCTCGATCACCCTATGGGGCCCATTG
AGAAGACACCTTCTACCTGTTTCAGCCCATGGAGGCCGTATGGGTTTGCGACTGCTGGGAACCCCACAG
GGCCATGAGACTGCCACGCCGCGTGGAGTCCCCGTTAGATAGCTTTAACTTGTGGCCGTCGAAAGGCGG
TGGAACATCGGCGCGAAGCCATTCTATTTCAAAGGTCCGACGAGCATGGAAATTGCATCCATTGAAGAA
CTTAGAACCCACCCTAGTGTTCGTCCCAAACTCTTGGGTGACTCGCCGTTAGACATTGGACACATACAGT

CGTCCGTGCCGCTAGGACATCCCCAGCTGCCTTTGCTCTCCCCAGCACAGGGACTACACCGTCTTGGCCT
GGTACGCACGATAAGAGTCTACTCCATTCCGCACAGATAAGTAGTTTCATGTAGGCATGCCTCAGTTGTG
ATGCCCCTTTCGGGCCCGTCCAAGTCACCGCAGCATTTAAGGTCCCATGGATTTGAGTTGAGGATTGGGT
GACAAGTAAACTGCCAGTCGCTCCTAAGGACCCACCTAGGGAGGGACCTTCCTGGCCATGCACCAGACC
ATTGTCTCCGGCCCTCGGACGCTCCCTAGTCGGGGATCACCCCTTCAAGCACGCTTCGGGTGGCTGGTTC
GAGGACCTGATGTTGACCTGCGATATTGCCAGTTGGGACTATTCCATCGGCGCCGTGAGCTTCGTGTGCA
CCGTACAGCAATTGCCCCGGGTAGGAATTGCGGTGCGCGCCGTCCTTCTTACACTTCGTTGCTCACCAAA
TCTTGGGCTGTGCCTGTGGGTAAGGCAATTTAACGGCTCAGCTGCCGATGCGCACCGACAGATAGTGAC
CGTCGAGCGGTTGCTGGGCGAGCCCGCGACTCATACTCGCATACCCGCCCTCGGATGCAGGCAAGTAAC
GGACCGGGGCCATTACTTGCTCATTTGCGGGATTGCAAGTGTGACCTCACCGATTCTCCACGGAATAGC
GCGTCGGTAGTACCGCCATCGTCAACGAACTTGAGAGTCAATCGATGGGACAGCCTGTAGACAACTACC
GGGACCACTACCCAGCAGTACCGAGATGCTACGAATGCGGGTTCCTAGGGCGAGCGTAACTCTACTGTT
CGAGTAGATCCTGGCGCGTGTGGGAGCCCGGGGCCTAACAGAGGCCTTATGAAACCCTCTCCCAGGACT
GCGTTAGTTAATAATCTGAGATCGAGGCGGCTCACTCGGGGACATAGTGGTTACAGGAGACCTAGCGTG
TATGCGGGTCCTTGGCAATGGTTCCGGATGAGCAGAACACTGCACCATGAGGACTTTGAGTCCAGCGGA
GTCTATGTCGGATCGCCGACGCGGAACCCCAGCAATGGCTTAACATTTTCGGCCAGGCGTGTGCATTTG
ATCGCGGCTGACGCAGTCATCAATTCTGTTGCAGAAACATTCTGCGTGAGTGCTTACACATAGTCCGTCC
AATAGCCTGGTCTCATTGGTCGCGCCAGCTCGGGGCCTCCACCCGACACGGCACACCTTCACTGAGGAA
TCTGTGTGGTTCCTCGAAAGTGCTAGAGATCGTCTTAACCTCAGCTTGACACGTCGGATTTTGCTATCCC
ATATGCGAGTGGACGCCGGCGGGAAACTATCCAAATTGTCACGGAAGTCCGGGTACCGACTTCCCTTGT
TATCCGAAATCAAAACTGGGCGACCGGTACCGCGTCAGCGGGTATAGCTACAAGGTGGACGGTTACACA
TACCGGCGGGCCGACGCGCGAGTTATGCACTATTGGGTTGCTGAAAATTCTCATGAGCGCTACACTATG
GCTAACTCGTATCTTCTAATGCCAGAAGTGAGACCGGGAAAGAAATGACCCACGTTGTCACACCGATTC
GGCGTCGTGGCAAGCAATTTACCGGTACGGTTTGTAAGTTTGCCAGGATCCTATCTCCGGCGGCCGTCCT
ACACTCATCCTAAGGGAGGCTCCACACTCCTTGGATGGCACTCGGGGTGACCCCTTGGTCTGGGGCATG
GCACCGGCCATAGTTTCATCCCGGTTTAGGGACTGCGTCCGCTGCGTAGCTGCCTTTGCAGCACGCTACG
AGGGCAAGCGTCTGTGGAATACGGAACCATCCGCGCGCTTATTAACCCGTACATGTCGATTAGTGGTCC
AGTCCGTATGCTGGTATTAGATACTCAGGGCCACATTACAACGGCCCGTAGAATAATGAAGGATCGAAC
AATGCTCTTATGCGTGCCCAACGGGCTTCTACGGTACATCCGCTGGGTACAATACTAGCAGGTCTGAAG
AGCAGACGGGTGCGGTGTGAAGTGGATACCTTGTTGTGAGGCCGATGCCACTCAGCATGGCGCAGGCCA
GGTCATTCTACACACCACGCTGAGTGGTATGCATGACTGCGAGGAACGTCCCACACGCGGCTAGAGAAT
CTACTGTTGGGGCCTGCGTTCCGTTTGCTTAGGGATTGGGTAGTGTGCTCTGAGCTTCTCTGTGGATTCTT
CTTTGAGAGGTATCTACCGTCCACAATATAGCGCCTGGCTATGTCTGCGGTGGGCCGGCGTGTCAGTTGC
CGGAGTGACGGGGTGCTTTCCAATCGGGCCGCTCTCGAAACTCGCGCCGCCCATTCCGCTCTCACCCACA
GGCAAGAATGCAAAGTCAATCGTGGCTGGGCTAGTGTCATCAACATCGAGTTACTGAACCTGGCTCCAC
GGAGGAACGCCTTCGATTCTGTTCGGCGGACTATCACACAACCGCCTCAGACTCCGCGACTACACAGTC
AGGGGTTTGCCTACATTTCCGGAGGGGTTAGAAGCCGAATTTGGGGACCGGGAGCTTGCCCCTGGCACT
TCTTTGAAACGCTGACCGGAAGCAATGAGCGCTCGCCGAACTCCGGTCCTGTCTGAATCCTCCTTTATGG
GATCAGTACCGGCTTGGGGCCTCTGTATGCGCGTTGAGATTGGAGGAGTTTTGTAACCACCAGTATCTAA
CTTTCGTTACCTGACGGGGCTCACTGTGCAAACCGGCGATGCAATACACGTAAGTTGAAACCTAGCGAA
GCTGCTTTTCAACCGGTCCGAATGCTGCCATAGGACTAACACTCAGGACGTCGAGACGACCGTAAGGCT
GATGGAGGGTCTCCTTTCGGGTCGGTGCCGGCATCTACCTAAGAGGTCAATGCTTGGCATGGTCGGTTA
AGCCCCGTGTGGGACGTGCGGGTCCCATTGCGTTAGTAATTGTGCCACGTCCAACCCACATGAGCATGG
GGCTTCGCCCATACGTCGGGGTCCGCGGTAGAATCATTGAGTCGTCTCTTAGAGCCTGCAGGCTGTGTCA
ATGAAGTGGTAAAGGGCTGCGGTTGGCCGGAGCGGTAGTCCTTTAGGCTTCTCTTACACTTACTAACGTG
GCCATTGGGGTTACCCACCATAACGGGTCCGACTGGTGAGAAGAAGTGAGTCTAGCATGCCCACGAACA

AGAAATACTTCATGGTTAGAACGAGCGCTCCAGTGTACCCCTGTTTCCTGCGATCGTCGTTAGTGTATCT
AACCACCCTGTACGGCAAACACCACCAGGTGCTGTGATCCGATGCTCGGTCCGGCTGCTAGCTGTTACA
CGGTCGGGGTGGACAATTCTGGGGATGGGAAGACGGGATGAGCAAACTTGACGACTCAGAGCAGATCT
TTCTGGCCCGGCCAAACTAACTCGCCGACCTCCCTCAGTTCGACCAGAGGTGACTCACCGACCGTGCCTT
CGCGTGGTATTCTGTCGCGAGCGTTAGACCCGTTAGAGCAACGGAATCACACAGAGTAGGCGCGAGGTG
CAACTCTAAGATTAAGTCCCCATCTGGATCTTCTCGATCATGCATCTGCGTGCCACGGGATAGGCACCGA
ATAGGGGCGTGTTATGCTTCGGGAGCGAGATGTGGAATTAGGTAGCCGTGATCGATCGAGTCACAACGC
ATGTCCTTCCTCCCCGCTGATGTCATCCCTAGCGCATTTCGAATCTTTCCGCGACCTATGCGGCGCTGATC
AGTCCAGGGTCACCCTCGCTCACGCAGTATGTGGGTATGCCGGGCACGGATTATTGGATTGATGCTACG
ACATGTACAGACTTACACACAGGTTTGTAGCCGTCCGTGTCGAGCCCGTCCACCAGAGTAAGACTTCCG
GCATAAACCGCATCCGGTTTAGGGGCACGGCAAACAGTCGACCACTATCTGGAGATCGGGAGGCCCATC
AGCAGTTATCTGTTACCGGCGGCTTAGCACTCCCATATGGGTCGGTGGCCAAGATGTCGGCGGCTGCAC
GAGGTGCGGAAGTCATAATTGAGTACCGGACTTAATCGAGTGATCCACAATCGTATCCCGTGACCGTGA
CCGTTGTATCGCCGTGCGCCGTCTCTTCGTATGAAACTCCTGCGTCCATGGTTATGTCTGCTGGAACCCTT
AAGGGCCGGCCGACCCAACAAGATTCGCCTTGCCTGCTACTCCTCGCTGATAGTGAGTGTCTCTACTATA
AACAACTGGGCGAAGGGAACCTGCAGTTTGCGTTCATCGCTTCGAT

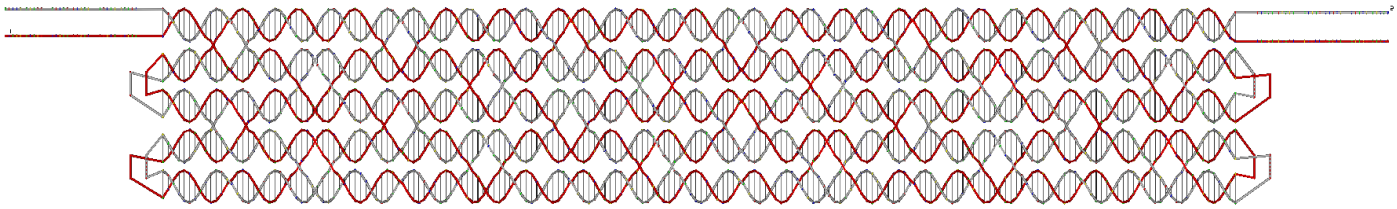

Figure S12-7. Design detail of strip-shape ssOrigami. Red strand is the forward strand and gray strand is the reverse strand.

Forward strand：

TACGGCACGTAAGCCTTGCATTGACTAGCCAACGTTTTGTGCCACGGCGCTATTGTGTCGTCGGTACACT
CGAGACGTCGCCACCTAGAGCTTGGAAGGTATCTTGTACACAGCGTACCGCTGAAGGCGATCGTAAGGC
CGAACAGTTATACGGTGTATTCATTATCCGATAACGAGCGTTTGAACCAGGCAGTTGTAAGGGTTCTCA
ATTGTTACGTAGCTTCGGCGTCCGTTTTTTTGCAAATAGCGAGCTACCAGTCGTAGCACCGATAGCGCGA
CTGGGGCAGTGCTGACGCGACATAAACACCTTGCGCTTTCGTTACGTTTTCTCGGCCATGTCTGACAACT
AGGCGGACTACACATGGAATTTAGTAAATGGCATCCTGAAGGCGAAATACCGCCGTCCAGTGACGACCT
TGATACTAGGTCGACCTCATGAGCTTTTTTTCAGTTATCTAGACTCAATCACCAAATATTGAGACGACCC
TGCTCTAATCTTCCCGCGGTTGCATGGATCGTAGGTTCCATCACGGTTAATGTAAGGGTAACCCTTCGAA
ACTGAGTCGGTTTAGTTGCGGCTCCCTCCTACTCTAAACCGGCGCCTGCCCCATTAGCGTGATGCCGGCG
TCACCAGCATCTAGTCCCTCGTCTTTTTTTGGGTGGGTCTTAGATGGGCGCGTCAATTCTGGAACCCAAG
CAAAATGCAGCCAGAACTGTTATCGATTGTCAGCATAGTTAGACTAGGCAAGTTTCTCCGTAGTTACCAT
AGGCAAAATAAAGGATAATGTGGCCCTCCAAGCTGTTGGGATAATTTCGCACATTTTAGGCTCAATTTC
GCGGGTAATTAGAGCAGCTTGGCTTTTTTTGCACAGCCGTACCACCACACTCCGTGCGTCTGATCCCGCT
TGGGTATTAGGGCCGACTGTTTTTGGGCTACAAGTTATCCTGATTTATCAGAGCAGAAGTTTATGAGTCG
CAAGGTTGTTTCCGAAAGCGATTACCGCTCGAACCCCCGGGACGGCATTTTGCGGTGTTTACGCACCCAT
GTCTTTCGAAGCCCACTGAGAAACAGCGACTAGATAATCGACCGCGTCCCAT

Reverse strand：

ACAGCGACTAGATAATCGACCGCGTCCCATTTCTCAGTGGGCTTCGAAAGACATGGAGAACCAAACACC
GCAGGCGTACGTCCCGGGGAGAGTAGCGGTAATCGCAAATAGAAACAACCTTGCGACTCATAAACTTCT

TCAGTGATAAATCATCCGCCCTTGTAGCCCATGCAAAGTCGGCCCTCATCTTCAAGCGGGATCAGACGC
ACGGAGTGTCGTGGCACGGCTGTGCTTTTTTTGCCAAGCTGCTCGACCTACCCGCGAATAGGAGCCTAA
AATGTGCGAAATTATCCCAACCGCTGCGAGGGCCACAGGCGGATTTATTTTGCCCTAGTTAACTACGGA
CGGATATGCCTAGTCTAACTATGCTGACAATCTGCTCGAGTTCTGGCTTACGCCTGCTTGGGTTATCGGT
TTGACGCGCCAGTATTAGACCCACCCTTTTTTTGACGAGGGACAATACTCTGGTGACGCCGGCATCACGC
TAATGAACATGGCGCCGGTTTGTTCGAGGAGGGAGCCTACACCAAACCGACTCTATCCGGAAGGGTTAC
CCTTACATTAACCGTGTGCTAGCCTACGATCCAAAAACCCGCGGGAAGACGTCTGCAGGGTCGTCTCCT
AATTTGGTGATTGAGTCTAGATAACTGTTTTTTTGCTCATGAGGTCTAATTAGTATCAAGAATAGTACTG
GACGGCAAGATGTCGCCTTCAGGATGCCATTTACTAAACTAGCAGTGTAGTCCGCTATGGTGTCAGACA
TCTTATTGAAAACGTAATATTTGCGCAAGGTGTTTATGTCGCGTCAGCACATGTTCAGTCGCGCTCCAGA
AGCTACGACTGGATACGCGCTATTTGCTTTTTTTCGGACGCCGACGTATCGTAACAATTGGTGCGTCTTA
CAACTGCCTGGTTCAAACGCTCCGAGCAGGATAATGAAGCAACTGTATAACTGTAATAAGTTACGATCG
CCTGCTCCGGTACGCTGTGTACAAGATACCTTCGCAGCGCTAGGTGGCGATTAGACGAGTGTACCACTA
TTACAATAGCGCGGTGGTACAAAACGTTATCCGGCATCGCGATTCATCTTCGCGAATC

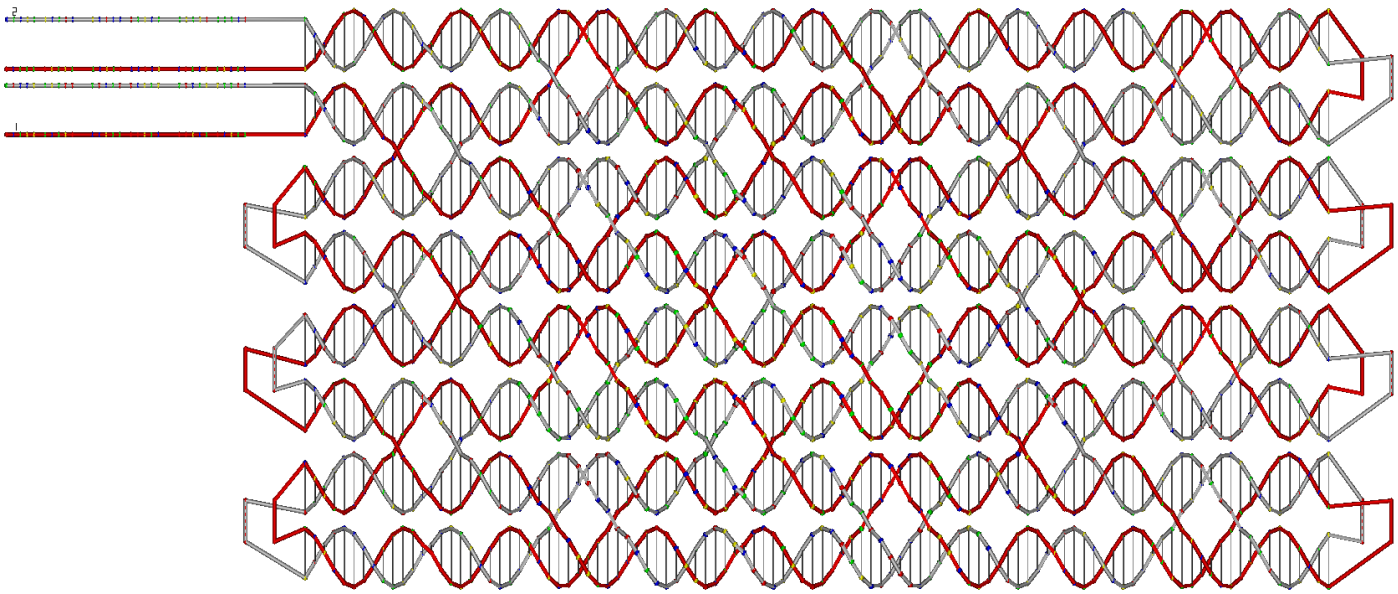

Figure S12-8. Design detail of rectangle-shape ssOrigami. Red strand is the forward strand and gray strand is the reverse strand.

Forward strand：

TACGGCACGTAAGCCTTGCATTGACTAGCCAGTAGTGTAACCCGTAATGACCCAGCCTATTATCGTCTCA
GTCTGCTGGGAGGTCAACCTCTGCGCTCTATAGAGTGGTAAAATGGCTCCGGACAGTGGAGTCAGCTTT
TTTTCAAAACCTGCCTGTCCGCCTACTCTCAAGTTCGAATGCAGGGATTATAGGATCGTTGAGATAGGGG
GGTGGAGGCTATCTCAGTGTGCTCTACGACATCAGTTATTTTTTTTTCCATAAACCAGACGGGAAGGAGC
GTATCAGAAGTGGGACCTCCTTACTATGCAACGCGCTGGTCCAAAATTAGACTATCAGTAACCCAAGAA
TTTGTACTCCAAACTTTTTTTGAATCTCCACCAAATTCCATGCCATGCGAGATCAATCTTAACGCAGAGC
CACTCGGCTGAGTGTGAACGTGACTTGCCTAGACTGTATCGCTTTCCGGTTTTAGACTTTTTTTAGGCTAA
AGCCGATCATCCTCCGGGGAGATAGCACGTGGCTGATTACAATTAGTAACGTCTTATCTAGAGCACTGC
GACATATGAAGCGAGCAGATACTTGAGACGTTTTTTTGGGTGAATCTATCTGCCGCGCTGTTATGTATGT
ATCGCCGGTGACCAGAGCGTAGAAGATTGGCCGAATGCATATAATAGAAAAGTAAGTCCATACTTATAT
AATATTTTTTTTTGCCTTGCTACTTACCAGGAATAACTAGGCAAATGTTAGGTACCTAATCGTTCTAGCTA
TAATGCCAGTACTACTGATTCGGTTAGAGTGTAGGGCCTCCAAGCTTTTTTTTTCCGGTCTTACCCTACAG
CGCTGGACCTGCTCACCCGACCCCATAAGAAAGCCTTTTGTGGACATGCCACCCGGTTCTGATGGCGGC
GCCTGCTCCCTCAGCCATGACAGCGACTAGATAATCGACCGCGTCCCAT

Reverse strand：

ACAGCGACTAGATAATCGACCGCGTCCCATCATGGCTGAGGGAGCAGGCGCCGCCACTTAAACCGGGTG
GCAGCCAATCAAAAGGCTTTAAAAGGGGGTCGGGTATCTCGGTCCAGCGCTCTATTTTAAGACCGGATT
TTTTTAGCTTGGAGGAAATAGACTCTAACCGTACCACTAGTACTGGCTAAATAGCTAGAACGATTAGGT
ACCTAACATTAATTTCGTTATTCCTGTGATCGAGCAAGGCAATTTTTTTTATTATATAAGTCGTAACTTAC
TTTTTAATCGTATGCATTCGTGTCCACTTCTACGCTAGACCCACCGGCGATACATACATAACAGCGCGGG
GCGGAGATTCACCCTTTTTTTCGTCTCAAGTCCGCCCTCGCTTCATATGATAGAGTGCTCTAGCTTTTACG
TTACTAATCAGCAGCAGCCACGTGCCCGACCCCCGGAGGAGTAAGTGCTTTAGCCTTTTTTTTGTCTAAA
ACCGGAAAGCGATACAGTCGAAATTAGTCACGTTCCCTATCAGCCGAGTGGCTAGGCGTTAAGATTGGA
GCAGCATGGCATGGCAGCACGTGGAGATTCTTTTTTTGTTTGGAGTAGTGCTGCTTGGGTTACTGTCGCT
CTAATTTTGGGGTCTCGCGTTGCATAGTAAGGAGGTCCCACTTTAAGTACGCTCCTTTACGGGTGGTTTA
TGGTTTTTTTAATAACTGATGTATGGGAGCACACTGGTCGGGCCTCCACCCCACACTCTCAACGATCCTA

TTTACCCTGCATTCGAACTTGAGAGTAGGCTGAGAAGCAGGTTTTGTTTTTTTGCTGACTCCATTCTCAG
GAGCCATTTAATCAGTCTATAGAGCGCCTAGGTTGACCTCCTGTAATACTGAGACGACGATTAGCTGGG
TCATCCCGTCTTACACTACTATCCGGCATCGCGATTCATCTTCGCGAATC

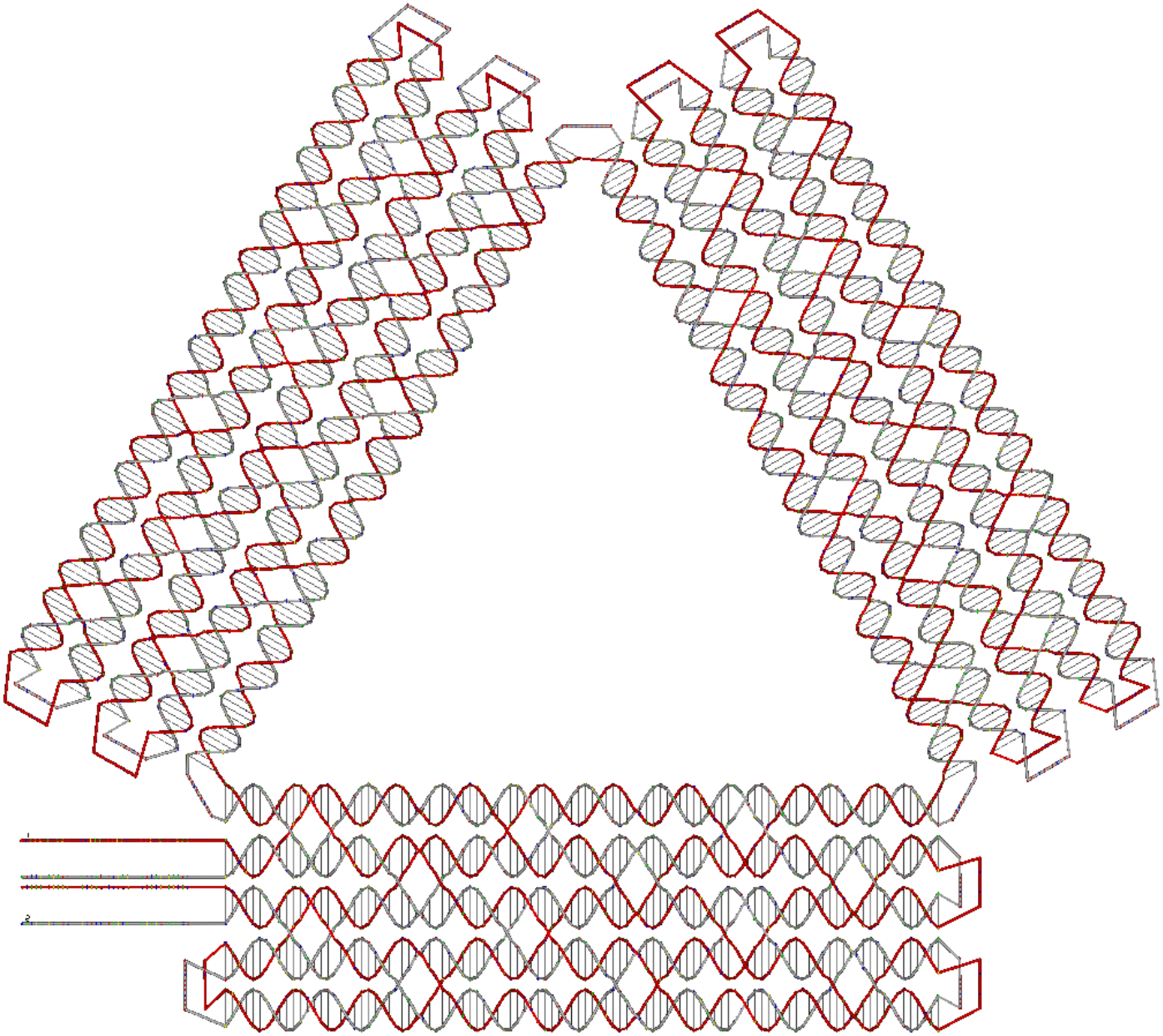

Figure S12-9. Design detail of triangle-shape ssOrigami. Red strand is the forward strand and gray strand is the reverse strand.

Forward strand：
TACGGCACGTAAGCCTTGCATTGACTAGCCAAAGTGGACGGTCTTTAGGTTCACAACTTGTTGGCCGATA
GGCCACACAGATGTTCTAGGGCACAAGGACGCAAAGCGGAATTGGGTGTAAGCCGGTCGGTTCGACTTT
ATTTATTTTACAGCTTTACCGGCTTGATACGGCCGGAGCTCCAGTGCTCCTACTTACAATGCATAGTCGG
ATTTTCTTAACGGAGTGTTTTTAGAAGGAAAGACATTAGAGTCGAGCTAGTTAAATAGGACGCAATCAC
CGAGGGCATAGGTTATCGCCTACTTTCGTGCCGAGATGGTCGCATGAAAGTGCCTGCTGAACTGATTCA
GATGGTCTGGGTTTTATTTATTTCCGAGGCTGGAGCGTGAACAGCGTAAACTGGTTGATACCTCTTCGAC
TATACTAACCTTAGAAATTTCCACTCCGCCCTCGCTTTTGCCATCTGTAGCCTTAGGCTTTTATTTATTTG
CATAACTTGTACAGAAACCATTACTGCTGTAGTTTTCATGGGACGCTTAGGTCTGGCAGTCGGGCGCCCT
GAGCTATCACATTACGAGACACGCTGATGGCATCCTTTATTTATTTCCTCATCTATCCACAAGTCAACGC

CACTGAATGAAACTTCACCATGGATAAAATGGATGTAGGCGATCCGCAAGTACAGCCCCCGGCCCCTGC
GACGTGTTTTTTGTTTATTTATTTTCGAAAATTTGTCGCATCCCCGCGAGATGTGTTAAATCTAGCGGTCG
GGAGCTTATATGTCAAACTAGCAATCTACCAGTTCAGTTTTTGTTGTGGGAAGGGATTCTAAGTCTGTGC
CTCGATCATATTTAGCAGATAGATAAGTCCGCCGAGCAAGCTGACAGTTTAGCAACTATGAGCGGACTC
GTGGGTATAGGATCGGACAAGAATTCTTTATTTATTTGAGTGTATCTAGAGTCTCGGTCCGGCAGCTCCT
TCTATGTCGTCTACCAGCTCACGCTGGTATAAACCATGGATTATCTGGCAATTCGCGCGCCAAGGCAACT
CGGTTTATTTATTTGAACGCTCGCTTGGCGCACCTCCCGCTCAAATCTGACCCGCGGGAAGATTTACCGG
CCCTCTAGGTGGTGATCTAGAGCGATAAAAACCGGACTCTTCCTGAAGAGTTTATTTATTTTCTATATCT
ACGATTTGAATCTGAGCCTACTCTGTAACGTGATGATGACTCGAGCCTGGCTCGGAATGTGTATAATTTG
ACAGATGATTCTGTGACAAGTTACGGGTTTATTTATTTTAGCATCGCGGTCACAGCACCGTCCCTGACAT
CTCATTATTTCCAGTGAGAGGAAGAACGTCTAGAACTTGCAAGGAGCTACTCCCCCTCAAATCGCTGGG
AGTCCTGTAATCGATAGTTGACCAGGATTAAACGAGATAAAGGCCCTGTGCCCACCCCTAGGGCGAGTA
GAACAACGTCGAGCATACTCACTAATATGGGCGGCAGTGAAGTTTATTTATTTTACTGGAAATTAAGAG
GCCACAATGCACACTCATGAACCCGAGGGGGTCCTTTTTGGTCTGTGGTAGTTATGTATCTCGTCAACTC
AAATAACTTAAGTACGGAAATTTATTTATTTCACTCTGAGATAAGTTTCCGGCTTGATCCGCTATATTTA
ACCAACTTAGGGGCTGAAAGAGGAATACCCAATGTTCCTTATTCGATTGATCTCTTATTGTTCGAGAACA
GCGACTAGATAATCGACCGCGTCCCAT

Reverse strand：

ACAGCGACTAGATAATCGACCGCGTCCCATTCTCGAACAATGTGCCATCAATCGAAATGCTCACATTGG
CTATTCCTCTTTCAGCCCCTAAGTAGGTTAAATATGCATTATCAAGCCGGATAAACGTCTCAGAGTGTTT
ATTTATTTTTTCCGTACTCGTTTAATTTGAGTTGTTCCCATACATAACTACCACAGACCAAAAAGGGTGT
GGTCGGGTTCATATATAGGCATTGTGGCGGCACAATTTCCAGTATTTATTTATTTCTTCACTGCCGCCCAT
ATTAGTGAGTTAAGGAGACGTTGTTCATCCGACCCTAGGGGTGAGGGTAGGGCCTTTATGGGAATTAAT
CCTGGTCAACTATCGATTACATTTATTTATTTGGACTCCCAGCGCCCAGAGGGGGAGTCAGAAGTTGCAA
GTTCGCTAAATTCTTCCTCTTCTTCCAAATAATGAGATGTCAGGGACGGTGCACGTACCGCGATGCTATT
TATTTATTTCCCGTAACTTGTACGTGAATCATCTGCACCAATATACACATTGTTCCTCAGGCTCGAGGGT
AGATCACGTTACAGAGTAGGCTCAGATTCTGGGCGTAGATATAGATTTATTTATTTCTCTTCAGGAATCT
CACGGTTTTTATGAGTCCAGATCACCACCTAGAGGGCCGGTAAACACTGGCGCGGGTCAGTTGGTGGCG
GGAGGTGACAGTCGCGAGCGTTCTTTATTTATTTCCGAGTTGCCGACTGTCGCGAATTGCAAATTAATCC
ATGGTTTATACCAGCGTGAGCTTCATCACGACATAGAACTTCTGGCCGGACCGATGAGATAGATACACT
CTTTATTTATTTGAATTCTTGTCCGATCCTATACCCACCGCTCTGCTCATAGTTTAGACGCTGTCAGCTTA
GGAACCGGACTTATCTAATTTCTAAATATGATCGAGGCACAGACTTATTTATTTATTTGAATCCCTTCCCT
CTGCAAAAACTGATCTTCAAGATTGCTAGCCATCTATATAAGCTCAGCGTCGCTAGATTTAACACATCTC
GCGGGGAGAAACAAAATTTTCGATTTATTTATTTCAAAAAACACTGTTTCGGGGCCGGGGAGGGTGCTT
GCGGATCCCCACGATCCATTTTAAGTCGAGTGAAGTTTCATTCAGTGGCGTTGACCAGAGGATAGATGA
GGTTTATTTATTTGGATGCCATCGCGATTTCTCGTAATGAGGCACCTCAGGGCGCCCGACTGCCAGACCT
ACCGACCCCATGAAAACCACCCTAGTAATGGTTTGTTCTCAAGTTATGCTTTATTTATTTAGCCTAAGGC
AGAACATGGCAAAAGCACGTCCGGAGTGGAAATTTCTAAGGTTAGTATTCCATGAGAGGTATCATGAAG
ATTACGCTGTTAATCGCCCAGCCTCGGTTTATTTATTTACCCAGACCATCTGAATCAGTTCAGCTGATAG
TTTCATGCGATTTGACCGGCACGAAACGTGGGGATAACCTATGGACGTGGTGATTGCGTCCTATTTAACT
AGCTTTTATTTATTTCGACTCTAATTTTTCGCCTTCTAAAACTATATCGTTAAGAAATACTCGCTATGCAT
TGTAAGTTGGAGCACTGGAGCTCCGGCCGTATCACCCCGATAAAGCTGTATTTATTTATTTGTCGAACCG
ATCGGGGTACACCCAATTAATGCTTGCGTCCTTACCCTCTAGAACATCTACCCCCCCTATCGGCCAACAA
GTTGTGAACCTCGAAAACGTCCACTTTATCCGGCATCGCGATTCATCTTCGCGAATC

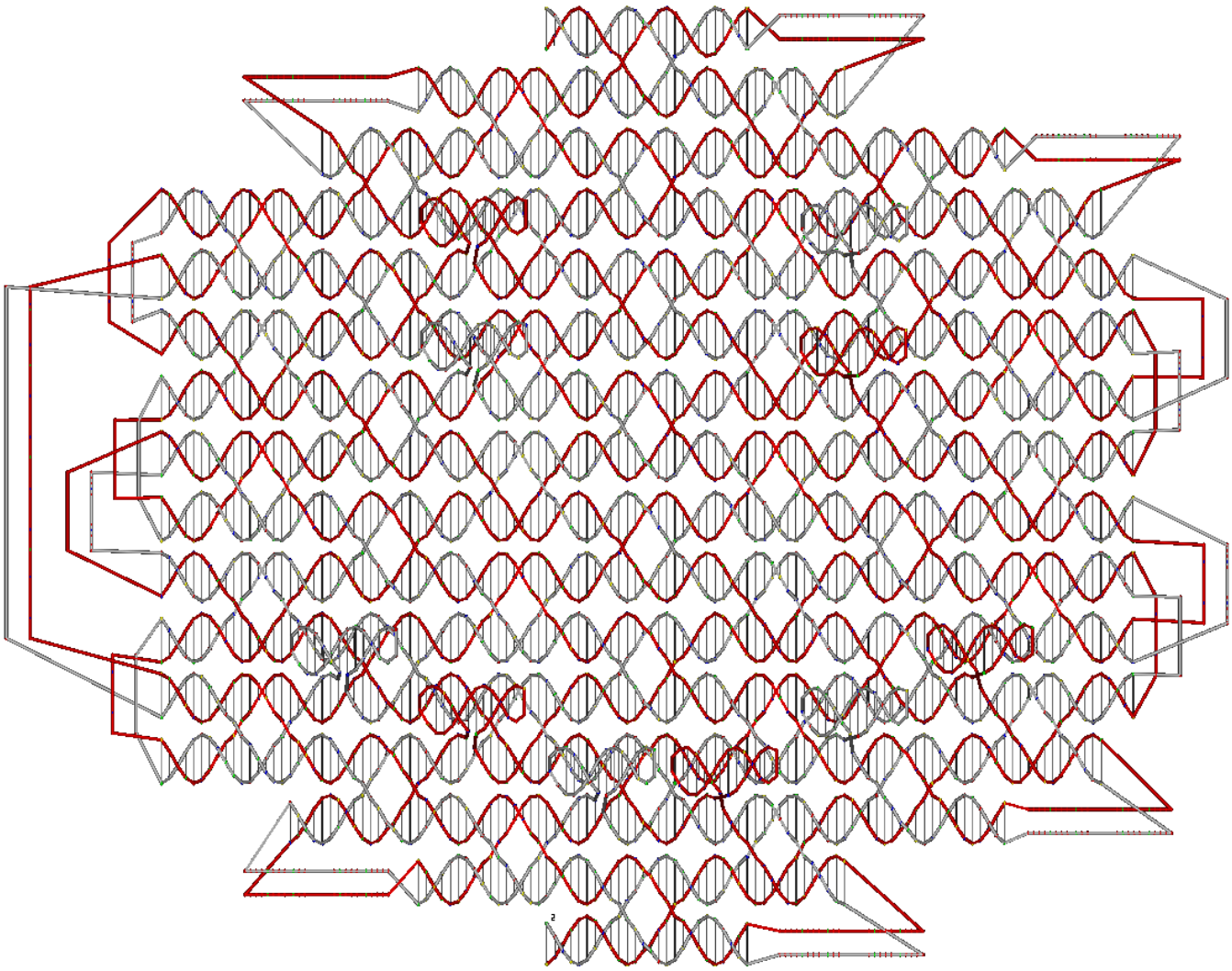

Figure S12-10. Design detail of hexagon shape ssOrigami with patterned smile face. Red strand is the forward strand and gray strand is the reverse strand.

Forward strand:

CACTTAGTAGGACTCGACTTCGTTCCGCACCACAACAGCCGACCAAACTCCATTACTTTGTGTACGGCCT
TGTCTTTATTATTTGAGGGCTAGTACCGTCGCTGTCAGAGATCCAATAATCGGCACGCCATGTACCCAAT
TACTGTTGGTCGATGCTGCCATCTAAGCGGTTTCTTTTCTTTCTTTCTTTCTTTTTTGCCAGTATGGTTAGT
GCCCGTTCACAGATCAGTTCACCAGTCCCGTTCAATCCCTCTGGCTAGCCTCATGGCAATGAGGGCTCCT
GGGAGCCAAATACACGATCTTGTAGTAGCAGTTTTTGTCCAGCTTTATTATTTTACCAGTGGACTCGAGT
TTAGGCATAGGTATCTTTACTACGTAGCTAGAGCAAGAAGTTACAAGGTCCGGCTTCCATCATGATGTG
ACGCACGGGAACTAAAGACTACTCAGATGTTACCCATTTATTATTTTAGAGCAACCAAGGGCTGAGCAC
CTTGATCCTTAATACCGCGCTGGTTGTCGAGAGAGACCCCACATCGTCGGGCAAACGTATATGAGTCAC
TACAGCGATTCCTATCCGTATAGGACCATGACCATGGTCACGCAGTGATCATACTTTTCTTTCTTTCTTTC
TTTTGAAAGAGCGTCATCCTCATTTGGGTGCACTTGATACGACCGAGACTTAAGTTAAGCGTGCATGAA
GTAAGCAGCCTTACCGATGTCAAGCACTAACGTGGCCTAAGTTTATTATTTATTCATACTCTACGCACTA
CAGTGGACAACCAGCTTTAACGCAGTCAATCCTTCGGTACTGGATTAGTCAATCTTATCCAAGATTGACA
ATTTTGTCATAGCGAATACGTTTGGTTTTCTTTCTTTCTTTCTTTTGCTAGCGACCGTGGATTCTGGTCCGA
CCAAATAAACCAAGAACCCAACAGGTTCAGGTATGTGGCACGCAGTCGTTTATTATTTCTTATTATTTCT
TATTATTTCTTATCATTTCGGAGACAAGCTGAGTCCACAACGCTTCGCACCAGACCCCAAAGATGGGGGT
TGCTTTCTGCAATTTGTCAGTGTTTTCTTTCTTTCTTTCTTTTGCCGAATGGTGCACCGTATAGAGAATGA

CCTAGATAGATGTGAAGTGAAAACTTTGGTTTTACACCGTACGGTGTGTAGGCTGCAATGGATCTTCCGC
GCCCTTGATTCCATAGTTTATTATTTCTCCGCCACTGTTAGTCGTTCCCCGCTACAAGGTCGTGACGTATG
ATGAATCATCATCTGTGAAACGTCCTCAGCATGGCGCTACTACCTACTTCGGGTTGACCTCTTTTCTTTCT
TTCTTTCTTTTCTGTCATACACATGAGGTGTAGCCTCAGGTGCCATTCGCAGAGGGTATATTAGGAAGGG
ACAGTGCGACTAACCAGTCTCGCTAGCAGTGAGGGTGACACCTTGCGTATACAAGAATCTTTATTATTTG
TTCTACTGGCCACATTTCTTGCTATGACTGCCTTACTTCGGTCATGCCCCTTCCACACGCTTGGTGACTAT
GACTAGCTCGCACCCAGATACTTCGTTAGAAGCGGACGGTCCTATTGTGCTTTATTATTTGAGGAGGAGG
AACTGCGCCCAAGATTCTATGTACAGGAGTGTCGTTTGGCCGTTTTTGCCTAGGACCCGTAGGTTTGACT
CTACTATTTGATAATAGTAGCTGTATAGCTACACGAAATGCACACGAGATTGCATTTTCTTTCTTTCTTTC
TTTTGCGCAGAACGATTTGGTTCATATAGCAAGCGCGAAAACAGTTCAAGTGTTGAAGTGATGTTCGGG
CAACTGCATCTCGAGAGACTAGTAGTTTATTATTTGACATTCAGCTCACTGTCAAAAGCTGACGTTGATC
GTCAAACGTATTCTGCCAGGTGGCAGTCGCGACTTCTAG

Reverse strand:
CTAGAAGTCGATCCACCCACCTGGCAGCGATCGTTTGACGATAGGATGCAGCTTTTGATGCTAGGCTGA
ATGTCTTTATTATTTCTACTAGTCTGCATGCATGCAGTTGCTGTAGTATCACTTCAATCGCTAAACTGTTT
TCATCCAGGCTTACACGCCCGTGTATAGTGTATTCACTAATATGAAGCCATGCGTTCTGCGCTTTTCTTTC
TTTCTTTCTTTTTGCAATCTCGGTTGGGTTTCGTGTAGTCCCTCACCTACGGGTTAAGTCCAAAAACGGCA
GGCTTACACTCCTGTGATACCAATCTTGGGCTCGAGGCCTCCTCCTCTTTATTATTTGCACAATAGGAGA
TCTCGCTTCTAACTCGTGTTCTGGGTGCGCTCCACTCATAGTCACTGGGGTTGTGGAAGGGTAGCATCCG
AAGTAAGTGGTTGATAAGATGATTCCATCTTCTAACTATTTAGAGCAAGAACTTGTACCAGTAGAACTTT
ATTATTTGATTCTTGTACAATTGAGGTGTCACCGGTAAGGCTAGCGAGAGAACCGAGTCGCACTGCTTGT
ACCTAATATACTTATACCGAATGGCACTTGGATCTACACCTCAGCATGGTGACAGTTTTCTTTCTTTCTTT
CTTTTGAGGTCAACCGTTTGGAGGTAGTAGCTGACATCTGAGGACGTGACTGGGATGATGATTACGCGC
ACGCGCACCAGGGTGCGAGTTACTTCTAACTTCACGACAGGATCGCGGGGAACGGGACCTAGTGGCGG
AGTTTATTATTTCTATGGAATCCGACTGGCGGAAGATCTCCCGTAGCCTACCACCGATAGTCTATCTAGG
CAACAGTCTATACGGTCAGGACTTCGGCTTTTCTTTCTTTCTTTCTTTTCACTGACAAACGAGTCAAAGCA
ACCCTGCTCATTGGGGTCTGCCATACAGCGTTGTGGGGTTCTCTTGTCTCCGTTTATTATTCTTTATTATT
CTTTATCATTCTTTATTACTTCGACTGCGTGTACAAGACCTGAACCTTGTGCATTCTTGGTTTCATGGCTC
GGACCAGACGACTGGGTCGCTAGCTTTTCTTTCTTTCTTTCTTTTCCAAACGATCGCGCTATGACTAGCGC
TTTACCGAAGGAGAGGGAGCGTTAAAGCGCAGTCTCCACTGTAGCAATTGGAGTATGAATTTTATTATTT
CTTAGGCCACAGGTCCGCTTGACATCCTCACTGCTGCTTACTATGCTAACGCTTAACTCCTAGGTCGGTC
GTATTAGCGACACCCATGTAGCGCCCTACACGCGGTATGCCGCGAATGCAACGTACGCTCTTTCTTTTCT
TTCTTTCTTTCTTTTGTATGACTAGCACGTGAATCGCCCGAACGACTCATATAAAGCCTCCCGACGATGC
AAGCGCTCTCTCGACCGGTTCCGCGGTATTACTTGTAAAGGTGCTCACAGTCGGGTTGCTCTATTTATTA
TTTTGGGTAACATAGAACCAGTCTTTAGTCATTGCGCGTCACATCGCGCGTGAAGCCGGACTCCCTTACT
TCTTGCTGTGGAGACGTAGTAAAACATAGTATGCCTAAAGCATGCTCCACTGGTATTTATTATTTGCTGG
ACAAACCTCGATACTACAAGAGAAGTAATTTGCTAGCGTATAAGATTGAACGGTTCACATGAACTGATC
CTATCGCGGGCACTAAGTGCGATGGCAATTTTCTTTCTTTCTTTCTTTTGAAACCGCTTTGAGCACAGCAT
CGACTCATTCTAATTGGGTAATGTCAGTGCCGTTCCTCGCGAGGAAACATTATATAATGTATTACTGAGG
CTCTGACAGCAGATCTACTAGCCCTCTTTATTATTTGACAAGGCCGCCATGCAAGTAATGGACGAAGTTC
GGCTGTTGGTCCTGGGAACGAAGTTTGCAGCTACTAAGTG

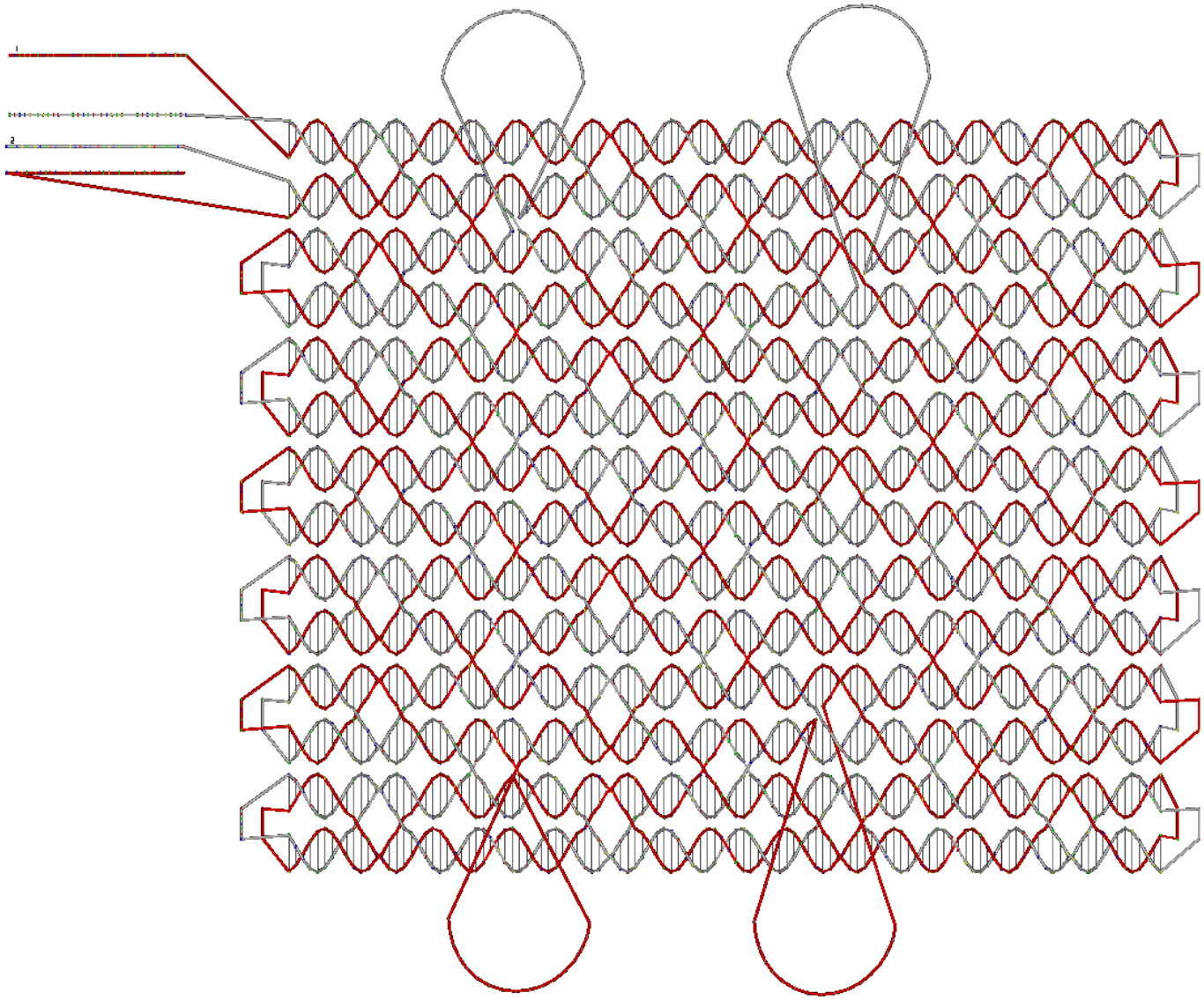

Figure S12-11. Design detail of rectangle shape ssOrigami with single-stranded loops for nanomaterial attachment. Red strand is the forward strand and gray strand is the reverse strand.

Forward strand：

TACGGCACGTAAGCCTTGCATTGACTAGCCGACAGGATGTAATGTTCGGCTTACAGAGGGATTCCTGCT
GTAACCGCAGCCTTGGATCTGCTAGACCACCGCTTCCAGCGATGGATAGTGACTGACTTAAATGTAATA
GGTGCGGTTTGTTCCAACACTTTGGCACGGTCACCTATAGTGTCGGTTGTTCTAAGCAGGTATATAATGG
CATATCCTTTCTGACCCACGGACAGGCAGCCCGACAACGCCTTACTCTATAATGTTTCGGTTGTACTGTG
ACCGATTCTTATAATTATACACGAGCCTCAATTGTTGAACTGGGCTTGTTTGTAATATAGGCTTGTCAAC
ACGTATTTACCAATCACTTGAACAACATTCCTAGATACTGTCACTAGGTTGACCGCTACTTCTTTCGGGC
CGTTTCGGTTGTACTGTGACCGATTCTTATGATTCATGCGTGTTCTTATCACACTCTTACTTAGTCATCAT
TTTACTCACTAAATTCCAAATTTACCGTAATGATGCGCTAAGATAAAGCGACAACAGGCCCCTGCACAA
GACAACAAGGCACGACGGCTTGTGAATAATAGCAATCTGACAACAAGGAGAGTGAATTGCGTACCAGT
AATTAGGCTCGATCTTACTCCGCAATTTACGGCAATATTCGGTTTGGAGACGCTATAAACGTACAACCTT
CTGTCGGACGGAGTCACCACCAGGAGCGAGTTGGCGGAGCAGAGCTCTCATTGCACCGAAACCACAAA
CCAGCCGGTTCAATGAGGCCTAGCCTGTATCCGAGAAGGATACCGCTGGTACAGAGCGGCTTAACTATC
CCATTATTCCGCTTAGATTATCGGAGTTTCGACAAGACAACAAGCCGCAATGGATCATGCTACAAGATC
CTCTTGTTAGTTCTAGTGGCACCTATTTCAACGTGGCTGCGCGTTTTTTGAGCCACGTGATGTGTATCTTA

GCATTCCATAGGCAACCCATAGAAGTTGAGGTTGGACGGATGGGTCAGACCCCTCGAAACAACCTCGGC
AGATTTTATTGTGCCTCTCGGTCCGCATGCTTTGGATGTTTGCTCGTATCTATGACTCGCACACTCACAAC
GTGTTAGATGTACTCATTACCTGGTCATTCCAGAATGTGCGAGAGACATAGGTAATAAATGCAACCAAG
CGTCTACTTATATTATTCACCAAGCGACAGAGCGGCAGCACCATATAATGCCAAATACTCTACTAGAGC
TTGACATGGGGTAGTTATACTGTCTGTGGCCGGACGAATCTACCCCAAATTGCGACGAAATTCCAATAC
CACGTGGTGAAAGCAAAATCGAAGCACCGCTAGTGTGCGGTGACCAGGCACGGTGCGGGGTGGCGGAG
TAAAAAAGCGTAGGCCTAAGATAGTGTTTGTATTTTACCAGGCGTTCAATCATGTTTCAGTGAGGCGGA
AATAATAGTTCATGGCCTCCAGTGGGTCATTATCATGTCATGTTCTTCGATGGCCATTACTACCAAACCC
TCATTGCCGGCTAATGCGAAAGTGGTAGTTGGCAACAGGTGGTCAGGGGAACTGCTAAGAAGCCGACA
CGCCAACGCCAATCTGGCTAGGAAACAGCGATAGTGGGCAGGGCACACGTGTTAAAGCTCTGGCCCCCA
TCTCGTGGCCTGTCTTTAACGTTCGAAAGGCTTGATTAATCTAGAGTGCGAGATGTATCGGAAATGGTTA
AAAGCGTGTGCAGGCGTCTGAGAACGTGGTCTTAGACACATACGATCTTTAATTGTAGTGAAGGCCTGT
ATTAATCGTACATTCTTGAAACAAGCGTATCGTGATCATTATTAAGTCCTTCCTTTGCCACGTATGAGTT
ATAGTCGAATTCTAGTCTGTATCGTTCGATAACATTGCATATAGCCACAGCGACTAGATAATCGACCGCG
TCCCAT

Reverse strand：

ACAGCGACTAGATAATCGACCGCGTCCCATGGCTATATGCTGGGGCATCGAACGATACAGACTAGAATT
CGATTCCTCCTCATACGTGGCTTCGGAAGGACTTAATCGGAATCACGATACCGGATATTCAAGAATGGG
GAAGTAATACAGGCACCAAGCACAATTAAAGCTTCCCTGTGTCTAAGGTCAGTTTCTCAGACGATCAGA
CACGCTTTTAGGCCATTCCGATACATATTACACTCTAGATTAAGGTGCCCTTTCGAACCCATTGGACAGG
CCACAGGCGACGGGCCAGAGCCAATGGACGTGTGCCCGTGTATCTATCGCTGTTTGCATGCCAGATTGG
CGTTGGCGTGTCGGCTGGCTACCAGTTCCCCTCACAATCTGTTGCCAACAGAGACTTTCGCATTTCCATA
GAATGAGGGTTTCTCTGTAATGGCCATGAGTGTACATGACATGACCGCGACCCACTGGAACCATTGAAC
TATTATGCTGTTCTCACTGAAACGCTTGTGAACGCCTGGCTGTTTACAAACACTATGCATAGCCTACGCT
TAACAGCTCCGCCACCCTGTTGTGTGCCTGGTCAACAACCACTAGCGGTGCAAAGATTTTGCTTTGTGTG
AGTGGTATTGGAATTTCGTCGCAATTTTCACTCGATTCGTCCGACATACGACAGTATAACGAGTGAATGT
CAAGCTCGCCAAGAGTATTTGGTTCTGTAACCGTTTTTCGGTTGTACTGTGACCGATTCTTCCTATTTCCG
ATATGGTGCTGCCTAGCAGTCGCTTGGTATGCCATATAAGTAGACATGATGTTGCATTTAGTATCAATGT
CTCTCGGAATGGTTGGAATGACCTGATACTGAGTACATCAACTCCGTTGTGAGTGTGTAATTCATAGATA
CGTCAGAACATCCAAAGTTGTCTGACCGAGAGGGACCACAAAATCTGCCCCGGACGTTTCGAGGGTCCA
CTACCATCCGTCCGTCCGGAACTTCTATGGGTTGCCTATGGAATGGTAGCCTACACATCACACCTAGCAA
AAAACGCCTTCCTACGTTGAAATATCAAGCACTAGAACTATCTACAGGATCTTGTGTCACGCTCCATTGC
GGGTAGATGTCTTGTCGATAACACGATAATCTAAAACAGCTAATGGGATAGTGCCTCCGCTCTGTACAG
AGAGTATCCTTCTGCTTGTCAGGCTAGGCATCTGAGAACCGGCTGGCTACTCGTTTCGGTGCTCAGATAG
CTCTGCTCCTAGTACTCGCTCCTGTCACACACTCCGTCCGACAGAAGGTTGTACGTGAGGAACGTCTCCA
AATTCGTAGATCCCAGTTCGGTTGTACTGTGACCGATTCTTAGTATTATCCCTATTGCCGTAAAAAATTG
AGTAAGATCCTGAGTTATTACTGGTAAATTTTTCACTCTCCTCGCACCCAGATTGCTATGGCATACAAGC
CGTCGTTAAGTGTTGTCTTGTCTGATGGCCTGTTGTAGAACAATCTTAGCGCGAAATTACGGTAAATTAC
GGACATAGTGAGTAAAATTTCGACTAAGTAACGAAGAGATAAGAACAAGACAAGTAGCGGTCAGTGGC
TTGACAGTATCATGCAATGTTGTTCAAGTGATTGGTAAATACGGAAGACCAAGCCTATATTCACTACAA
GCCCAGTGTCTTCATTGAGGCTCTGCCCAGGCGTTGTCGAGGAAGCTGTCCGTGGGAGCAAAAGGATAT
GCCGCGGTATACCTGCTTCGCTTTACCGACACTACTAAAAACCGTGCCAAGTTCTGGGAACAAACCGTTT
TAGTTACATTTAAACCACGCACTATCCATTCTCTGAAGCGGTGGTCGCTCTGATCCAAGGCGTTGTTTAC
AGCAGGACCGAATCTGTAAGCCGGCCCCAACATCCTGTCATCCGGCATCGCGATTCATCTTCGCGAATC

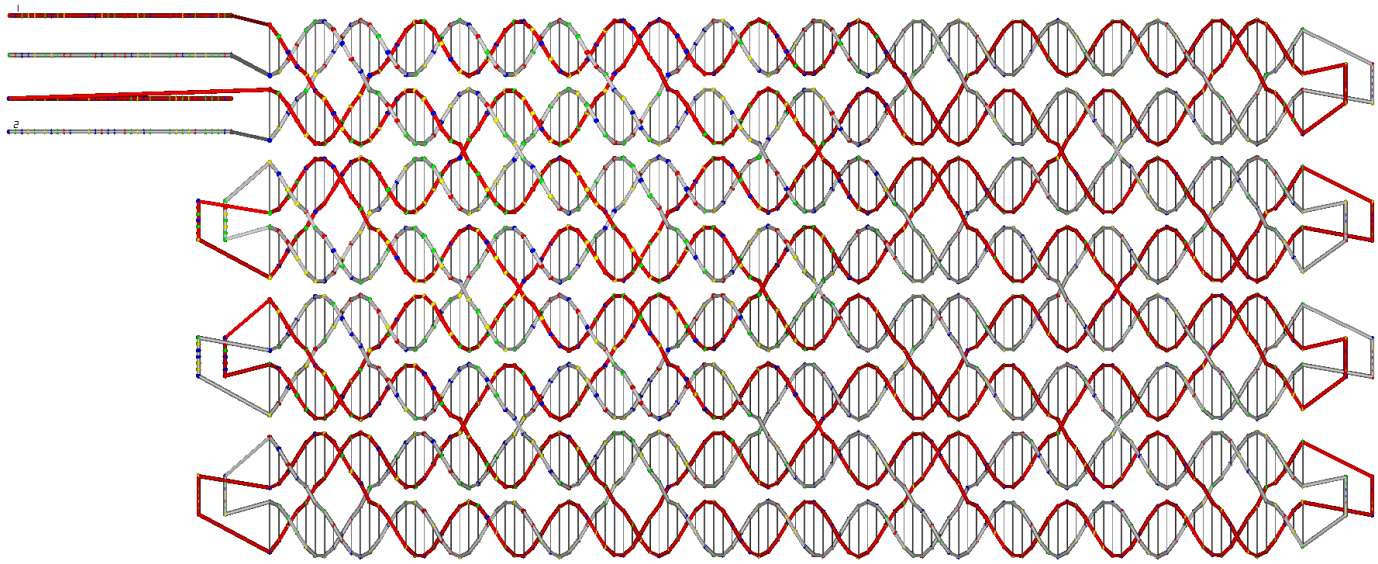

Figure S12-12. Design detail of rectangle RNA ssOrigami with 6bps locking domains. Red strand is the forward strand and gray strand is the reverse strand.

Forward strand:

TACGGCACGTAAGCCTTGCATTGACTAGCCTCAAGAGAGCCGGAAGGGATCTCCGCCTGTGCATGGGAC
TGCGCAGGTGCATGCCCGGGCGAGAGTAGTTGTCAACCGGCTCATCTGCTGGATCGCTCTACAGATGAT
GCCCACGAGCTATTCACGCGCATCACTGATACAGATGGTCATGCACGTGTACGAAACCAACCTTCATTG
TATATGGACCCAGATAGACTCCACTATAAGTGTGGAGATACGGGTAGGCCTTAATACCTCATCACTGGA
ACCATTAAGCTCTCGGGCAACTACGCGGAGCGCGTGATTAAATAATTACTGCTCAACAACAGAGTCATA
CCTTTCCCACGTTGCTGCATCAGCTCCCTACTACATTATCGCTCTCAAACGCTGAGATAATGGGCAATCC
TAACATCAAGATCGCTGGAGGTTGACGTCCCTATATGTGCAGCCCTGAACCATCCGATGGATCCTCAAC
CGACGCAACACGTTGCAGCTGAATATAGTCCGCTAGGGCTCAGCTGATGTCATGAGTGTGTTCAATTTCC
TAGGAGTCTGCACAACTGCTAACCCGCTAATGAAGGACAACTTACCTGAAAGCCCTACCGAAGCTCTGG
AGAGGGTTGGGTTAGTGACCGCCCTCTCAAACACCGGCCGGGCCTCCTCGTTCACGAAAGGGTATATAT
ACTGGTAAGACATCGATATGCGCAGTGGTGTAATAGCGCGCCGTGGGTACAGCGAGCTCCTACTATACT
ATGTTCAGCTCGAAATCGAACTTGTCGTCTCCTGAGCTCATCGGAGCTCTGTAAAGTACCTAAATTGTTG
ACGGTTTCTTATATAGTTCATGTAAGCCTCTGCAGATTGCCACGAGGTATAGAGGCCGGGCAATCGACTC
CCGACCGCTCAAGTTCTCTTGGTTGTCCGCTAGAATGCTGGCTTCCTCCCTTTATTTAATGAAGGAGAGA
CTAGATGAGTCGTATGAGGCTCTGTTCTACAGCGACTAGATAATCGACCGCGTCCCAT

Reverse strand：

ACAGCGACTAGATAATCGACCGCGTCCCATAGAACGTATATTCATACGACTCATCTAGTCTCTCCTTCAG
AACGTAAAGGGAGGATTACCACATTCTAGCGCCGCAACAAGAGAACTTTGATGTTCGGGAGTCGGTCCC
ACGGCCTTTATGACTCGTTGGGACCTGCAGAGGCGATCCAGAACTATATAATTGATCGTCAACAATTTA
GGTACTTTACAGAGCCCGCCCGAGCTCAGGAAACACAAAGTTCGATTTAAACGAGAACACGAAGGAGT
AGGTCGTTTCTGTACCCACGTCTCCATATTACACCAAGGTGAATATCGATGTCAGCCAGGTATATATACC
GCGTGGTGAACGAGGAGGCCCGGCCGGTGTTTGCTGGAGCGGTGATAATTCCAACTCCAGCCAGAGCTT
CGCTGATGCTTTCAGGTAATTGCGGCTTCATTAGCCGCCCGGCAGTTGTGCATAAAGGTAGGAAATTGG
ACGACCTCATGACATCTTAAGCGCCCTGCTGACATATATGCTTAAGCAACGTGTTGCGTCGGTTGAGGAT
CCGGGCGGTGGTTCAGGGCATATACTATAGGGACGCCCATATCCAGCGATCTGAGCGGTAGGATTGCCG
TGTGTCTCAGGGAAGTTGAGCGACACACTAGTAGGGAGGTAGGGCAGCAACGTGGCACGCGTATGACT
CTGTTGTTGAGCAGTAATTACGTTCTCACGCGCTCCAGGCGGTTGCCCGAGAGGTGTAGGGTTCCCGCGT

CGAGGTCTACACGCCTACCCGTAGCGCGCCACTTATAGTCCTTTATATCTGGGTCCTGCACAAATGAAGG
TTGATCAAGTACACGTGCATGACCATCTGTATCAGCGACTGGCGTGCCAATGGCGTGGCAGTCGTCTGT
AGAGCTTACATGCAGATGAGCCTATGGGCAACTACTCTGGGTTAGGCATGCACCTTCACCTTCCCATGCA
CGCGTAGAGATCCCTTCCATATACCTTGAATCCGGCATCGCGATTCATCTTCGCGAATC

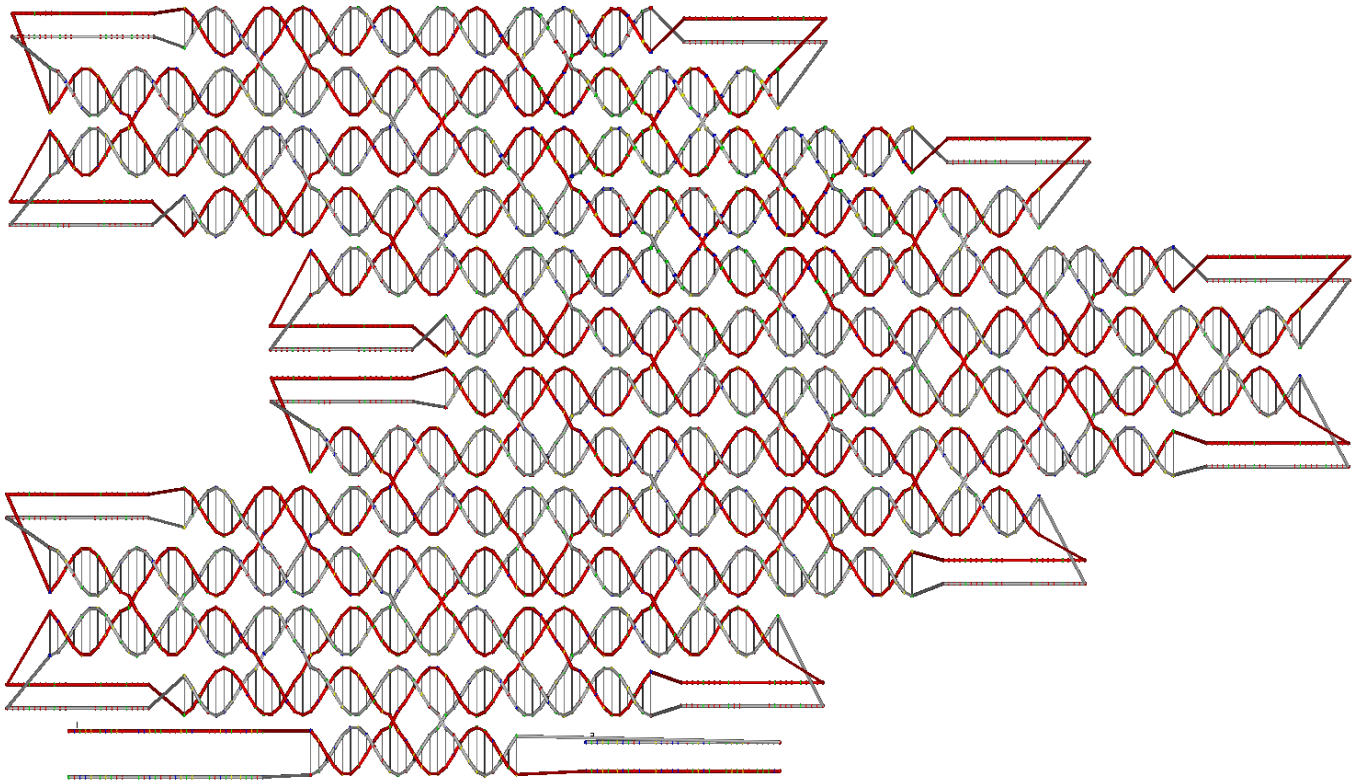

Figure S12-13. Design detail of heart-shape RNA ssOrigami with 6bps locking domains. Red strand is the forward strand and gray strand is the reverse strand.

Forward strand：
TACGGCACGTAAGCCTTGCATTGACTAGCCAGTTGTCTAACATGCAAGTTTCCCTATGGTCTCGCACGTC
CTTCTGTAAGAAGTATAGCGTGTCGCCCCTGGTTACGCACTCGATACGAGAAATCTAAGGACAGCTGCC
TTCCGGGATGGTGACAGTTTTCTTTCTTTCTTTCTTTTTACAACGAATCTCCTTCATATTGTCCCCCACGG
GCAGGGGAGCCGTTGTCATGCTAAACCATGGTACGACAACAATCCTCCTCGACTGCTGACCCGCGCGCC
CCGTGCCGGATGTCCATCTTAGCCTTTTCTTTCTTTCTTTCTTTTTAGTGTCGCGCGATCACGCTCGTGTAT
AACCATTCCTGGACTAAACTCAGACCCCGCCGATGCCTCCGTAAGCACAGGTAACGGCGTACAGACGAA
TGGATCTCACACTGTATGTGAGCGTTCAAGTTTTCTTTCTTTCTTTCTTTTCACGTTACCTCATCCTGAAGT
GCTACAACGTGGGATTTTTAGATGGTAGCTGTAGGTCTGTTTTCTTTCTTTCTTTCTTTTACTTTCGCAAA
GGGTGGTTTCCGACCTTTCGCATGGCGCTCGCGATTCGTAGTCTCGCACTTTTCTTTCTTTCTTTCTTTTAG
TATTGATACAGTGGTATTATGGAACAGATATTTATTGGAGTTGTGGCCCCCTCTCGGTTTTTCTTTCTTTC
TTTCTTTTACTGTGACCCGAATAAACGTACCTGCCATGTGCAGCAGAGCTTCATCGTGGAGCTTTAGGAC
CACTAACGCGGGCGGCGTGTCCTGAGTGGCACAGGATTGTCAGAGCTGCTAGCCATCATCCCTAGAAGG
AATGACGGTGCCGGGACCACGAACACTTTTTTCTTTCTTTCTTTCTTTTCCCCTTTTCCGCTTAGAAGGAT
GCGCCTATCGTCTAGATAAGGACCATTCAGAGGTCCACAAAGCCCGTAATTGACGTGCGAATGTCGGCA
AGACGAAGACCCTATTGGTGCACATATTAAATCAGTTTTCTTTCTTTCTTTCTTTTGATATGGGGAACGTG
GTCCGCCGGGGAGGCCACCGCATGGTCTGGGGTTAGTGCGCGGCGGCTACCAGAGTACGAATCTCCTAA
GTCGGAAAGGACAACAACACAATATGACGCTCTGTCTCCATTTTTTCTTTCTTTCTTTCTTTTGCCGGACT

CAGGCGACACCACTGCACCAGAATTGATTCCCCAACGAGGCAGGGCTCGGCATTTTCTTTCTTTCTTTCT
TTTCGTTACATGGAGTATTAATGAACGGCCGAGGAGCAAGGTGTTAAAGCCGCGACACCAGAGTTTTCT
TTCTTTCTTTCTTTTAGCCGCGACACGAGACCCGGATTATCGCCGTATGTCCGATGGAGATGGTTTAGCC
TCCGCTTTTCTTTCTTTCTTTCTTTTACCAGGCGCTAGACCTGGGCTTGGAAGGACATCTAGCCGGGCGCG
AGGGGTACCCCAGCGACAGCGACTAGATAATCGACCGCGTCCCAT

Reverse strand：
ACAGCGACTAGATAATCGACCGCGTCCCATCGCTGGGGTATTGCATGCGCCCGGCTAACTGGTCTTCCA
AGCCGTGATCTAGCGCCTGGTTTTTCTTTCTTTCTTTCTTTTGCGGAGGCTAATTACACTCCATCGGACGC
GCGGCGATAATCCGGGTACGGTGTCGCGGCTTTTTCTTTCTTTCTTTCTTTTCTCTGGTGTCCTTACATTA
ACACCTTGCTCGCAGGCCGTTCATCTGAGTTCCATGTAACGTTTTCTTTCTTTCTTTCTTTTTGCCGAGCCC
AACTGGGTTGGGGAATCTACCATGGTGCAGTGGCACGTGCTGAGTCCGGCTTTTCTTTCTTTCTTTCTTTT
AATGGAGACACGAGTGCATATTGTGTTAACGGCCTTTCCGACTCGTTACATTCGTACTCTCAGCCTCGCC
GCGCACCCACCCCAGACCATGCGTATATATCCCCGGCGGTTTATTTTCCCCATATCTTTTCTTTCTTTCTT
TCTTTTCTGATTTAATCCAGCAACCAATAGGGTATATCTCTTGCCGACACGCGAGCGTCAATTACGCCAC
GTGTGGACCTCTTAACATTCCTTATCTAGCCGTGGGGCGCATCCTATATTCCGGAAAAGGGGTTTTCTTT
CTTTCTTTCTTTTAAGTGTTCGTCCCGGAGGCACCGTCATAACTGGTAGGGATGATCACATACAGCTCTG
ACAGACACATGCCACTCAGACGAATCCGCCCGCGTTTTCCACCCTAAAGCTCCACGATGAAGCTCTGCTT
GCTGGGGCAGGTACGACCACGCGGGTCACAGTTTTTCTTTCTTTCTTTCTTTTACCGAGAGGGTATATAA
ACTCCAATAACTTCGTGTTCCATAATGTGGAAGTATCAATACTTTTTCTTTCTTTCTTTCTTTTGTGCGAG
ACTGACACGCGCGAGCGCCACTCGCGAGGTCGGAAATAACCCTTTGCGAAAGTTTTTCTTTCTTTCTTTC
TTTTCAGACCTACAAGGCTGATCTAAAAATCGGCTTTTGTAGCACTTTGTGTCGAGGTAACGTGTTTTCTT
TCTTTCTTTCTTTTCTTGAACGCTGGCTAGCAGTGTGAGATATGTTAGTCTGTACGCTAGGAGCTGTGCTT
ACGCCAGTTTCGGCGGGGTTAATACTTAGTCCAGGATGTAATATACACGAGCCAGGTCGCGCGACACTA
TTTTCTTTCTTTCTTTCTTTTGGCTAAGATGACCAGTCGGCACGGGGCATACGGGTCAGCAGTCTGCGAG
GATTGTTGTCGAATTCTGGTTTAGCATGCCGTTGGCTCCCCTGCACGATAGGGACAATATCCAGTTGATT
CGTTGTATTTTCTTTCTTTCTTTCTTTTCTGTCACCATGGTCCCAGGCAGCTGTCGAATATTTTCTCGTATG
AGCGTCGTAACCAGGGCACGTGCGCTATACTTGCGGCTGAAGGACGTGCCGTACCATAGGGAAACCCCC
TCGTTAGACAACTATCCGGCATCGCGATTCATCTTCGCGAATC

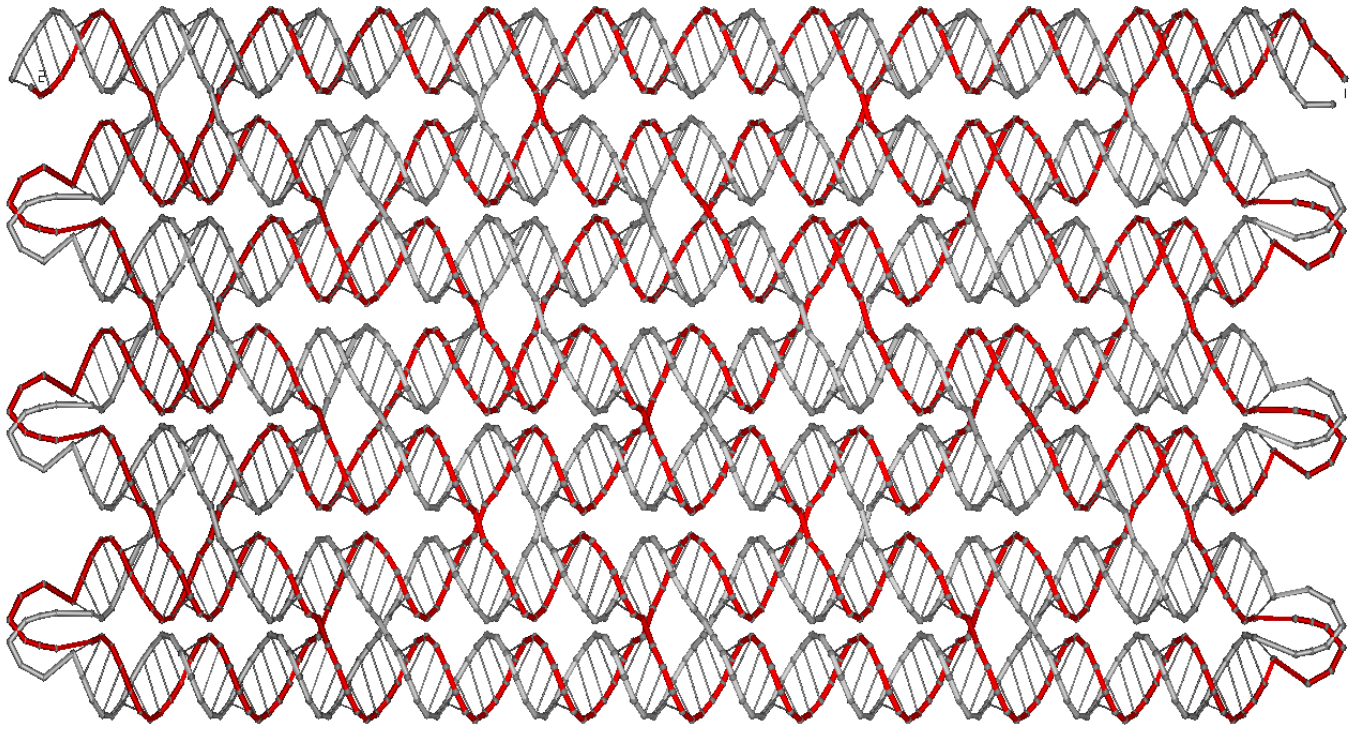

Figure S12-14. Design detail of rectangle RNA ssOrigami with 8bps locking domains. Red strand is the forward strand and gray strand is the reverse strand.

Forward strand：

GAATTCTAATACGACTCACTATAGGGAGAGGATCCGAACACTAGCCATAGCAGTTCGCTGAGC
GTAATGTGTATGAAACATCATAAGTTCAGTGCTACATTGAAGCGAAGAGCCAATGACTCGTTC
GTGTCATACTCATCAACGGAGTGTTGACTAAGCCGAAAAAACATAGTCCGACTACACACCAGA
CACGTTTGACCCTCAGTCGATTAACTGCAAGTCGCAAACAAGCTGACGTACAGTAACGACTCG
TCACTGTACTGATGATTCCACAACTGCTAATGCACGAAAAAAGGAGTAGTGTGTCAGATCGAC
AAGACTTAACCACGATTCCTGATGCATTGACTTACCATCGACTCAACTGACAAGGGACCACGC
AGAGGTGAATGAGTCAGGACTTTGTAGTCGGAGTCGGAAAAAACACCAGTCACAATGTATCGT
ACGCTTGCTACTAGGAGCTCGTCATGACGTTGAGAGCCTGTTAACTAGACACGTTCCTAAGGGT
TAGCCACACATTAATATCGGGCCTGACACAGGACACGAAAAAAGAAGGTGCTGTTAGTTGGAC
AGGTACTATCATCTCAAGTCGATAGTCCAAGTAGGTTTGAACCATGCATAGCTTGTATCAGGTC
ATCGCCTCAAACGTTAGGTGTCACATTGTGGAATCGCAAAAAACATACCGACTTCCATTATGG
GACACGTCGCTTATTCTTGGTAAGTAGAAGTTGCCATCGTAGTCGCACGACCTACTTATGACGA
ACTTCGGTTAAGTGGCTGACGTACTAACAGTGCGTGCAAAAAAGACCTACGAAGCCAGAGTTC
GTTCCAGTGTGAAAGTGCACATCACGAGTTGTGCCAATGCACGTTGCATCGAGAGTTAATCCC
GTCTTAAGTAGCAAGGCACCTGAATGGAAGTTGATTCGTCTAGA

Reverse strand：

TCTAGAAATAGACGAATCATGCTGATCTCAGGTGCTCACTTGATTAAGACGGCTGTTTATCTCG
ATGCCTTCAATGTTGGCACAAATGCATCAGTGCACTTATGATAGTGAACGAACTCTGGCTTCGT
AGGTCAAAAAAGCACGCAAGCATGTAACGTCAGCCTAACGCTTGAAGTTCGCAGGTGTGAGGT
CGTGCCTTGTTTGTGGCAACTGTCATGACCCAAGAATAAGCGACGTGTCCCATAGATCAGCAC
GGTATGAAAAAAGCGATTCGTGAGGTAGACACCTAGATACTCTGGCGATGACAGTCATTGAGC
TATGCGAGTCGATAACCTACTTGGACTATCGACTTGAGTCACACTGACCTGTCCATACATGCTC
ACCTTCAAAAAACGTGTCCGCACTATAGCCCGATATCTCGTACAGGCTAACCTCGTTACTCGTG

TCTAGTTAACAGGCTCTCAACTCTACTTAGAGCTCCTATCAAGTGACGTACGATTACCTCACAC
TGGTGAAAAAACCGACTCAAGATTTGAAGTCCTGTGAGTATGACCTCTGCGTGGTCCCTTGTCA
GTTATGGTTCAGGTAAGTCACTCGTGATGGAATCGTAAGCGTTACTTGTCGATTATAGTGCCTA
CTCCAAAAAACGTGCATCTTGATCAGTGGAATCATCAGTACAGTGACGAGCTTAGGAAGTACG
TCAGGACTACGACGACTTGCATAAACAGGACTGAGGGAGAGTATCGTCTGGTGCAAATCTTGA
CTATGAAAAAACGGCTTAGTCAACACTCCGTTGAACTCATTCACACGAACGCTGATACAGCTCT
TCGAACGTGCATAGCACTGACACACCTGTGTTTCATTGTACGAGCGCTCAGCGTGATCAAGTGG
CTAGTGTTCGCTCGAGCTCTCTCCCTTTAGTGAGGGTTAATTAAGCTT

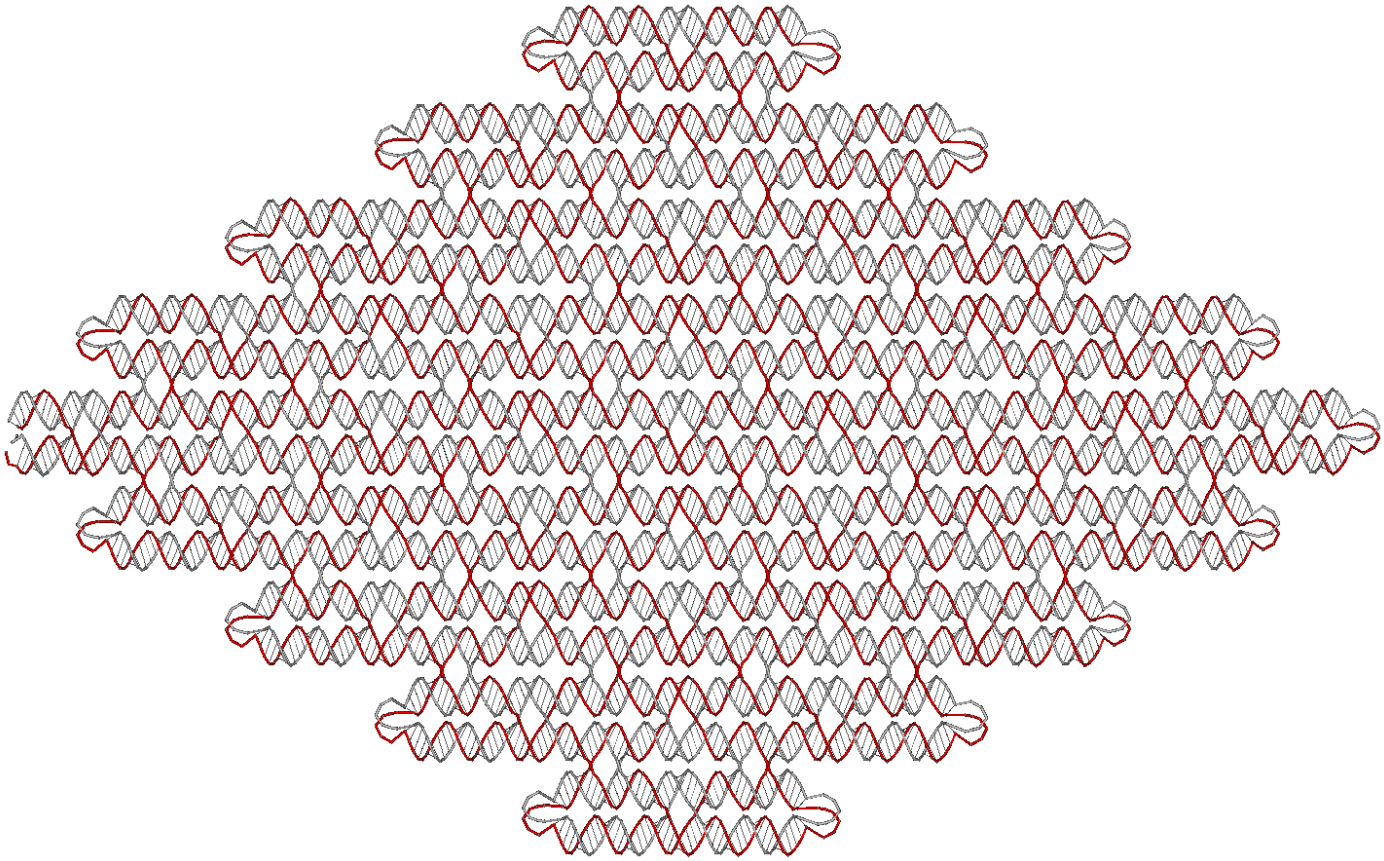

Figure S12-15. Design detail of 9 × 9 RNA ssOrigami containing 6337 nt with 8bps locking domains. Red strand is the forward strand and gray strand is the reverse strand.

Forward strand：

GAATTCTAATACGACTCACTATAGGGAGAGGATCCAACATGGAGTGCGGATATGGTTCGCTAA
GGGATTCCCTGAATGCGAACTCTATCAACTGTCGATACCTGGAGACGATGCTGATCGACCTGTC
ATGGGCGAAAACCTATACCGATGTAAACTCCGTATATTCATTTTGCTCTAGTCCAGTCCTGGAG
GTTACTTCGGAAAAAAGTACCGCAGTGGTGAAGCGTGTCCTCCATACACCTCCGCAAGGTATT
CACTTTTGTGATCATAGTTATGGGTGTATGAGGATATGCACTTCACTATGCAGATGTGAGATAG
ATGTCCGTGGGCAGATGTCAGCGAACCGCGAAGACTCGCAATGAAAAAACGAGTGAAGGGCG
TCTTGGCGCGTCCTTGTCTCACCCAACTGGCTTGTGGTTAGAGCTTGACTCTGGGATATGACCA
TCTTGGTCACTAATTTAGGACTGCCCTAACCTCCCTAATGGATGCGGGTGATAAGTTCTGAATG
TCACGTTTGCAAATAGCCCTTAATGTTCCCGTACTGTGGCACGAGCAAAAAACCTTACACCTAA
GGCGATACTCACTTCAACTGTGTGTATCACATTAGGTGCCTACGGTAAACTCATCGTCTAGTTC
TGGGACTGTTTCGTCTGGTTGAACGTTATAATAGACACGATACCTGGTTCTACCATTCGCCGAT
CCATTTGGTCTTCGAAAAAACGAGGGAGAATCACTCTATCAAAGATGCACCTCGTAGCGAGTG

AGTGGAACTTCATAAAGGGAAGTCATGGCCGGTCAGACTTCTGGCACTGATATGCAACATCAG
TACAGTCTTAAGTTCCAGCCGAAAGTGCGGTTGGCATCTCTTAGGACACAGAGCGATTTTGGAC
TGGTAGCTGACCGCATGAAAAAAGGAACGACGTGTCGAAAGGTCCCGGTAGTAGCTCCCTCAT
TCCACTTGGCTAAACGTTCAACACGTATCGAGTTGGTTTAGGTAGTTCGCAGACGCACAAACG
AAGGCAGGTAAAACTTGGCAAGTTGCGTCGTGGCACGTCATACCAGTGTTGAAAAAACGGCTA
TGTAGTGTCTAGCTGTCAATACCCGTACCCATCTGATGGTTGCAGGATGATTAGGTCGAAACGA
AGTCTCTGATCTGAGGTCGTCTGAAGCTAAGTAATACCTGGCTAACTTGACTAACTCGTACTCA
TACTCAGCTTTCTCACATTCTGTGCTCAAAATCTGCATTGACTGCAACGGTCCAAAAAAGCGAC
CTTCTGTGTGAATATGAATACTAAGCGGGAGTTGAAGAATAGCTCACAGACAGACACAACCTA
CAAAATGAATGAGCAGTCCGTGTAAGCTCGCATTGCTCACTTCAGCCTTCGGGCGCTATAGCCA
TTATTATGATCCAACTCGATCGAAAAAAGGTACTACGTAGATTTGGCCGACACCAGATTGCCC
GTACCGACAATGCGGTTTCTTTGTAAACTGGGCACTTACGATCATAGGGAGCTGGTTACGAAC
GGCATCCGACAGGAATCTAGCTCGATGCATGGGATAGTACTGTCCACATCCAGCCGTCCCAGA
GATAGGTAGATTGGGAAAAAACGATCGGTACTGATCTCTGGTGTCTGACAAACACCTCCGCAC
TCATTTGAGCATGAGCCAATGTATAAGTTGCACCAGAATCGCTCTGGTATGTCTAACATCTGCA
ACATCTTAAGGGCAGTCATGACTACTGACCGTAGTCGGCTAGAGCACCGTGAGGCCAAATGAT
CCTCCAGAAAAAAGCACTGAGTTGACACCATCCGAGAGTATGGAGCACTAGCTATCATGACGA
GGTTCCCAGTTGAAGTCAGAATCTTGATGGACGAAGCCTACTACTACCTGCTGTTGGTACATGG
ATAAGATTGGCTTAGTAGGTCATCCAAGACTGGGCCTTGGAAAAAACCACGGTTTGTGACCAT
GATCGTCCCATGCATACTGAAATCATCACTAGTTGCGGAGTACGAGTCGAGCTGTGCAGTGCA
AACTAATCCCTTTCGGCGGTCACATAGTCCTGAACGCCGTCCTTATCACCGAAATCTTCCAACA
AAGCATGGCTCGTATAGGTGCCCAGTCGACTACTGGATACTGGAAAAAACGGACTTTAGACAG
CACCCTCAATCTATGATCGGTCCAGTGGTTAGTTCGTTTCTGCGAGTTTACCTTGCATCAGGAT
ATGACACCTCGGGTGTTGAAGCCTGAATAGAGAGCCGGTTCGATCTTGTGTCTACTGAACGCA
GTGTAGCGTTAGCAAAAAAGACACTATCCTGAAGCACGCTATGTTCGTAATTCAGCCGACTCG
CATTATTGCTGGAGCTTCAGCTCGGCCTTGACTGAGTGCACTCAGGCATATCAGTCAACACAGC
AACTTCCTACGACTGTCCTAAATCAACACTGCTAGTCACGTGTGTCTATCGTCTCGACCTGCAA
GCATGGGTGTCGTCGAAAAAAGCTCACGCTGTACAACCTTCACCCCATAGTGATAGCCACAGA
AAAGCCTCTGAACACCAACCAGACGGTCGAAAAGAAATGTAAGCTCACTGCGTCTGGTGCGTT
GACAAGAAGACCCATTATGAGCTTACGTGCTCTCACGTAGGCACTATCCAAAAAAGGAGTAAA
GGCGAACGTTCGCAGCAGTTTACTCGGTGGTTTATCTCTGAGGTCACGTCGACCTAAGTCCCAT
GATGACGTCCAGACAACCTTCCCTTGCTTCCAAGGCTTTGGAGGTATGCTAGAGTCAAGAATTA
CTCTGCATCGAGTCATCAAGCATTCAGTACTATTAGATTGGAGCACGACACAAAAAAGCATCT
TCAATTAGGCTTATCTGAGACATCTGGTCAGGTCACCGAGTACCAGATGTCGGTAGAACCAAA
GATGACATAACAGTGATCAACCGCAACTTACTGTACCCTACACGAGATATGTCCGCTATAGCG
TCAAACGCAGGTACTGCGATGGAAAAAACAGCAGTAGCACAGGCTTAACATCAATCTGGTGGT
CACCTCTATAGGGCTAGAGTGACGGGTATCGGTTATGACAGTGTTGCAGTCAGCAGGTGCATT
GTCTTCGTCGAGCAGTAAGCGGATAGACAAGGGTCGACTTGGTCTATTATCATGTAACACTCCA
TTACCTGGTCTAGA

Reverse strand：

TCTAGAAATAGACCAGGTACCACTACATTACATGAAGTCTTCGCAAGTCGACAGGCTATAATC
CGCTTCAAATGGAACGAAGACACGACTTAAGCTGACTGGGTATGACTCATAACCGTGCTGTTG
CACTCTAGGTTGGATCAGGTGACCAGTTACGCTATGTTAAGCCTGTGCTACTGCTGAAAAAACC
ATCGCGCATTGTCCGTTTGACATGCGATAGGACATATCCAACCATCGGTACAGTCGTAATACGT
TGATCACCCACTCACCATCTTTGTACAGGTAGACATCTGGACAAGCCAGACCTGACGTAAACG

TTCAGATAAGTAGCGAACAAGATGCAAAAAAGTGTCGTGCTCCAATCTAATAGTAGAGTAGAC
TTGATGACCATCTATCGAGTAATTCACAGTGAAAGCATACCGTGTCTATCTTGGAAGCTCAACT
CAGTTGTCTGTTACCTGCCATGGGACTACTCCATCCGTGACCTGCTGAAGTAACCACCGATGTT
GAGTCTGCGAACGTTCGCCTTTACTCCAAAAAAGGATAGTTATGATCGGAGAGCACACCATTG
TATAATGGGTGATCAGAGCAACGCACGTACATATGTGAGCTTAGTCTGACCTTCGACCGCACTC
GTTGTGTTCAGAAAGATGGTTGTGGCTAAGCAACCAGGGTGAAGGACAGTTGACGTGAGCAAA
AAACGACGACACCCATGCTTGCAGGTCCACAGACAAGACACACTCCTCATACAGTGTTGACGT
CACGAAGTCGTAGTCCCAGAATGTGTTGACAACGGACTCTGAGTGCCTAAACCAAAGGCCGAG
GAAATTGGCCAGCAATCTCATTCATCGGCTGAAGAGACGGTATAGCGTGCTTCAGGATAGTGT
CAAAAAAGCTAACGATTCCTGTCGTTCAGTGCTCTTTCGATCGAACCTAGCCAGGATTCAGGCC
GTGCTTACCGAGGTGTAGACTGTAGATGCAAGTATCGCAGGCAGAAACGTAGGGAGGACTGG
ACCTACGACTCATTGAGGGTTGACAGGTAAGTCCGAAAAAACCAGTATCCAGTAGTCGACTGG
GCTATTGCTGGAGCCATGGAATACCTGAAGATTTCCATATCGCGGACGGCGCCTAATGTTATGT
GACCTTGTATGAGGATTAGTCAAGTGGACACAGCTCGTTATCGCTTCCGCAACGCTATTCTATT
TCAGTACTCTTTCAACGATCATGGTCACAAACCGTGGAAAAAACCAAGGCATGTGGACGGATG
ACCATCACTTGCAATCTTATAGAAAGCTCAACAGCATCCTTATCTAGGCTTCGAGAGATGCGAT
TCTGATCATTGGAGGGAACCTCACGTGACAAGCTAGTGAGATGATTTCTCGGATGTACGGAGTT
CAGTGCAAAAAACTGGAGGATCATTTGGCCTCACGGCCAAGGTACCGACTACTCACCACTGTC
ATGACTAGTCAAGGGATGTTGCGCCTTAGGGACATACCACTTGGTACCTGGTGCATCGACACG
ATTGGCTCACATGTGACTGAGTGCGCACACAGATGTCAGACAGTCGTCTACAGTACCGATCGA
AAAAACCCAATCTACCTTAGACGACGACGGCTGGCCAGTCTTAGTACTATTGAAAGAGTCGAG
CTAGCTACACTGCGGATGCCACCGTCTCCCAGCTCCCGCCTACGTTAAGTGCCACTCAACAAAA
GAAACCAGTACCTGGGTACGGGAGCGTAACTGTCGGCCAAATCTACGTAGTACCAAAAAACGA
TCGACCCTATAGATAATAATGTATCGCATGCCCGAAGCAGAGATAGAGCAATGCACAATGGTA
CGGACTGAATGCGAGTTTTGTAGGGAAAGAGCGTCTGTGATAGTGATGTCAACTCCCCAAGTG
ATTTCATATTGAGGTGTTAGGTCGCAAAAAAGGACCGTTGCAGTCAATGCAGATGTCACATGC
AGAATGTGCCATGTACGAGTATGAAGCGATAATAGTCAAGTGGCTCTCTTATTACTTCCAATTT
CACGACCTCACTTCTTGTACTTCGTTGATGGAGTATCATCCTGTCGTGTAGAGATGGGTCAACA
GCATGACAGCTAGACACTACATAGCCGAAAAAACAACACTCAACACTGGTGCCACGAGTATTA
CGGCCAAGTTGACGTCATCTTCGTTTGATATGTACCGAACTACACTCAGTCACTCGATACTAAG
CACGCGTTTAGCTTGCACTGATGAGGGAGGATAAGGAGGGACCTTACTTATACTCGTTCCAAA
AAACATGCGGTCAGCTACCAGTCCAAGTACCAAGTGTGTCCTATCCATCAACAACCGCATCAT
ACAATGGAACTTACATATCCTCTGATGTTAGTCCGTTGTGCCAGAACATTTCTTGGCCATGATG
AGTTGATATGAAGTTTGTTATGTTCGCTACGTTAAGTCGCTTTGATAGAGTGATTCTCCCTCGAA
AAAACGAAGACACTGCTCGTCGGCGAATTACCTGTACAGGTATCTCCAAAGCTATAACGTTAA
CGAGTGCGAAACAGGAAGTTGCCTAGACGATCTGCGATACGTAGGCATTCAGGACGATACACA
CTCCAATGATGAGTATCAGATGTTATGTAAGGAAAAAAGCTCGTGCCACAGTACGGGAACACC
TTGACTTATTTGCAAGTCATGATTTCAGAACGCGATATGCGCATCCATAACTAACCTTAGGGCA
TCGTGACGTTAGTGACCGGCTTTTCCATATCCCTTCACTGTGCTCTAACCTACTCGGTGTTGGGT
GTATAGCCTACGCGCCAAGACGCCCTTCACTCGAAAAAACATTGCGTAATAGACCGGTTCGCT
ACGTTTACCCCACGGATCGATGCATCACATCTGTGGTTGCTAGTGCATAGTGACTAGCACCCAT
AAGAGTCGTAACAAAAGTCTTTGTTGTGCGGAGGTAATCATCTGACACGCTGGTCAGTAGCGG
TACAAAAAACCGAAGTAACCTCCAGGACTGGATACCTTGGAAATGAATAGTGTCAACTTACAT
CGCAGCAATATTTCGCCCAGCTGTCTACGATCAGCTGTCTGTGCAGGTATCGTTGTACAGTAGA
GTTCGTCTACTCGGAATCCCTCCTAATTGCATATCCGTGTAGTGGGTTGGATCCTCTCGAGCTCT
CCCTTTAGTGAGGGTTAATTAAGCTT

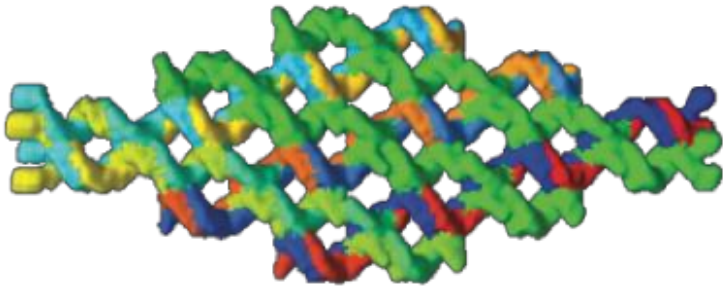

Figure S12-16. Design detail of automatically designed 3x3 diamond-shape ssOrigami in the helix surface view mode. The strand of the ssOrigami is composed of the forward strand and the reverse strand. The colors represent the indices of the bases, which start from the blue base and end with the red base.

Forward strand:
TACGGCACGTAAGCCTTGCATTGACTAGCCTTCTAACGCGCGTACAGTGTTCGCAGATCCCAGAAATCG
ATGGCCGATACGATAGCACAATTTCTTTCTTTCTTTCTTTCTTGATTAGGAGTGTTGGGCGGTAACCTCCT
ACTTCCCGAGACTTATCAGACTGCCACGCACTTTCTTTCTTTCTTTCTTTCACGCGTCGGGCTTACGATAG
AGAGAGGGTTCCTGGGCAGACACAGCTGACGGTTCATGCTTTCTTTCTGGCCCGTCGGCAGCTGCCAGA
GCGGCCCGTAAGCCGAATGAGCGTATCTAAGGTCATATTTCTTTCTTTCTTTCTTTCTATCGTCTCATCAG
AGCGCCAGTCCGAAAGTAGTTCACTGAAGACGACCCATCGGCTCGTCTTTCTTTCTTTCTTTCTTTGCTCC
CCTTTCGTAAGTGGCGCAAGAGTCTGTCACTGGTGGACACTGTAGTGGGCTTCTTTACAGCGACTAGATA
ATCGACCGCGTCCCAT

Reverse strand:
ACAGCGACTAGATAATCGACCGCGTCCCATCTTGAAGCCCACTCCAGTATCCACCAGTGTCTGATTCTTG
CGCCAAAGTCCAAAGGGGAGCCTTTCTTTCTTTCTTTCTTTCCGAGCCGATGGGAACCCTTCAGTGAATC
ATGTTCGGACTGGCTTCTGGATGAGACGATTTCTTTCTTTCTTTCTTTCTTTATGACCTTAACCACCCTCAT
TCGGCCCCAACGCCGCTCTGGTCAATGCCGACGGGCCTTCTTTCTTTCATGAACCGTCATTGATGTCTGC
CCAGGTCGTCTCTCTCTATGGACTTCCCGACGCGTTCTTTCTTTCTTTCTTTCTTTTGCGTGGCAGACAGA
CAAGTCTCGGGACATGAGAGGTTACCGTTACGGACTCCTAATCTTTCTTTCTTTCTTTCTTTCTATTGTGC
TATGGTGGTGGCCATCGATGCTCTGGATCTGCGAATACTGGACGCGCGTTATCTATCCGGCATCGCGATT
CATCTTCGCGAATC

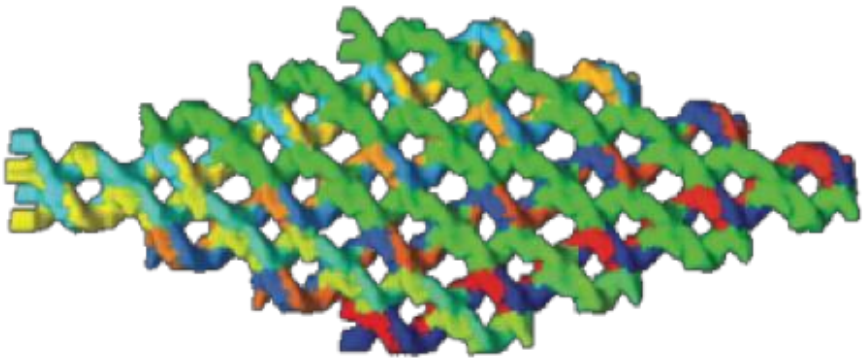

Figure S12-17. Design detail of automatically designed 4x4 diamond-shape ssOrigami in the helix surface view mode. The strand of the ssOrigami is composed of the forward strand and the reverse strand. The colors represent the indices of the bases, which start from the blue base and end with the red base.

Forward strand:
TACGGCACGTAAGCCTTGCATTGACTAGCCTCTGATAAGTGTGGGCCGCTCCCAAGTGCTCCTTCCCTCC
AGGTGTTCGTTGACCACCGTCCGGAGCTTTAAACTGCTTCTTTCTTTCTTTCTTTCTTACCCAGGGGACGC
CCCCCAGCTGAGGAGCCCGTAAAAATCGACCAGTTCTTAACGCACATGGCCCCAGTCACAGCTTTCTTTC
TTTCTTTCTTTCCGTTAACCTTCTAATTCCCGAGACTTATCAAGGCCGAAGGAGCGAACGATGGGCTTCA
CTATTATCGGAATGTCTTCTTTCTTTCTTTCTTTCTTACTCCTAATCGTCGGGTCCGATCTGTCCTACGATA
GATAGAGGGTTCCTGGGCAGACACAGGTGGCTGTTCATTCTTTCTTTCTGGCTCGTTGGCACCTGCTTCA
GTGAATCATGTAAGACGATTAGGCCATTGAACAACGCAAAATCGGATTGGCTTTTTCTTTCTTTCTTTCTT
TCTATTTCTCCTGGAAGGAATAGGCGACTTCTACAGTTTCGCAGACTTGATTCTTGCACCAACGACCCAT
CGGCTCGTCTTTCTTTCTTTCTTTCTTTGCTCCCCTTTCGTAGGTATTGGTAGTATACCAATGTCCACGGCG
GGCTAAGACAGGTTGTTCTGACGTGCAAGTTTTCTTTCTTTCTTTCTTTCTTCGGCCCAACGCTCCGGTTG
GGACAGCCACTGCATGTGGCGGTAATAGACTATGACCTGGACGCCCCAACTTACTTCACAGCGACTAGA
TAATCGACCGCGTCCCAT

Reverse strand:
ACAGCGACTAGATAATCGACCGCGTCCCATTCTGTAAGTTGGGCCCGACAGGTCATAGTATTATTCCGCC
ACATGGGGGCGCTGTCCCAACCCGATAGTTGGGCCGATTCTTTCTTTCTTTCTTTCTTACTTGCACGTAAC
GAAAACCTGTCTTAAGTGACCGTGGACATCGTTCGACTACCAATAAAGTCCAAAGGGGAGCCTTTCTTT
CTTTCTTTCTTTCCGAGCCGATGGGAACCTGGTGCAAGAGTCTATTCTGCGAAACAACTGGAGTCGCCTA
TGCGTTCCAGGAGAAATTTCTTTCTTTCTTTCTTTCTTAAGCCAATCCGCGGCCGCGTTGTTCAAGATCGT
AATCGTCTTAATTAGTTCACTGAAGTCCATGCCAACGAGCCTTCTTTCTTTAATGAACAGCCATGGATGT
CTGCCCAGGTCGTCTCTATCTATGGACTTACAGATCGGAGCGTCCGATTAGGAGTTTTCTTTCTTTCTTTC
TTTCTGACATTCCGAAATAATTGAAGCCCATTGGTATCTCCTTCGGCATAGACAAGTCTCGGGACATGAA
AGGTTAACGTCTTTCTTTCTTTCTTTCTTTCTGTGACTGGCGATCTGTGCGTTAAGTGTAGATCGATTTTTA
TCACTTCCTCAGCTGGCAGTGGTCCCCTGGGTTTTCTTTCTTTCTTTCTTTCTGCAGTTTAAATATCGGGA
CGGTGGTCCAGAACCACCTGGAGGGAACGCGCACTTGGGAGATTTTCACACTTATCTTCATCCGGCATC
GCGATTCATCTTCGCGAATC

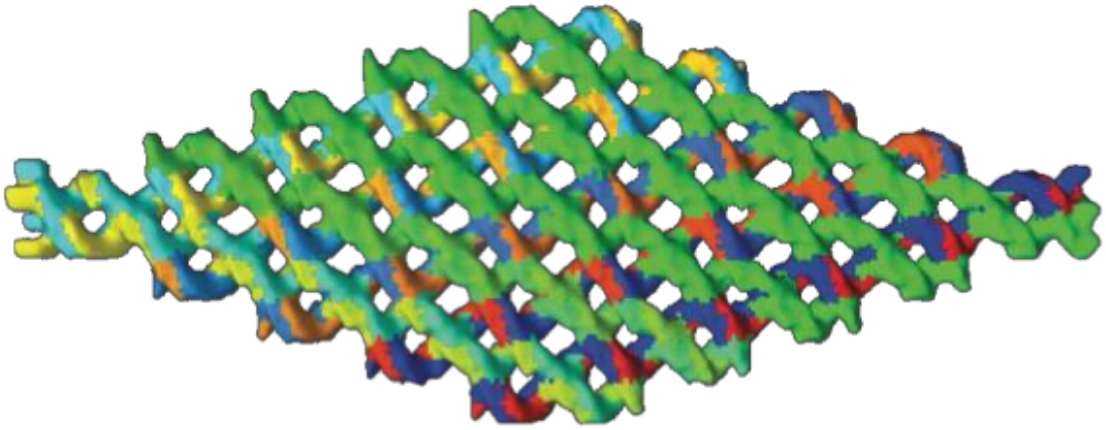

Figure S12-18. Design detail of automatically designed 5x5 diamond-shape ssOrigami in the helix surface view mode. The strand of the ssOrigami is composed of the forward strand and the reverse strand. The colors represent the indices of the bases, which start from the blue base and end with the red base.

Forward strand:

TACGGCACGTAAGCCTTGCATTGACTAGCCTTCAACTCTGGCCGAGCACATTGGGGACGTCTGTCGATA
AACGGAGAGTCGATCTCGACTTAGTTTGTCTATACACTCGACCTCGGAAGGTAATTCTTTCTTTCTTTCTT
TCTTGTGCAAGTCCGGTTCCCCACCGTCTTGAGTCTCGCTGGACACGCGTTGGTAGAGGCAGGACGTGAT
CTAAGGGGAGGAGAGCGGCTAGGGCTTTCTTTCTTTCTTTCTTTCAACGAACAGAGCGACTACATTTTTC
CCTTATCGAAGGAGAACAGGGAAGCGTTGTTCACGCCACCCAGCTGATGAGCCCATAAAAATAGATTCT
TTCTTTCTTTCTTTCTTCCCGAGACTTATCAAAACCGAATGAGCGAACGATGGGCTTTACTATTAAAGAC
GATTATGTCGGTCTGCGAAACCTGGAAGTGCGTTAAGCTTTCTTTCTTTCTTTCTTTCAAGGTTAACGCTA
ATCTTCACTGAAGATCGGGTCCGATCTGTCTTACGATAGATAGAGGGTTCCTGGGCAGACACAGATGAC
TGTTCATTCTTTCTTTCTGGCTCGTTGGCATCTGTGGTGCAAGAGTCTATATGTCCACTGTGGGCTTCCAG
GTGACAAGACAAACGAGACGCAGGTCGTGGAGCGACATTTCTTTCTTTCTTTCTTTCTGCTCCCTTCCCTC
AATCTGCGATTTAAGACTCTCGTTGGGACCCACTGCATGTGGCTGCGTTCGACTACCAATAACGACCCAT
CGGCTCGTCTTTCTTTCTTTCTTTCTTTGCTCCCCTTTCGTAAGAGGTCATATTATTATTAATCGGCCGCTT
CCCTGGCCTAGGTCTAAACTCGATTCTAAACGACTCAGGCGTCCCCTTTCTTTCTTTCTTTCTTTCTCTAA
GTGGTGGAAATTTGTATTACTTCACGTCCCGCGGTAGTCCCACAGCAAGCCAATCCGACAATATCGATG
GGGACGCCCCAACTTACTCTTTCTTTCTTTCTTTCTTTATGTCTAATTGATTAGCTGGTGTAGACTGTTAC
CAAGTATCAAGTCGCATGCGAGGCTATAGCCTGAGTGTAGCGTGCTCCGCATCGGTTTTTACAGCGACT
AGATAATCGACCGCGTCCCAT

Reverse strand:

ACAGCGACTAGATAATCGACCGCGTCCCATCTTAACCGATGCGTCCGAGGCTACACTCATCTCCTAGCCT
CGCATGAATAGTGATACTTGGTTCCAGTCTACACCAGGAACTCAATTAGACATCTTTCTTTCTTTCTTTCT
TTCGTAAGTTGGGCCCGATCCATCGATATTCGGAAATTGGCTTGCGATAAGACTACCGCGGGAGGCTAA
GTAATACAGACAGACACCACTTAGTTCTTTCTTTCTTTCTTTCTTGGGGACGCCTGCCTGATTTAGAATCG
CAACGCGACCTAGGCCTTACTCGCGGCCGATTTAATAGAATATGACCTAAGTCCAAAGGGGAGCCTTTC
TTTCTTTCTTTCTTTCCGAGCCGATGGGAACCTATTGGTAGTATACCACAGCCACATGGTGGCGGTCCCA
ACGAGATATGTAAATCGCAGCAAACTGGAAGGGAGCTTCTTTCTTTCTTTCTTTCTTTGTCGCTCCAGCA
AGAGCGTCTCGTTGGAACCGTCACCTGGAAAGTGACAGTGGACATTTTGATTCTTGCACCATCAATGCC
AACGAGCCTTCTTTCTTTAATGAACAGTCATTGATGTCTGCCCAGGTCGTCTCTATCTATGGACTTACAG
ATCGGAGCGTCCCTTCAGTGAAGAGTTCCGTTAACCTTTCTTTCTTTCTTTCTTTCTTTCTTAACGCACTA

ACAGGTTTCGCAGATTCCGATAATCGTCTTAATAATTAAAGCCCATTGGTATCTCATTCGGTATAGACAA
GTCTCGGGTTTCTTTCTTTCTTTCTTTCTTCTATTTTTATCACTTCATCAGCTGGCAGTGGTGAACAACGCG
AGTAAGTTCTCCTTCTGTGGGGGAAAAATGTCTATTCTCTGTTCGTTTCTTTCTTTCTTTCTTTCTTTCCCT
AGCCGCGGCTATCCCCTTAGATAGCCTCCTGCCTCTACAGTTTAGTGTCCAGCGCATATCAAGACGGTGG
TGTCTTGGACTTGCACTTTCTTTCTTTCTTTCTTTCTTTACCTTCCGTCTTGCAGTGTATAGAATTGAGAAG
TCGAGATTCAGGCTCCGTTTATCAATTTCCGTCCCCAATCTCGGAGGCCAGAGTTTCTATCCGGCATCGC
GATTCATCTTCGCGAATC

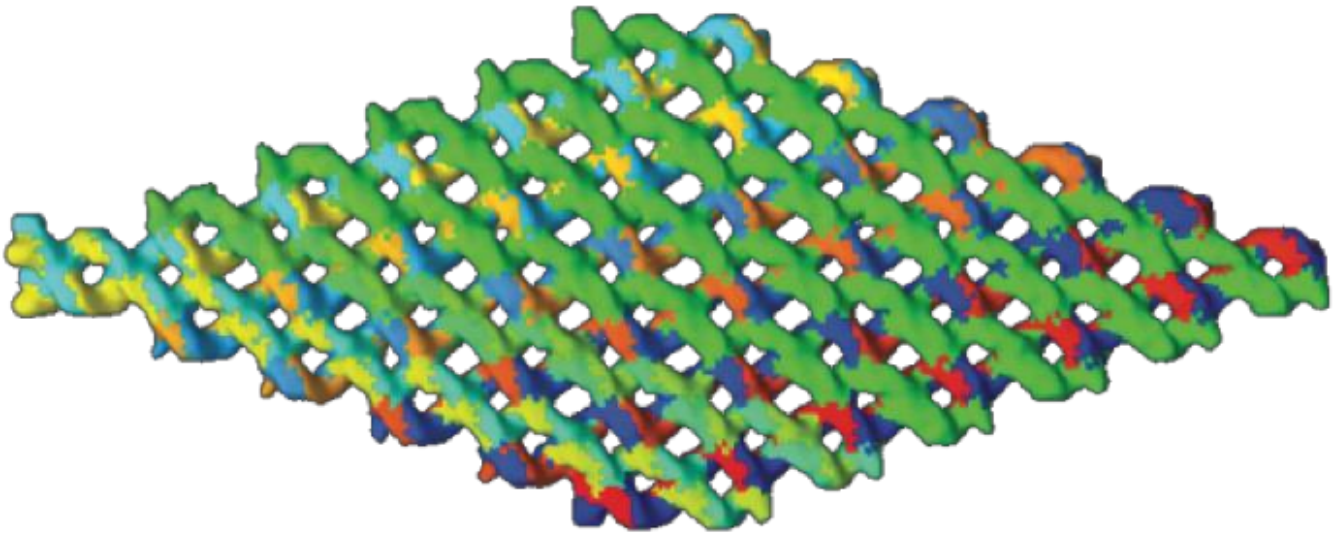

Figure S12-19. Design detail of automatically designed 6x6 diamond-shape ssOrigami in the helix surface view mode. The strand of the ssOrigami is composed of the forward strand and the reverse strand. The colors represent the indices of the bases, which start from the blue base and end with the red base.

Forward strand:
TACGGCACGTAAGCCTTGCATTGACTAGCCTCTATCAGAGGGCCTAGACCTTTGTTATGAAAACTGTCGG
ACTCCACCCGGACGTCGATATGATCACCTTCCACTAATCATGCATAACCATAGGACAACCAGAGTCTCG
TTCTTTCTTTCTTTCTTTCTTTTGACCGGGGGTGGTTACCGACAGCAGCCAGCCCACACGATCGTCCGGGA
GCAGATTTTGGGGACAATAACCGAAAGTGGCGGCTACACTTTTCTGTGGATAAACGCTTTCTTTCTTTCT
TTCTTTCGTAGAGGCAGGACGTGACCTAAGGTGAGGAGAAACGAGACGCAGGGAGAACTATTGAGTCC
GTGAAGGGAGCCGGCAGAGGTCGAGATAGAGGCCGGCGTCCCCGATTCTTTCTTTCTTTCTTTCTTGTGT
CCAGCGCGGTGGGACCTAGGCCTTGCACTCGTTGGGACAACAGAGTCACCTGGAGCGACTACATTTCTC
CCTTATCGAAGGAGAACAGGGAAGCGTTGTTCACTTTCTTTCTTTCTTTCTTTCACCGAATGAGCGAACG
ATGGGCTTTACTATTAAAGACGATTATGTCGGTCTGCGAAACCTGGAAATGTCCACTGTAAGTGCAGCC
ACATGTTTAGTCATCAGCTGGTTCTTTCTTTCTTTCTTTCTTAAGTCTCGGGTTAACGTCTTGCACCACTA
ATCTTCACTGAAGATCGGGTCCGATCTGTCTTACGATAGATAGAGGGTTCCTGGGCAGACACAGATGAC
TGTTCATTCTTTCTTTCTGGCTCGTTGGCATCTGTATTGGTAGTATACCAAATCGGCCGCTTCCCTACTAC
CGCGGGAGGCTGTAATACATCCAGAAACTGTAACATTAACACCATTTTACCGCTTTCTTTCTTTCTTTCTT
TCTGCTACAAACAAGTTTTCAGCTCTTTAGCACCTCATCCGAGGATCTCCTAGCCTCGCATCCCACAGCA
AGCCAATTAATAGTATATGACCTACGACCCATCGGCTCGTCTTTCTTTCTTTCTTTCTTTGCTCCCCTTTCG
TAAGCCATCGATATTCGGAACCAAGTATCAAGTCGCGTCGTCTTGCGCGGCTAGAGTTCGCATCCCCATT
CGCGTGTCCAACGGACTAGCGGGCTTTCTTTCTTTCTTTCTTTCTGCTGGGTTTCGTGATCCCCGGCGCTT
AGCAGACCTTCGGGACCACGGATGTGTCGCTCTTAACGGGAACCTGTCTTCCAGTCTACACCAGGGACG
CCCCAACTTACTCTTTCTTTCTTTCTTTCTTTATGTCTAATTGATTAGGGCTTCACTTGTGCGTTATGGAGT

CTGTGCAATGTATAGAGGTAAATCGGGCCAGGGAGCTGGCAGTTTTAACCAGCAGATTTAGGATTGTTT
CTTTCTTTCTTTCTTTCTGTGCGGACCCGTTGTCAAGTCCAGCCATAGGAGTCCGTTATTCGGCCTTTTTT
AGAATTAAAGACAACGCAGTTACTAAACCACTGCGCCACAAGGTTTGATATAGTTCACAGCGACTAGAT
AATCGACCGCGTCCCAT

Reverse strand:
ACAGCGACTAGATAATCGACCGCGTCCCATTCTCTATATCAAACGTTAAGGCGCAGTGGTCTATTAACTG
CGTTGCCACCGATTCTAAAAAACTCTCAATAACGGACAACCACGGCTGGACTTCTCATTGGGTCCGCACT
TCTTTCTTTCTTTCTTTCTTCAATCCTAAAGCATGAGGTTAAAACTTCAAACTCCCTGGCCCCTCTGCCCT
CTATACATCGGACAGACTCCATACACTTAAAGTGAAGCCGAACTCAATTAGACATCTTTCTTTCTTTCTT
TCTTTCGTAAGTTGGGCCCGATCTGGTGTAGACTGTTAGACAGGTTCCTCTGTTGAGCGACACATTACCT
GTCCCGAAGGCCGGACAAGCGCCGGGTTAGCTGAAACCCAGCTTCTTTCTTTCTTTCTTTCTTGCCCGCT
AGTCCGGGTGACACGCGAAGGCCATTGCGAACTCTCTCCCTGCAAGACGACGAATAGTGATACTTGGCC
GACAATATCGATGGAAGTCCAAAGGGGAGCCTTTCTTTCTTTCTTTCTTTCCGAGCCGATGGGAACCAGG
TCATATAATTATTATTGGCTTGCGATAAGATGCGAGGCTATAGCCTCCTCGGATGCCACTTTAAAGAGCT
GTACCAATGTTTGTAGCTTCTTTCTTTCTTTCTTTCTTGCGGTAAAATGTCTAGAATGTTACAGTTGAAAG
ATGTATTACCACGTCCCGCGGTAGTTTACTCGCGGCCGATTCGTTCGACTACCAATATCAATGCCAACGA
GCCTTCTTTCTTTAATGAACAGTCATTGATGTCTGCCCAGGTCGTCTCTATCTATGGACTTACAGATCGGA
GCGTCCCTTCAGTGAAGAGTTCTGGTGCAAGACCTTGTCCCGAGACTTTTTCTTTCTTTCTTTCTTTCTCC
AGCTGATGAATAGACATGTGGCTGACGCACCAGTGGACATTAACAGGTTTCGCAGATTCCGATAATCGT
CTTAATAATTAAAGCCCATTGGTATCTCATTCGGTTCTTTCTTTCTTTCTTTCTTTTGAACAACGCGAGTA
AGTTCTCCTTCTGTGGGGGAGAAATGTCTATTCTCCAGGTGACCGTTAAGTCCCAACGAGTCCGAGGCCT
AGGTCTCTTTACGCTGGACACTTTCTTTCTTTCTTTCTTTCTTCGGGGACGCGAGAGTCTATCTCGACGAT
TTACGGCTCCCTTAGGTAACTCAATAGTTAGCCGCGCGTCTCGTTGGCTATCACCTTAGGTAGCCTCCTG
CCTCTACTCTTTCTTTCTTTCTTTCTTTCGTTTATCCATTTCAAAGTGTAGCCGAGGTGCTCGGTTATTGAT
GGCCAAATCTGCTCTCTGCTGATCGTGTGGGTTTGATGCTGTCGGTTCCTATCCCCGGTCAATTTCTTTCT
TTCTTTCTTTCTCGAGACTCTGAATGAGCTATGGTTATTCTGCTTTAGTGGAAGAGCTAAATATCGACGTC
CGTTGGGAGTCCGACTTGGTACATAACAAAGGGTGTTGCCCTCTGATTTCATCCGGCATCGCGATTCATC
TTCGCGAATC

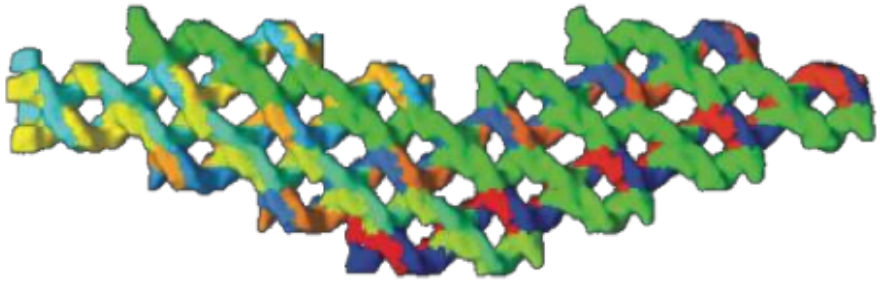

Figure S12-20. Design detail of automatically designed 4x4 heart-shape (L-shape) ssOrigami in the helix surface view mode. The strand of the ssOrigami is composed of the forward strand and the reverse strand. The colors represent the indices of the bases, which start from the blue base and end with the red base.

Forward strand:
TACGGCACGTAAGCCTTGCATTGACTAGCCTTTTCGCGCTAATGCGCGGGGTGGGGGTGCGCCTCCTATG
ACCGACCCACTCAACGTCGCTGCCTGCGTTGCTTGCTCTTTCTTTCTTTCTTTCTTTCGGATTGAGTCTCTT
ATGTCGAAGCGACTAAGTTTGGGTGCACTTGGGAAGGCGTATAATATTGTGCTTGGTAAATTCTTTCTTT
CTTTCTTTCTTCGGATTCTCGCCCGGAACACCGAGATATGCGGCTTTGCATCACTTTCTTTCTTTCTTTCTT
TCCCGTTGCCCTGAGTACGTAGCCTGGCTTCCAGCTGCCCTCTCCTTTCTTTCTTCCAGGTTTCCTGGAAA
ACTCCTACTAAGGGTGCCGAGGGGGACAATAACAAGTAAACTTAATCCGACGCGACCTTTCTTTCTTTCT
TTCTTTCTAGCTCCCCGTGAGGCGTGGTTCAATGGGGACCATCTCGCTGTCCGCATTTTGGTTCGGGATA
GGGCGCCAGCGCTTCTCTGCGCTGGCGCGTACTCCCGAACCAAAACGGCCTTTCTTTCTTTCTTTCTTTCT
CTGATCCCATACTTAGTGGTGCTGAACGCCGTCTGTCGTCTGTCTTTCTTTCTTTCTTTCTTTTAAGTTCGC
AGCAGGCCCCCTTTATAGAATTCCTCTCGAGCTCTTACAGCGACTAGATAATCGACCGCGTCCCAT

Reverse strand:
ACAGCGACTAGATAATCGACCGCGTCCCATTTTAGCTCGAGAGATAAGATATAAAGGGGAGATGATGCG
AACTTACTTTCTTTCTTTCTTTCTTTCCAGACGACAGAGTGGGTTCAGCACCATTTTCGATGGGATCAGTT
CTTTCTTTCTTTCTTTCTTACAGCGAGATTCCCAACATTGAACCAGTTGGGACGGGGAGCTTTCTTTCTTT
CTTTCTTTCTTGGTCGCGTCGCCGCGCGTTTACTTGTCACAGCCCCCCTCGGCTCCGGGAGTAGGAGTTA
AGCGGGAAACCTGGATTCTTTCTTTGAGAGGGCAGCCGCTTGCCAGGCTACCCTATCAGGGCAACGGTC
TTTCTTTCTTTCTTTCTTTTGATGCAAAGGGCCGTATCTCGGTGTACCCTTCGAGAATCCGTTTCTTTCTTT
CTTTCTTTCTTTTACCAAGCGCTGTGTTATACGCCTGGTCCCGTGCACCCAACGAAAATCGCTTCGACGA
ATTCGACTCAATCCTCTTTCTTTCTTTCTTTCTTTAGCAAGCAACTCATCTAGCGACGTTGACGGCGTCGG
TCATAGCCCAACCACCCCCACCGATTAAATTAGCGCGACTTATCCGGCATCGCGATTCATCTTCGCGAAT
C

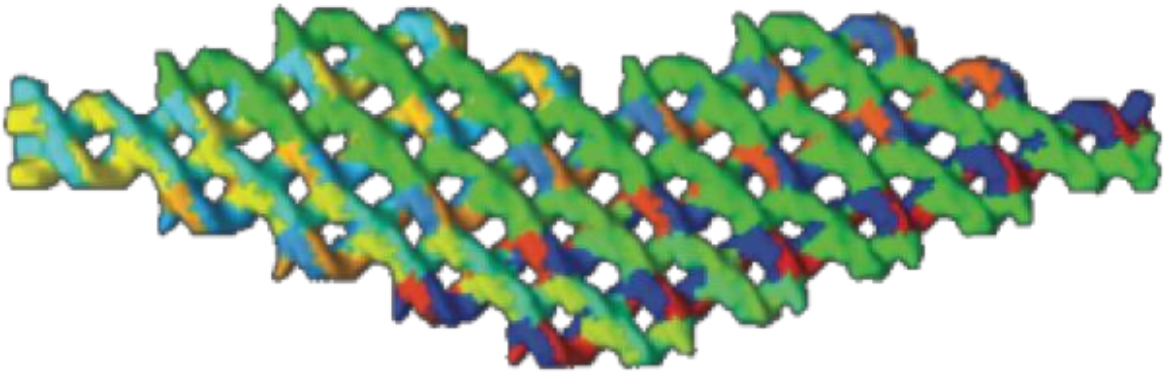

Figure S12-21. Design detail of automatically designed 5x5 heart-shape (L-shape) ssOrigami in the helix surface view mode. The strand of the ssOrigami is composed of the forward strand and the reverse strand. The colors represent the indices of the bases, which start from the blue base and end with the red base.

Forward strand:
TACGGCACGTAAGCCTTGCATTGACTAGCCTTCCTTATGTCTGGAGAGATATCCGCGACGGAGATTGTCA
TGGAAGGCGCGGGGTCGATGGGACGACTACAACAACACAGCCCCAAGGGAGTGTTCTTTCTTTCTTTCT
TTCTTTGTGTACGGGAACAAGTTTCTCGCCCTTATCTGCCATCCAAACCGGGGATTCGCGGCCTGAGTAG
GGCAATAGCGCTACACTCGTCAGGTCTTTCTTTCTTTCTTTCTTTCATTACGCAGTACCTTACTCTGCGTT
CTGGACTCCTTTGACATCTCACAATTTGGGACTTGAGGGCGATAGAGGCGGGATGCAGAAGGGTATTCT
TTCTTTCTTTCTTTCTTAACGAGCCTATCCTTCAGACACCTATTCCTTCTTATTTACCTAGGGTGTCCAGCG
CCTCTTTCTTTCTTTCTTTCTTTCACACTGCGCACACGCGCAAGCAGTGGAGCCGCTCTGAACCTGTCACT
GAGTCAAGATACTTTCTTTCTGGGGGGTATGCAGTGAGACCAAGTACGCGCGAAAGCATGCGGCATCCC
GGGGTAATTATCAGGCTGGGAGTATTGGGCTGCTTATTGGATTTTCTTTCTTTCTTTCTTTCTTTGGGAAA
GACTAGGGGTACCCACTCAGATAACTCTTACAGTGACCCCCACATTTTCCGAAGGATCTATTATCCTGTA
GACCTGTAAATGTCTTTCTTTCTTTCTTTCTTTCCTCTCCCGTCGCGTGTTTCTGAGACTCCGCGGACGCCT
CCCTGTGAGCAACAAATGATACTTGCCCTAGAATGCGCGCCTTCATAGCTATTTCTTTCTTTCTTTCTTTC
TCGTATTAGAGAGGAGCTTGTCGGCCGTACTCACTGGAGCTCGGCACCCGTTTGTGGGCTCTTTCTTTCT
TTCTTTCTTTTGGCCTTCCATAAGGTGCCTCGGGTTTTACCAAGCCAATGTCTCTCTCAGGCAAACCCTTT
ACAGCGACTAGATAATCGACCGCGTCCCAT

Reverse strand:
ACAGCGACTAGATAATCGACCGCGTCCCATCTTGGGTTTGCCTGATACGGACATTGGCTTGTAGCAACCC
GAGGCTGTATATGGAAGGCCACTTTCTTTCTTTCTTTCTTTCGCCCACAAACAGTCCACGAGCTCCAGGC
TACCCGGCCGACAAATCTCCCTCTAATACGTTCTTTCTTTCTTTCTTTCTTTAGCTATGAAACGTGTCATT
CTAGGGCCCCGGTCATTTGTTGATGTCGGGGAGGCGTCCACCCTGTCTCAGAAACACGCCACGGGAGAG
GCTTTCTTTCTTTCTTTCTTTCCATTTACAGGGCGGCTGGATAATAGATTCAGCGGAAAATGTGCCCTCAA
CTGTAAGAGCAGTATGAGTGGGTACGTCGTCTCTTTCCCAATTCTTTCTTTCTTTCTTTCTTATCCAATAA
GGGAATGAATACTCCCACTTGTTTAATTACCCCGGATGACCGCATGCTTGAAGGAGTACTTGGTCGGTTT
TCATACCCCCCTTCTTTCTTTTATCTTGACTAAAACCCAGGTTCAGATCTACACCACTGCTTGGGCGTGTG
CGCAGTGTTCTTTCTTTCTTTCTTTCTTTAGGCGCTGGACGCGGAAGGTAAATAAGCTGAAATAGGTGTC
TTCGCGCTAGGCTCGTTTTTCTTTCTTTCTTTCTTTCTTACCCTTCTGTCATCCGCCTCTATCGGGGGTCAG
TCCCAAATCGACATATGTCAAAGGGGGTGCGAACGCAGAGTATACAACTGCGTAATTCTTTCTTTCTTTC
TTTCTTTACCTGACGAGTGGTAAGCTATTGCCCGGTAGCGGCCGCGAATCAAGTATTTGGATGGCATACT

GGGGCGAGAAAGCCTGACCCGTACACATTTCTTTCTTTCTTTCTTTCTCACTCCCTTGCATTCCTGTTGTT
GTACCCTAGCCATCGACCCACACGTTTCCATGACAGCTCCTGTCGCGGATACGTATCCAGACATAAGTCT
ATCCGGCATCGCGATTCATCTTCGCGAATC

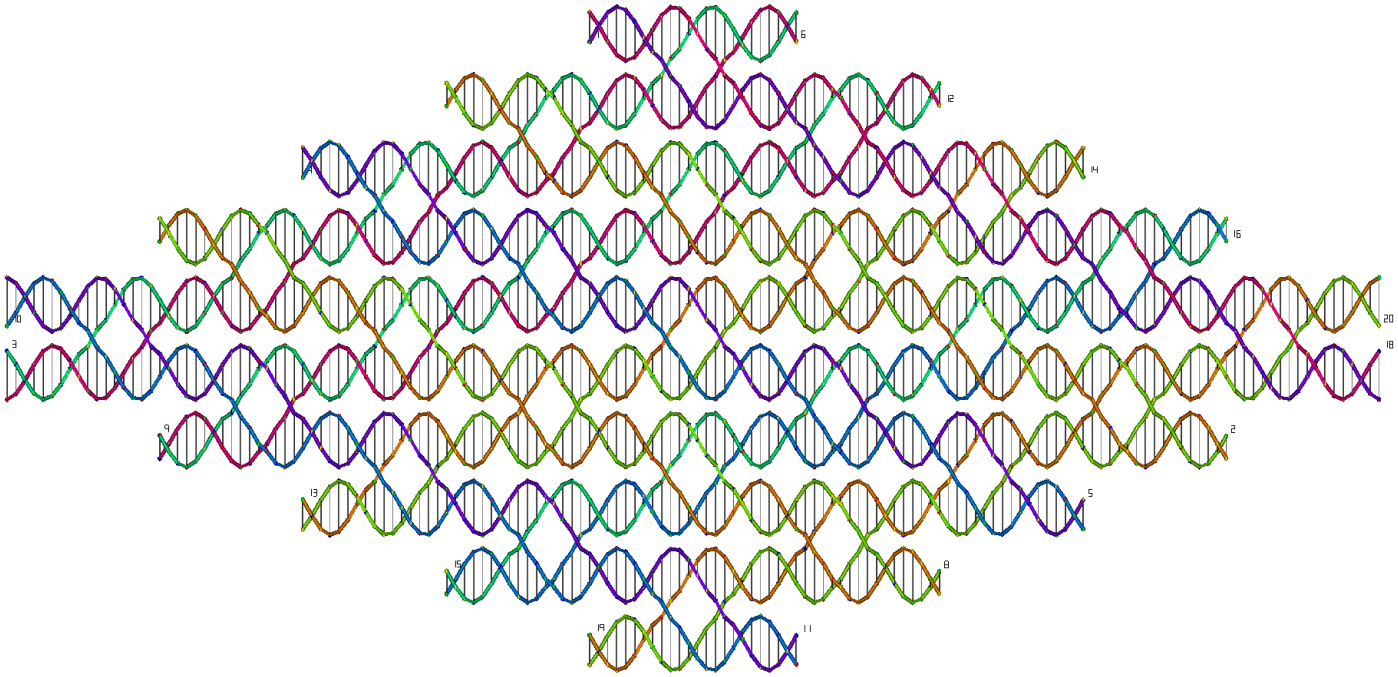

Figure S12-22. Design detail of 20-strand version of 5 × 5 diamond-shape ssOrigami.

1:
CGGTCGTCACCAATATCGTAATTGAGCCAACCTCAACGCGGGTCCGATGCGGCATGAGGCTGACACGCC
ATGGCAGGCATCGATTGGG
2:
CCCAATCGACTGAAGCCATGGCGTGCCATACTCATGCCGCAATCTATCCGCGTTGAGTTAGCATCAATTA
CGATGAAACTGACGACCG
3:
AAACAGATCGCACTCAGCGGTCTCGTAGATCGAGTGTCTCTACCTGAGACAAGGATCTGTTTCACAAGG
CCTTGTGACTTCCGCTAGTC
4:
CCTCGAAGTGATTGATCTAGCGTAGGCTCTACCGTTCGGCTCGCCCTCTGCAACATGAAGATCGGTCGCC
AAGCACCGATGTCGGTCC
5:
GGACCGACAGGTTGTCTTGGCGACCTCGTCCCATGTTGCAGAGTGTGAGCCGAACGGAAATAACTACGC
TAGACTCAGGACTTCGAGG
6:
GACTAGCGGAAATGGCAAGGCCTTGTATTGGAGATCCTTGTTCAATCTAGAGACACTCGCGCCACGAGA
CCGCAGAGCACGATCTGTTT
7:
CCGGCTGTGGGCGCGAGGTGCCGTGGCGTCTGCAAGACACAGCGCTCTGTTGATATCGCCCAGGTCTAC
GACAGTTGAGTGTTGGGCG

8:
CGCCCAACACTGGGTTGTCGTAGACAAAATCGATATCAACAATAAGGTGTGTCTTGCCCAGTACACGGC
ACCTCGATCTCACAGCCGG
9:
TCATAGTAAAGACGTCAGGATAGAATACTGGGAAGATGCCATTATTTCCCATATGTTTGCTAATCGTGG
ACTCCACGTCATGGCAGCC
10:
CAGGATCTAGTGCTCTATGGGATTAGGTCTAGGACCTTCCGGCGGGTCGGTTTGTGCATACCAGATGTTA
ACGTGACCGGCAGTCAAGT
11:
ACTTGACTGAGGCACACGTTAACATTCGCATTGCACAAACCCACACACCGGAAGGTCACGTCTCTAATC
CCATTGAGTGCTAGATCCTG
12:
GGCTGCCATGAGACCGAGTCCACGAGTTGGCAACATATGGGTAGAGCTGGCATCTTCAGACGCTTCTAT
CCTGCTAGACTTACTATGA
13:
CAGATCATCTGTGTGTGGCCGGATGCCTTATCGGGTCTCGTCACACTCGGGCACAGAATAGATCTCTAAG
AGACACGTGCCCAAAGCG
14:
CGCTTTGGGCCACGCTCTCTTAGAGTCGGACTCTGTGCCCGAGGGCGACGAGACCCGGAGCGCCATCCG
GCCAGACCCGGATGATCTG
15:
GGGACGTGCATGCGACCCACGTCGTGATTTTGTTCCACTTGGGACGAATGTCGAAGTGTATGGTGCATTA
CCCGTAGGCTACATCTGG
16:
CCAGATGTAAGTTTTGGGTAATGCATCAGCCACTTCGACATGATCTTCAAGTGGAACCTGGGCACGACG
TGGGCTGGTAGCACGTCCC
17:
CTGATAGGCCCATTTCTAATTTCGCGGTCTCTTACACGGGTGCGTGGTCTTCCTCTGAAAACTGGAGCCA
CAGGGAGGGACACTCGCTT
18:
AAGCGAGTGTCGGCATCTGTGGCTCCGCCTACCAGAGGAAGACACGTGACCCGTGTAAGACGTGGCGA
AATTAGAAGTCAGCCTATCAG
19:
CAGGCTCGTGTGCCTTGGAGATGGAACCCAGCTGGAGCGAGACAACCAGATGGGATCCTTCAGCCCATG
ACAAATGCCGCACAGGCAGC
20:
GCTGCCTGTGCCCTCCTTGTCATGGGTGCCTGGATCCCATCTTCGGTGCTCGCTCCAGCTCAACTCCATCT
CCACCGGTCACGAGCCTG

To study the knotting complexity of a structure, we introduce a novel dynamic relaxation model to simplify the knot structure without changing its knotting complexity. In this model, both the 3' and 5' ends of a 3D ssOrigami model are fixed while the remaining part of the strand falls under simulated gravity. The falling process will relax the unknotted crossings, and thus simplify the diagram. For example, if a structurally "complex" 3D knot model is actually an unknot (crossing number 0), the relaxation will simplify the model into an untied loop (unfolding). On the other hand, if a 3D knot model is knotted, the crossings will be kept during the falling process.

[Movie-1] Dynamic animation to demonstrate the knot relaxation process of a simple DNA hairpin.

[Movie-2] Dynamic animation to demonstrate the knot relaxation process of a paired double helical DNA with antiparallel crossovers analogue.

[Movie-3] Dynamic animation to demonstrate the knot relaxation process of RNAse (PDB: 1GQV).

[Movie-4] Dynamic relaxation to demonstrate the knot relaxation process of Telomerase (PDB: 3KYL).

[Movie-5] Dynamic relaxation to demonstrate the knot relaxation process of Group II Intron (PDB: 3EOH).

[Movie-6] Dynamic relaxation to demonstrate the knot relaxation process of 16S rRNA (PDB: 1L94).

[Movie-7] Dynamic relaxation to demonstrate the knot relaxation process of acetohydroxy acid isomeroreductase (PDB: 1YVE-L).

[Movie-8] Dynamic relaxation to demonstrate the knot relaxation process of an anti-parallel ssOrigami model shown in Fig. S4-8.

[Movie-9] Dynamic relaxation to demonstrate the knot relaxation process of a parallel ssOrigami model with 16bp crossover distance shown in Fig. S5-2.

[Movie-10] Dynamic relaxation to demonstrate the knot relaxation process of the 3 × 3 ssOrigami model.

[Movie-11] Dynamic relaxation to demonstrate the knot relaxation process of the 4 × 4 ssOrigami model.

[Movie-12] Dynamic relaxation to demonstrate the knot relaxation process of the 5 × 5 ssOrigami model.

[Movie-13] Dynamic relaxation to demonstrate the knot relaxation process of the strip-shape ssOrigami model.

[Movie-14] Dynamic relaxation to demonstrate the knot relaxation process of the rectangle-shape ssOrigami model.

[Movie-15] Dynamic relaxation to demonstrate the knot relaxation process of the triangle-shape ssOrigami model.
[Movie-16] Dynamic relaxation to demonstrate the knot relaxation process of the rhomboid-shape ssOrigami model.

References and Notes

1. J. Chen, N. C. Seeman, Synthesis from DNA of a molecule with the connectivity of a cube. *Nature* **350**, 631–633 (1991). doi: 10.1038/350631a0; Medline

2. E. Winfree, F. Liu, L. Wenzler, N. Seeman, Design and self-assembly of two-dimensional DNA crystals. *Nature* **394**, 539–544 (1998). doi: 10.1038/28998; Medline

3. W. Shih, J. Quispe, G. Joyce, A 1.7-kilobase single-stranded DNA that folds into a nanoscale octahedron. *Nature* **427**, 618–621 (2004). doi: 10.1038/nature02307; Medline

4. P. Rothemund, Folding DNA to create nanoscale shapes and patterns. *Nature* **440**, 297–302 (2006). doi: 10.1038/nature04586; Medline

5. Y. He, T. Ye, M. Su, C. Zhang, A. E. Ribbe, W. Jiang, C. Mao, Hierarchical self-assembly of DNA into symmetric supramolecular polyhedra. *Nature* **452**, 198–201 (2008). doi: 10.1038/nature06597; Medline

6. J. Zheng, J. J. Birktoft, Y. Chen, T. Wang, R. Sha, P. E. Constantinou, S. L. Ginell, C. Mao, N. C. Seeman, From molecular to macroscopic via the rational design of a self-assembled 3D DNA crystal. *Nature* **461**, 74–77 (2009). doi: 10.1038/nature08274; Medline

7. H. Gu, J. Chao, S.-J. Xiao, N. C. Seeman, Dynamic patterning programmed by DNA tiles captured on a DNA origami substrate. *Nat. Nanotechnol.* **4**, 245–248 (2009). doi: 10.1038/nnano.2009.5; Medline

8. S. M. Douglas, H. Dietz, T. Liedl, B. Högberg, F. Graf, W. M. Shih, Self-assembly of DNA into nanoscale three-dimensional shapes. *Nature* **459**, 414–418 (2009). doi: 10.1038/nature08016; Medline

9. H. Dietz, S. M. Douglas, W. M. Shih, Folding DNA into twisted and curved nanoscale shapes. *Science* **325**, 725–730 (2009). doi: 10.1126/science.1174251; Medline

10. E. S. Andersen, M. Dong, M. M. Nielsen, K. Jahn, R. Subramani, W. Mamdouh, M. M. Golas, B. Sander, H. Stark, C. L. P. Oliveira, J. S. Pedersen, V. Birkedal, F. Besenbacher, K. V. Gothelf, J. Kjems, Self-assembly of a nanoscale DNA box with a controllable lid. *Nature* **459**, 73–76 (2009). doi: 10.1038/nature07971; Medline

11. A. Rajendran, M. Endo, Y. Katsuda, K. Hidaka, H. Sugiyama, Programmed two-dimensional self-assembly of multiple DNA origami jigsaw pieces. *ACS Nano* **5**, 665–671 (2011). doi: 10.1021/nn1031627; Medline

12. S. Woo, P. W. K. Rothemund, Programmable molecular recognition based on the geometry of DNA nanostructures. *Nat. Chem.* **3**, 620–627 (2011). doi: 10.1038/nchem.1070; Medline

13. D. Han, S. Pal, J. Nangreave, Z. Deng, Y. Liu, H. Yan, DNA origami with complex curvatures in three-dimensional space. *Science* **332**, 342–346 (2011). doi: 10.1126/science.1202998; Medline

14. B. Wei, M. Dai, P. Yin, Complex shapes self-assembled from single-stranded DNA tiles. *Nature* **485**, 623–626 (2012). doi: 10.1038/nature11075; Medline

15. Y. Ke, L. L. Ong, W. M. Shih, P. Yin, Three-dimensional structures self-assembled from DNA bricks. *Science* **338**, 1177–1183 (2012). doi: 10.1126/science.1227268; Medline

16. D. Han, S. Pal, Y. Yang, S. Jiang, J. Nangreave, Y. Liu, H. Yan, DNA gridiron nanostructures based on four-arm junctions. *Science* **339**, 1412–1415 (2013). doi: 10.1126/science.1232252; Medline

17. R. Iinuma, Y. Ke, R. Jungmann, T. Schlichthaerle, J. B. Woehrstein, P. Yin, Polyhedra self-assembled from DNA tripods and characterized with 3D DNA-PAINT. *Science* **344**, 65–69 (2014). doi: 10.1126/science.1250944; Medline

18. Y. Ke, L. L. Ong, W. Sun, J. Song, M. Dong, W. M. Shih, P. Yin, DNA brick crystals with prescribed depths. *Nat. Chem.* **6**, 994–1002 (2014). doi: 10.1038/nchem.2083; Medline

19. K. E. Dunn, F. Dannenberg, T. E. Ouldridge, M. Kwiatkowska, A. J. Turberfield, J. Bath, Guiding the folding pathway of DNA origami. *Nature* **525**, 82–86 (2015). doi: 10.1038/nature14860; Medline

20. T. Gerling, K. Wagenbauer, A. Neuner, H. Dietz, Dynamic DNA devices and assemblies formed by shape-complementary, non–base pairing 3D components. *Science* **347**, 1446–1452 (2015). doi: 10.1126/science.aaa5372; Medline

21. E. Benson, A. Mohammed, J. Gardell, S. Masich, E. Czeizler, P. Orponen, B. Högberg, DNA rendering of polyhedral meshes at the nanoscale. *Nature* **523**, 441–444 (2015). doi: 10.1038/nature14586; Medline

22. F. Zhang, S. Jiang, S. Wu, Y. Li, C. Mao, Y. Liu, H. Yan, Complex wireframe DNA origami nanostructures with multi-arm junction vertices. *Nat. Nanotechnol.* **10**, 779–784 (2015). doi: 10.1038/nnano.2015.162; Medline

23. R. Veneziano, S. Ratanalert, K. Zhang, F. Zhang, H. Yan, W. Chiu, M. Bathe, Designer nanoscale DNA assemblies programmed from the top down. *Science* **352**, 1534 (2016). doi: 10.1126/science.aaf4388; Medline

24. N. Avakyan, A. A. Greschner, F. Aldaye, C. J. Serpell, V. Toader, A. Petitjean, H. F. Sleiman, Reprogramming the assembly of unmodified DNA with a small molecule. *Nat. Chem.* **8**, 368–376 (2016). doi: 10.1038/nchem.2451; Medline

25. D. Liu, G. Chen, U. Akhter, T. Cronin, Y. Weizmann, Creating complex molecular topologies by configuring DNA four-way junctions. *Nat. Chem.* **8**, 907–914 (2016). doi: 10.1038/nchem.2564; Medline

26. G. Tikhomirov, P. Peterson, L. Qian, Programmable disorder in random DNA tilings. *Nat. Nanotechnol.* **12**, 251–259 (2017). doi: 10.1038/nnano.2016.256; Medline

27. S. L. Sparvath, C. W. Geary, E. S. Andersen, Computer-aided design of RNA origami structures. *Methods Mol. Biol.* **1500**, 51–80 (2017). doi: 10.1007/978-1-4939-6454-3; Medline

28. S. M. Douglas, J. J. Chou, W. M. Shih, DNA-nanotube-induced alignment of membrane proteins for NMR structure determination. *Proc. Natl. Acad. Sci. U.S.A.* **104**, 6644–6648 (2007). doi: 10.1073/pnas.0700930104; Medline

29. G. P. Acuna, F. M. Möller, P. Holzmeister, S. Beater, B. Lalkens, P. Tinnefeld, Fluorescence enhancement at docking sites of DNA-directed self-assembled nanoantennas. *Science* **338**, 506–510 (2012). doi: 10.1126/science.1228638; Medline

30. A. Kuzyk, R. Schreiber, Z. Fan, G. Pardatscher, E.-M. Roller, A. Högele, F. C. Simmel, A. O. Govorov, T. Liedl, DNA-based self-assembly of chiral plasmonic nanostructures with tailored optical response. *Nature* **483**, 311–314 (2012). doi: 10.1038/nature10889; Medline

31. S. Douglas, I. Bachelet, G. M. Church, A logic-gated nanorobot for targeted transport of molecular payloads. *Science* **335**, 831–834 (2012). doi: 10.1126/science.1214081; Medline

32. Z. Jin, W. Sun, Y. Ke, C.-J. Shih, G. L. C. Paulus, Q. Hua Wang, B. Mu, P. Yin, M. S. Strano, Metallized DNA nanolithography for encoding and transferring spatial information for graphene patterning. *Nat. Commun.* **4**, 1663 (2013). doi: 10.1038/ncomms2690; Medline

33. W. Sun, E. Boulais, Y. Hakobyan, W. L. Wang, A. Guan, M. Bathe, P. Yin, Casting inorganic structures with DNA molds. *Science* **346**, 1258361 (2014). doi: 10.1126/science.1258361; Medline

34. J. Fu, Y. R. Yang, A. Johnson-Buck, M. Liu, Y. Liu, N. G. Walter, N. W. Woodbury, H. Yan, Multi-enzyme complexes on DNA scaffolds capable of substrate channelling with an artificial swinging arm. *Nat. Nanotechnol.* **9**, 531–536 (2014). doi: 10.1038/nnano.2014.100; Medline

35. J. B. Knudsen, L. Liu, A. L. Bank Kodal, M. Madsen, Q. Li, J. Song, J. B. Woehrstein, S. F. J. Wickham, M. T. Strauss, F. Schueder, J. Vinther, A. Krissanaprasit, D. Gudnason, A. A. A. Smith, R. Ogaki, A. N. Zelikin, F. Besenbacher, V. Birkedal, P. Yin, W. M. Shih, R. Jungmann, M. Dong, K. V. Gothelf, Routing of individual polymers in designed patterns. *Nat. Nanotechnol.* **10**, 892–898 (2015). doi: 10.1038/nnano.2015.190; Medline

36. P. C. Nickels, B. Wünsch, P. Holzmeister, W. Bae, L. M. Kneer, D. Grohmann, P. Tinnefeld, T. Liedl, Molecular force spectroscopy with a DNA origami–based nanoscopic force clamp. *Science* **354**, 305–307 (2016). doi: 10.1126/science.aah5974; Medline

37. F. Kilchherr, C. Wachauf, B. Pelz, M. Rief, M. Zacharias, H. Dietz, Single-molecule dissection of stacking forces in DNA. *Science* **353**, aaf5508 (2016). doi: 10.1126/science.aaf5508; Medline

38. T. G. Martin, T. A. M. Bharat, A. C. Joerger, X.-C. Bai, F. Praetorius, A. R. Fersht, H. Dietz, S. H. W. Scheres, Design of a molecular support for cryo-EM structure determination. *Proc. Natl. Acad. Sci. U.S.A.* **113**, E7456–E7463 (2016). doi: 10.1073/pnas.1612720113; Medline

39. A. Gopinath, E. Miyazono, A. Faraon, P. W. K. Rothemund, Engineering and mapping nanocavity emission via precision placement of DNA origami. *Nature* **535**, 401–405 (2016). doi: 10.1038/nature18287; Medline

40. N. A. W. Bell, U. F. Keyser, Digitally encoded DNA nanostructures for multiplexed, single-molecule protein sensing with nanopores. *Nat. Nanotechnol.* **11**, 645–651 (2016). doi: 10.1038/nnano.2016.50; Medline

41. C. Lin, M. Xie, J. J. L. Chen, Y. Liu, H. Yan, Rolling-circle amplification of a DNA nanojunction. *Angew. Chem. Int. Ed.* **45**, 7537–7539 (2006). doi: 10.1002/anie.200602113; Medline

42. C. Lin, X. Wang, Y. Liu, N. C. Seeman, H. Yan, Rolling circle enzymatic replication of a complex multi-crossover DNA nanostructure. *J. Am. Chem. Soc.* **129**, 14475–14481 (2007). doi: 10.1021/ja0760980; Medline

43. Z. Li, B. Wei, J. Nangreave, C. Lin, Y. Liu, Y. Mi, H. Yan, A replicable tetrahedral nanostructure self-assembled from a single DNA strand. *J. Am. Chem. Soc.* **131**, 13093–13098 (2009). doi: 10.1021/ja903768f; Medline

44. C. Geary, P. W. Rothemund, E. S. Andersen, A single-stranded architecture for cotranscriptional folding of RNA nanostructures. *Science* **345**, 799–804 (2014). doi: 10.1126/science.1253920; Medline

45. C. X. Lin, *et al.*, In vivo cloning of artificial DNA nanostructures. *Proc. Natl. Acad. Sci. U.S.A.* **105**, 17626–17631 (2008). doi: 10.1073/pnas.0805416105; Medline

46. C. Ducani, C. Kaul, M. Moche, W. M. Shih, B. Högberg, Enzymatic production of 'monoclonal stoichiometric' single-stranded DNA oligonucleotides. *Nat. Methods* **10**, 647–652 (2013). doi: 10.1038/nmeth.2503; Medline

47. N. C. Seeman, The design and engineering of nucleic acid nanoscale assemblies. *Curr. Opin. Struct. Biol.* **6**, 519–526 (1996). doi: 10.1016/S0959-440X(96)80118-7; Medline

48. X. Zhang, H. Yan, Z. Shen, N. Seeman, Paranemic cohesion of topologically-closed DNA molecules. *J. Am. Chem. Soc.* **124**, 12940–12941 (2002). doi: 10.1021/ja026973b; Medline

49. Z. Shen, H. Yan, T. Wang, N. Seeman, Paranemic crossover DNA: A generalized Holliday structure with applications in nanotechnology. *J. Am. Chem. Soc.* **126**, 1666–1674 (2004). doi: 10.1021/ja038381e; Medline

50. D. Han, S. Jiang, A. Samanta, Y. Liu, H. Yan, Unidirectional scaffold-strand arrangement in DNA origami. *Angew. Chem. Int. Ed.* **52**, 9031–9034 (2013). doi: 10.1002/anie.201302177; Medline

51. L. Jaeger, N. B. Leontis, Tecto-RNA: One-dimensional self-assembly through tertiary interactions. *Angew. Chem. Int. Ed.* **39**, 2521–2524 (2000). doi: 10.1002/1521-3773(20000717)39:14<2521::AID-ANIE2521>3.0.CO;2-P; Medline

52. A. Chworos, I. Severcan, A. Y. Koyfman, P. Weinkam, E. Oroudjev, H. G. Hansma, L. Jaeger, Building programmable jigsaw puzzles with RNA. *Science* **306**, 2068–2072 (2004). doi: 10.1126/science.1104686; Medline

53. C. J. Delebecque, A. B. Lindner, P. A. Silver, F. A. Aldaye, Organization of intracellular reactions with rationally designed RNA assemblies. *Science* **333**, 470–474 (2011). doi: 10.1126/science.1206938; Medline

54. L. Jaeger, A. Chworos, The architectonics of programmable RNA and DNA nanostructures. *Curr. Opin. Struct. Biol.* **16**, 531–543 (2006). doi: 10.1016/j.sbi.2006.07.001; Medline

55. J. W. Alexander, G. B. Briggs, On types of knotted curves, in *The Annals of Mathematics, Second Series* (Annals of Mathematics, 1926), pp. 562–586.

56. J. W. Alexander, Topological invariants of knots and links. *Trans. Am. Math. Soc.* **30**, 275–306 (1928). doi: 10.1090/S0002-9947-1928-1501429-1

57. K. Murasugi, *Knot Theory and Its Applications* (Springer Science and Business Media, 2007).

58. M. L. Mansfield, Are there knots in proteins? *Nat. Struct. Mol. Biol.* **1**, 213–214 (1994). doi: 10.1038/nsb0494-213; Medline

59. F. Takusagawa, S. Kamitori, A real knot in protein. *J. Am. Chem. Soc.* **118**, 8945–8946 (1996). doi: 10.1021/ja961147m

60. W. R. Taylor, A deeply knotted protein structure and how it might fold. *Nature* **406**, 916–919 (2000). doi: 10.1038/35022623; Medline

61. J. R. Wagner, J. S. Brunzelle, K. T. Forest, R. D. Vierstra, A light-sensing knot revealed by the structure of the chromophore-binding domain of phytochrome. *Nature* **438**, 325–331 (2005). doi: 10.1038/nature04118; Medline

62. H. Lee, E. Popodi, H. Tang, P. L. Foster, Rate and molecular spectrum of spontaneous mutations in the bacterium *Escherichia coli* as determined by whole-genome sequencing. *Proc. Natl. Acad. Sci. U.S.A.* **109**, E2774–E2783 (2012). doi: 10.1073/pnas.1210309109; Medline

63. M. Wang, M. Zyracki, A. Kimoto, M. Tinnus, D. Parker, P. Jones, J. Schaeffer, D. Amago, F. Mazzoldi, E. Groban, Autodesk Molecule Viewer; https://moleculeviewer.lifesciences.autodesk.com (2017).

64. S. Horiya, *et al.*, RNA LEGO: Magnesium-dependent formation of specific RNA assemblies through kissing interactions. *Chem. Biol.* **10**, 645–654 (2003). doi: 10.1016/S1074-5521(03)00146-7; Medline

65. More formally, previous scaffolded origami work and the DNA brick work demonstrates the construction of a size n object using $O(n)$ number of components; the unimolecular ssOrigami demonstrates the construction of a size n object using one component; the two-strand case represents its construction using $O(1)$ components; the 20-strand case represents its construction using $O(\sqrt{n})$ components.

66. S. Williams, K. Lund, C. Lin, P. Wonka, S. Lindsay, H. Yan, Tiamat: A three-dimensional editing tool for complex DNA structures, in *International Workshop on DNA-Based Computers* (Springer, 2008), pp. 90–101.

67. W. B. R. Lickorish, *An Introduction to Knot Theory* (Springer Science and Business Media, 2012), vol. 175.

68. V. Biou, R. Dumas, C. Cohen-Addad, R. Douce, D. Job, E. Pebay-Peyroula, The crystal structure of plant acetohydroxy acid isomeroreductase complexed with NADPH, two magnesium ions and a herbicidal transition state analog determined at 1.65 Å resolution. *EMBO J.* **16**, 3405–3415 (1997). doi: 10.1093/emboj/16.12.3405; Medline